CRUSTAL STRUCTURE ACROSS THE SOUTHERN APPALACHIANS AND ATLANTIC COASTAL PLAIN: CONSTRAINTS FROM TELESEISMIC RECEIVER FUNCTIONS AND NEW PERSPECTIVES FROM MAGNETIC MODELING

by

ELIAS HORRY PARKER JR.

(Under the Direction of Robert B. Hawman)

ABSTRACT

The Southeastern Suture of the Appalachian Margin Experiment (SESAME) is an 85-station broadband seismometer array deployed across the southern Appalachians and Atlantic Coastal Plain. Receiver functions analyzed in this study complement previous active-source reflection and refraction experiments and provide new constraints on crustal structure across the crystalline southern Appalachians. Receiver function Ps conversions combined with previous wide-angle results confirm the presence of a localized crustal root (up to ~58-km crustal thickness) beneath the high elevations of the Blue Ridge province in northern Georgia and western North Carolina. Low average crustal Vp/Vs ratios (1.69-1.72) determined from H-k stacking indicate that the continental crust across the Carolina terrane and parts of the Inner Piedmont has a felsic average composition. Forward modeling of Ps conversions in relatively high-frequency (2-3 Hz) receiver functions provides new constraints on the nature of velocity contrasts along the Appalachian detachment. In the Blue Ridge, a 3.5-km-thick, high shear-wave velocity layer (Vs=3.9 km/s) is consistent with underlying passive-margin metasedimentary rocks dominantly comprised of quartzite and/or dolostone. In the Inner Piedmont, conversions from the top and base of a low-Vs zone (3.1 km/s) at depths of 5-9 km are interpreted as a package of metasedimentary rocks or a shear zone characterized by radial anisotropy. High-amplitude negative conversions beneath the Carolina terrane at 10-13 km depth are consistent with high-Vs arc rocks (4.0 km/s) overlying sheared rocks with lower Vs (3.2 km/s). H-k stacking results and forward modeling are consistent with models showing that the Alleghanian detachment extends southeastward beneath the peri-Gondwanan Carolina terrane. Beneath the Atlantic Coastal Plain, the Suwannee suture zone is interpreted to mark the Late Paleozoic Alleghanian collision between Laurentia and Gondwana, though the coincident Brunswick Magnetic Anomaly (BMA) is interpreted to result from Central Atlantic Magmatic Province intrusions. New magnetic models assuming a contrast in remanent magnetization between two crustal blocks suggest that the anomaly can also be explained as an effect of continental suturing. Additional constraints on the velocity structure across the Atlantic Coastal Plain from the SESAME array are needed to differentiate between models for the source of the BMA.

INDEX WORDS: southern Appalachians, Atlantic Coastal Plain, receiver functions, crustal structure, Blue Ridge crustal root, Appalachian detachment, Alleghanian orogeny, Suwannee suture, South Georgia basin, Brunswick magnetic anomaly, remanent magnetization, Central Atlantic Magmatic Province

CRUSTAL STRUCTURE ACROSS THE SOUTHERN APPALACHIANS AND ATLANTIC COASTAL PLAIN: CONSTRAINTS FROM TELESEISMIC RECEIVER FUNCTIONS AND NEW PERSPECTIVES FROM MAGNETIC MODELING

by

ELIAS HORRY PARKER JR.

MS, University of Georgia, 2010

BS, University of the South, 2002

A Dissertation Submitted to the Graduate Faculty of The University of Georgia in Partial Fulfillment of the Requirements for the Degree

DOCTOR OF PHILOSOPHY

ATHENS, GEORGIA

2015

CRUSTAL STRUCTURE ACROSS THE SOUTHERN APPALACHIANS AND ATLANTIC COASTAL PLAIN: CONSTRAINTS FROM TELESEISMIC RECEIVER FUNCTIONS AND NEW PERSPECTIVES FROM MAGNETIC MODELING

by

ELIAS HORRY PARKER JR.

Major Professor: Robert B. Hawman
Committee: Karen M. Fischer
Alberto Patiño-Douce
Michael F. Roden

Electronic Version Approved:

Suzanne Barbour
Dean of the Graduate School
The University of Georgia
August 2015

ACKNOWLEDGEMENTS

I would like to thank Rob Hawman for his dedication and support as we navigated the country roads of Georgia and explored the southern Appalachians.

The SESAME project was truly a group effort, and I would like to acknowledge the numerous undergraduates, graduate students, and others that participated in the field work over the course of the four-year seismometer deployment. I would also like to thank the station hosts for their support of the project.

This work was funded by National Science Foundation grant EAR-0844154 to R.B. Hawman. Financial assistance from the Miriam Watts-Wheeler Fund, the Gilles and Bernadette Allard Award Fund, the Joseph W. Berg Scholarship in Geophysics Fund, and the University of Georgia also supported this research.

TABLE OF CONTENTS

Page

ACKNOWLEDGEMENTS iv

LIST OF TABLES viii

LIST OF FIGURES ix

CHAPTER

1 INTRODUCTION AND LITERATURE REVIEW 1

INTRODUCTION 1

DISSERTATION OVERVIEW 5

GEOLOGICAL AND GEOPHYSICAL CONSTRAINTS ON THE TECTONIC DEVELOPMENT OF THE SOUTHEASTERN UNITED STATES 6

2 CRUSTAL EVOLUTION ACROSS THE SOUTHERN APPALACHIANS: INITIAL RESULTS FROM THE SESAME BROADBAND ARRAY 17

ABSTRACT 18

INTRODUCTION 18

DATA AND METHODS 19

CRUSTAL STRUCTURE ACROSS THE SOUTHERN APPALACHIANS 20

DISCUSSION 22

CONCLUSIONS 24

3 CONSTRAINING LITHOLOGIC VARIABILITY ALONG THE ALLEGHANIAN DETACHMENT IN THE SOUTHERN APPALACHIANS USING PASSIVE-SOURCE SEISMOLOGY 33

ABSTRACT....34

INTRODUCTION 34

REFLECTION PROFILING ACROSS THE SOUTHERN APPALACHIANS ..35

DATA AND METHODOLOGY....36

RESULTS 37

DISCUSSION....40

CONCLUSIONS 42

4 CRUSTAL MAGNETISM, TECTONIC INHERITANCE, AND CONTINENTAL RIFTING IN THE SOUTHEASTERN UNITED STATES....49

ABSTRACT....50

INTRODUCTION 50

ALLEGHANIAN OROGENY 52

MESOZOIC CONTINENTAL RIFTING....53

CRUSTAL STRUCTURE ACROSS THE BMA AND ECMA 54

PREVIOUS MAGNETIC MODELS 55

REMANENT MAGNETIZATION OF LOWER CRUSTAL ROCKS 55

NEW MAGNETIC MODELS....56

DISCUSSION....58

CONCLUSIONS 59

5 ERRATUM FOR CRUSTAL MAGNETISM, TECTONIC INHERITANCE, AND CONTINENTAL RIFTING IN THE SOUTHEASTERN UNITED STATES...........66
CORRECTION FOR MAGNETIC MODELS...67
6 CONCLUSIONS 69
SOUTHERN APPALACHIAN CRUSTAL STRUCTURE 69
CRUSTAL STRUCTURE ACROSS THE ATLANTIC COASTAL PLAIN 70
FUTURE WORK...72
REFERENCES 75
APPENDICES
A SUPPLEMENTARY MATERIAL FOR CHAPTER 2...100
B SUPPLEMENTARY MATERIAL FOR CHAPTER 3...110

LIST OF TABLES

Page

Table 2.1: Crustal thickness and Vp/Vs estimates for selected SESAME stations 30

Table 2.2: Crustal thickness and Vp/Vs estimates for selected TA stations.................................32

Table B1: Events used in the calculation of receiver functions for each station 128

LIST OF FIGURES

Page

Figure 1.1: Regional maps of the SESAME array 15

Figure 2.1: Maps of seismic deployments 26

Figure 2.2: Stacked receiver function traces from stations along the D-line 27

Figure 2.3: H-k stacking analysis 28

Figure 2.4: Map showing the H-k stacking results and estimated crustal thicknesses using Ps delay times for selected SESAME and TA stations 29

Figure 3.1: Map of the SESAME array and reproduction of ADCOH line 1 43

Figure 3.2: P-SV conversions at station W33 44

Figure 3.3: Stacked receiver function traces ($\alpha = 7.0$) compared with synthetic seismograms generated for three models of the upper crust 45

Figure 3.4: P-SV conversions and interpretive cross-section 47

Figure 4.1: Aeromagnetic map (red = high; blue = low) of the eastern margin of North America showing the approximate locations of existing seismic profiles crossing the Brunswick magnetic anomaly (BMA) and East Coast magnetic anomaly (ECMA) 61

Figure 4.2: Map showing magnetic profiles and reproduction of COCORP lines 11-15 62

Figure 4.3: Observed total magnetic intensity (dots) and magnetic models (solid line) 63

Figure 4.4: Conceptual tectonic model for the southeastern United States 65

Figure 5.1: Corrected magnetic models for Chapter 4 68

Figure A1: Stacked receiver functions from stations along the N-S trending W-line, including station D20 from the NW-trending D-line 104

Figure A2: Receiver function gathers and stacked traces for stations D02 and D05 in the Carolina terrane using Gaussian values of 2.5 and 5.0 105

Figure A3: Receiver function gathers and stacked traces for stations D15, D17, and W35 using a Gaussian value of 2.5 106

Figure A4: H-k stacks for selected SESAME and TA stations 107

Figure A5: Stacked receiver function traces for selected TA stations projected onto a NW-trending line passing through stations V50A and Z54A...108

Figure A6: Variation in Ps delay times across the southern Appalachians 109

Figure B1: P-SV conversions at stations D20, D21, and D22 113

Figure B2: P-SV conversions at stations D18 and D19 114

Figure B3: P-SV conversions at stations D14, W31, D17, and W31.5 115

Figure B4: P-SV conversions at stations Y52A and Z52A...116

Figure B5: P-SV conversions at stations W29, W30, D12, W54A, and X54A..........................117

Figure B6: P-SV conversions at stations D03-D07 and Z53A 118

Figure B7: P-SV conversions at stations D03 and D08 119

Figure B8: Bootstrapped receiver-function stacks...120

Figure B9: Distribution of events used in the calculation of receiver functions 127

CHAPTER 1

INTRODUCTION AND LITERATURE REVIEW

INTRODUCTION

Southeastern Suture of the Appalachian Margin Experiment

The Southeastern Suture of the Appalachian Margin Experiment (SESAME) is an 85-station seismometer array that operated from 2010-2014 across the southern Appalachians and Atlantic Coastal Plain. SESAME is an EarthScope flexible-array experiment deployed in conjunction with the arrival of the USArray Transportable array in the southeastern United States. Both arrays have provided a significant dataset to study the lithospheric structure of the region using seismic methods. The broad goal of SESAME is to characterize processes associated with continental suturing, terrane transport, and extension along the southeastern margin of North America. Improved constraints on the deep structure of this region are needed to assess the dynamics of the Late Paleozoic Alleghanian continental collision, as well as potential reactivation of inherited structure during rifting of the supercontinent Pangea and emplacement of the Central Atlantic Magmatic Province.

The geometry of the deployment (Figure 1.1A) is largely motivated by previous Consortium for Continental Reflection Profiling (COCORP) and Appalachian Ultradeep Core Hole (ADCOH) studies. COCORP lines crossing the Atlantic Coastal Plain in southern Georgia image a prominent set of dipping reflectors interpreted as the crustal-scale Suwannee suture zone marking the boundary between Laurentian (North American) and Gondwanan (African/South American) continental crust. The South Georgia basin, a 6-7 km deep Mesozoic rift basin, is also imaged beneath the Atlantic Coastal Plain south of the suture. The N-S trending SESAME transects (lines W and E) are roughly coincident with COCORP profiles showing the Suwannee suture and South Georgia basin. The dense station spacing (~5 km) on these lines coincides with the location of prominent dipping seismic reflectivity on COCORP profiles and the Brunswick magnetic anomaly (Figure 1.1B).

North of the proposed suture, COCORP and ADCOH profiles indicate that a low-angle detachment extends laterally ~250 km beneath the Appalachian fold-thrust belt and crystalline southern Appalachians. The Appalachian detachment, or décollement, is interpreted to separate overthrust terranes from underlying Cambrian-Ordovician passive-margin sediments and North American, Grenville-age basement. Stations along the NW-trending SESAME profile (line D) crossing the Blue Ridge, Inner Piedmont, and Carolina terrane are also roughly coincident with COCORP and ADCOH lines showing the underlying detachment (Figure 1.1A). Stations in northern Georgia and western North Carolina also sample the high elevations of the Blue Ridge Mountains and associated crustal root, which is marked by the Appalachian gravity low (Figure 1.1C).

Field Work

SESAME is a collaborative effort between Brown University, the University of North Carolina, and the University of Georgia. The array consisted of 85 broadband seismometers deployed across Georgia, Florida, North Carolina, and Tennessee. Seismometer installations were completed during three summer field seasons from 2010-2012, and the entire array was demobilized in May 2014. Prior to each field season, suitable locations for seismic stations were identified using Google Earth, and landowners were then identified and contacted to obtain permission for station installations. We met with each station host individually to determine the exact placement for the seismometer after considering noise sources, visibility, and site access. Private landowners hosted the majority of stations, though several sites were located in state parks.

During the summer of 2010, an initial array of seven seismometers was deployed along the W-line in west Georgia (Figure 1.1A). Six of the stations were constructed using the traditional vault method, which involved pouring a concrete base inside a buried plastic barrel. At station W15, a second seismometer was deployed using the direct-burial method, which involved burying the seismometer directly in the ground and using compacted sand to stabilize the instrument. A comparison of the data quality between the vault and direct burial methods showed that the two methods yielded comparable recordings (Parker et al., 2011). For the next two field seasons, seismometers were deployed using the direct-burial method because of the advantage of the simplified installation procedure. In the summer of 2011, stations were deployed along the remainder of the W-line and portions of the NW-trending D-line. In the summer of 2012, the D-line was completed and stations were installed along the E-line. The entire array was demobilized in May 2014, so recording times for stations range from approximately two to four years.

Throughout the experiment, 'service runs' were conducted every six months to obtain data and perform station maintenance. Typical field issues related to seismometer functionality included moisture/water, power problems (battery and solar panel), and occasional vandalism. Special trips to remote parts of the array were often necessary to address outstanding issues after completion of regularly scheduled 'service runs'.

This substantial data set is archived with the Incorporated Research Institutions for Seismology (IRIS) Data Management Center (DMC). With the exception of a few stations, the bulk of the data is proprietary to the University of Georgia, University of North Carolina, and Brown University until two years after completion of the experiment. At this time, the data will become publicly available to the seismological community.

SESAME Outreach

The scientific research is also accompanied by an outreach component. We have provided station hosts with data examples of earthquakes recorded by their individual stations, and we have shared the results of our preliminary scientific findings. We have also participated in numerous educational outreach projects for elementary and middle school students at the Georgia Mountain Research and Education Center in Blairsville, GA and a middle school in Lincolnton, GA. As of April 2015, we have conducted educational programs involving small-group activities (10-15 students) for over 1250 students.

Research Groups and Data Analysis

A variety of seismic methods are being employed to address the scientific questions associated with this study. The research group at Brown University is using a combination of SKS-splitting measurements, Pn phase analysis, Sp receiver functions, and Rayleigh wave analyses to investigate lithospheric structure and anisotropy within both the lithosphere and asthenosphere. Researchers from the University of North Carolina are focused on P-wave tomography methods to analyze the velocity structure of the lithospheric mantle. The group from the University of Georgia is using Ps receiver functions (H-k stacking method, forward modeling), SsPmp analysis, and PKIKP arrivals to study crustal structure. The contributions from receiver function analyses comprise the seismic component of this dissertation.

DISSERTATION OVERVIEW

This dissertation is comprised of three published manuscripts. In Chapter 2, an analysis of receiver functions from stations located northwest of the Fall Line within the crystalline southern Appalachians is presented (Parker et al., 2013). These data provide improved spatial coverage of Moho topography and new constraints on average crustal composition across the region. The main contribution of this study is the identification of low average crustal Vp/Vs ratios across the Inner Piedmont and peri-Gondwanan Carolina arc terrane. The low Vp/Vs values are indicative of a felsic average crustal composition. In terms of southern Appalachian crustal structure, this result is important because it supports models of overthrusting of the Carolina arc terrane over Grenville basement during continental collision, rather than lateral accretion of an intermediate-composition arc complex. Globally, the well-constrained low Vp/Vs ratios support the hypothesis that parts of the continental crust may be more felsic than typically thought. Receiver function Ps conversions from both SESAME and USArray Transportable Array stations also indicate that a localized crustal root (up to ~58-km crustal thickness) is present beneath the high elevations of the Blue Ridge in northern Georgia and western North Carolina.

In Chapter 3, a detailed analysis of receiver functions places new constraints on the nature of shear-wave velocity (Vs) contrasts along the Alleghanian detachment (Parker et al., 2015). There are two main contributions from this paper: 1) A high-velocity layer beneath the Blue Ridge is consistent with underlying passive-margin metasedimentary rocks dominantly composed of high-Vs quartzite and/or dolostone. 2) A velocity inversion beneath the Carolina terrane marks the contact between high-Vs arc lithologies and lower-Vs passive-margin metasediments or sheared basement gneisses. Again, this study reinforces the overthrust nature of accreted terranes within the southern Appalachians. In terms of methodology, the ability to correlate observations from relatively low-frequency receiver functions with higher resolution seismic reflection images is an important contribution.

In Chapter 4, an alternative magnetic model for the Brunswick Magnetic Anomaly (BMA) in southern Georgia is presented (Parker, 2014). The model is based on the assumption that contrasts in remanent magnetism between Laurentian crust and a Gondwanan crustal fragment (Florida block) are responsible for the long-wavelength magnetic low, in contrast with previous models based on induced magnetism associated with Mesozoic mafic intrusions. A modeling error was discovered in Parker (2014), and the corrected models are presented in Chapter 5. The error does not change the premise that the BMA is caused by contrasts in remanent magnetization associated with continental suturing, and the magnetic models have important implications for interpreting seismic results from the SESAME array and USArray Transportable array.

GEOLOGICAL AND GEOPHYSICAL CONSTRAINTS ON THE TECTONIC DEVELOPMENT OF THE SOUTHEASTERN UNITED STATES

Tectonic Overview

The geologic structure of the eastern margin of North America is a product of the complex formation and break-up of the supercontinents Rodinia and Pangea (Hatcher, 2010). The Grenville orogeny (1.3-1.0 Ga), a Himalayan-type continental collision that occurred during the formation of Rodinia, affected the Laurentian margin from present-day eastern Canada to Texas (Hynes and Rivers, 2010). Proterozoic rifting of Rodinia and development of the Iapetan passive margin forms the basis for understanding the subsequent Paleozoic evolution of the Laurentian margin (Thomas, 2010). Cambrian-Ordovician passive-margin strata, including an extensive carbonate platform, were deposited over extended Grenville continental crust on the Iapetan margin (Thomas, 1991; Hatcher, 2010). Paleozoic convergence along the Laurentian margin is characterized by island-arc collision and terrane accretion during the Taconic (Ordovician) and Neoacadian (Devonian-Mississippian) orogenies (Hatcher, 2010; Hibbard et al., 2010). The Permo-Carboniferous Alleghanian orogeny occurred during the formation of Pangea as North America and Africa collided (Hatcher, 2010). In the Mesozoic, continental rifting and break-up of Pangea resulted in the development of onshore Triassic-Jurassic rift basins, emplacement of mafic rocks of the Central Atlantic Magmatic Province (~201 Ma), and ultimately the formation of the Atlantic passive margin (Schlische, 1993; Hames et al., 2000).

Terranes of the Crystalline Southern Appalachians

The crystalline southern Appalachians are comprised of distinct terranes that were thrust over Laurentian (Iapetan) passive-margin strata during the Alleghanian orogeny, driving fold-and-thrust belt development in the Appalachian foreland (Cook et al., 1979; Hatcher et al., 1987; Hatcher et al., 2007). The major provinces include the Blue Ridge, Inner Piedmont, and Carolina terranes, though there are important internal boundaries within each terrane. The present configuration of the terranes is largely a product of the Alleghanian collision, but the surface geology provides insight on the Paleozoic evolution of the Laurentian margin prior to continental collision. A simplified description of the regional geology, including geophysical constraints on subsurface structure, is presented below.

The Blue Ridge province lies east of the Appalachian foreland basin and is bounded by the Brevard zone on its eastern flank. Middle Proterozoic Grenville basement rocks consisting primarily of granitic gneisses are preserved in the western Blue Ridge (Carrigan et al., 2003; Anderson and Moecher, 2009). Isotopic and geochronologic studies of Mesoproterozoic basement blocks in the southern Appalachians suggest that these rocks (Grenville inliers) were formed during continental collision between Laurentia and Amazonia at ~1.2 Ga (McLelland et al., 2010). In western North Carolina and northern Georgia, clastic sequences are representative of sediments deposited within a Neoproterozoic intracontinental rift basin (Ocoee Supergroup) and along the Iapetan rifted margin (Ashe-Tallulah Falls sequence) (Chakraborty et al., 2012). In the eastern Blue Ridge of Alabama and Georgia, metasedimentary (Wedowee-Emuckfaw-Dahlonega basin) and metavolcanic rocks (Hillabee Greenstone, Pumpkinvine Creek Formation) are interpreted to have formed within an Ordovician back-arc basin to the southeast of the Laurentian margin (Holm-Denoma and Das, 2010; Tull et al., 2014). Plutonism (e.g. Elkahatchee batholith) and high-pressure metamorphism (e.g. Lick Ridge eclogite) record deformation associated with Taconic subduction and arc collision during the Ordovician (Miller et al., 2006; Anderson and Moecher, 2009). Cambrian-Ordovician passive-margin metasedimentary rocks are present within the Grandfather Mountain window in western North Carolina (Bryant and Reed, 1970).

The Inner Piedmont is bound to the west by the Brevard zone and to the east by the Central Piedmont suture zone. These rocks provide evidence for basin sedimentation and arc collision, but the exact timing and nature of the collision is debated. Merschat et al. (2005) suggest that middle-to-upper amphibolite facies para- and orthogneisses of the Inner Piedmont were deformed within a middle-to-lower crustal channel during the Neoacadian orogeny in the Late Devonian-Mississippian. Alternatively, Anderson and Moecher (2009) suggest that the Piedmont was underthrust beneath the Laurentian margin during the Ordovician Taconic event based on high-pressure eclogite now preserved within the Blue Ridge and seismic reflection profiling (see below).

The peri-Gondwanan Carolina superterrane is composed of felsic-to-mafic metaplutonic and metavolcanic rocks formed in a Neoproterozoic / Early Paleozoic island-arc setting (Dennis and Wright, 1997; Hibbard et al., 2002; Dennis et al., 2004). Again, the timing and nature of accretion remain controversial: the Carolina terrane may have initially collided with North America during the Ordovician-Silurian Cherokee orogeny (Hibbard et al., 2012) or the Late Devonian-Mississippian Neo-Acadian orogeny (Merschat et al., 2005; Hatcher, 2010; Sinha et al., 2012). Although the timing of accretion is debated, the Carolina terrane likely experienced significant translation in a Middle Paleozoic dextral shear system along the Laurentian margin prior to the Alleghanian continental collision (Hibbard and Waldron, 2009; Hatcher, 2010; Hibbard et al., 2010; Sinha et al., 2012).

The Alleghanian Orogeny

The Late Paleozoic Alleghanian orogeny is characterized as an oblique transpressional collision between North America and Africa (Hatcher, 2010). Appalachian fold-and-thrust belt evolution was driven by indentation of the Blue Ridge-Inner Piedmont allochthon as it was thrust over the Laurentian margin (Hatcher et al., 2007). Deposition of Pennsylvanian and Permian clastic wedge sediments in the Appalachian foreland basin also records uplift and erosion associated with thrust sheet emplacement during the Alleghanian collision (Secor et al., 1986; Becker et al., 2006).

Consortium for Continental Reflection Profiling (COCORP) and Appalachian Ultra-deep Core Hole (ADCOH) experiments across the crystalline southern Appalachians and Atlantic Coastal Plain indicate that accreted terrains were transported over the continental margin along a low-angle detachment known as the southern Appalachian décollement (Cook et al., 1979; Hatcher et al., 1987; Hubbard et al., 1991; Cook and Vasudevan, 2006). Strong sub-horizontal reflectors can be traced laterally from beneath the Appalachian Valley & Ridge fold-thrust belt southeastward beneath the Blue Ridge and Inner Piedmont to a depth a 10-15 km, but the reflectivity package loses coherency beneath the Carolina terrane and Atlantic Coastal Plain (Iverson and Smithson, 1983). The detachment is interpreted to extend southeastward beneath the Carolina terrane and Coastal Plain (Phinney and Roy-Chowdhury, 1989; Cook and Vasudevan, 2006). The basement rocks beneath the detachment are interpreted as Grenville-age continental crust (Hatcher et al., 2007).

Alternatively, Hibbard et al. (2010) suggest that the detachment terminates beneath the Carolina terrane. They reinterpret northwest dipping reflectors on COCORP line 1 (Cook et al., 1979) as the suture between Grenville basement and the Carolina terrane. Using the same reflection data, Anderson and Moecher (2009) suggest that the Inner Piedmont was underthrust beneath the Laurentian margin during the Taconic orogeny and currently lies beneath the Charlotte belt of the Carolina terrane. However, Cook and Oliver (1981) consider westward dipping subduction in this location unlikely because subduction-related plutonism would have disrupted the continuity of passive margin sediments imaged on COCORP line 1 beneath the Inner Piedmont. This is consistent with the interpretation that Taconic subduction occurred a significant distance (~300 km) from the present Laurentian margin (Tull et al., 2014).

A preserved section of the interpreted Alleghanian collision zone known as the Suwannee suture trends roughly E-W in southern Georgia (Figure 1.1A-B). On COCORP lines crossing the Atlantic Coastal Plain, steeply dipping reflectors coincident with the Brunswick Magnetic Anomaly are interpreted to mark a deep crustal suture zone between Grenville basement and an allochthonous crustal block of Gondwanan origin (McBride and Nelson, 1988). The dipping reflectivity along the suture zone is interpreted to merge with reflectors marking the Appalachian detachment on COCORP line GA-15 (McBride et al., 2005). The suture zone is inferred to be a Late Paleozoic feature that formed during the Alleghanian collision. Hibbard et al. (2010) suggest that the interaction of the Suwannee terrane with the Laurentian margin occurred as early as the Late Devonian.

The Gondwanan Suwannee terrane is a composite of upper-crustal lithotectonic units identified in drill cores across the Coastal Plain southeast of the suture (Chowns and Williams, 1983). It consists of a felsic volcanic unit in southeastern Georgia (Paleozoic or Proterozoic), a thick succession of Ordovician-Silurian-Devonian sedimentary rocks, and a granitic plutonic complex (Osceola granite). The Paleozoic sedimentary and granitic rocks correlate with lithologies in western Africa, indicating a Gondwanan origin (Chowns and Williams, 1983; Dallmeyer et al., 1987). The relatively undeformed nature of sedimentary rocks comprising part of the Suwannee terrane suggests that the Alleghanian event was largely transpressional with a major strike-slip component (Mueller et al., 2014).

Late Alleghanian extension

Extensional tectonics partly obscure the relationship between transpression and convergence associated with the Alleghanian collision, particularly within the rifted hinterland. Late Alleghanian (~274 Ma) extension occurred along fault zones along the eastern margin of the exposed crystalline southern Appalachians (Snoke and Frost, 1990; Maher et al., 1994; Steltenpohl et al., 2013). In the Carolina terrane, exhumation of high-grade rocks along the boundary between the Kiokee belt and greenschist-facies Carolina slate belt indicates significant extensional deformation affected this part of the orogen (Snoke and Frost, 1990). The generation of A-type granites (294-296 Ma), recently identified in drill cores from southernmost Georgia and northern Florida, suggest a derivation during orogenic collapse or transpression, rather than subduction or crustal thickening (Heatherington et al., 2010).

Mesozoic rifting

The Appalachian orogen was rifted in the Mesozoic, leaving a fragment of Gondwana (Suwannee terrane / Florida block) attached to North America. The South Georgia basin is the southern-most rift in a series of onshore Mesozoic basins that formed along the Atlantic margin during Triassic-Jurassic rifting (McBride, 1991; Schlische, 1993). Drilling data across the Coastal Plain show that the South Georgia basin contains Triassic red-beds (Chowns and Williams, 1983). Seismic reflection data in western Georgia indicate the basin is ~6-7 km deep (McBride, 1991). Interpretation of faulting suggests that the basin is bounded to the north by a south-dipping normal fault, but the behavior of the fault at deeper levels in the crust is unknown. It may sole into a mid-crustal, shallow-dipping, sub-horizontal detachment near the brittle-ductile transition or extend deeper into the crust (McBride, 1991). Clendenin (2013) interpreted the eastern compartment of the South Georgia basin in terms of mylonitic core complex formation.

Central Atlantic Magmatic Province

Prior to the opening of the Atlantic Ocean, extensive magmatism associated with the emplacement of the Central Atlantic Magmatic Province occurred at ~201 Ma on four continents (Hames et al., 2000; Callegaro et al., 2013). In North America, the exposed dike swarms extend from Georgia to New England. In the southeastern U.S., most of the mapped dikes within crystalline rocks of the southern Appalachians terminate in the Inner Piedmont near the Brevard zone (King, 1961). Borehole data across the Atlantic Coastal Plain show that a network of dikes and sills intruded buried sedimentary basins; the sills are up to ~120 meters thick in some boreholes (Chowns and Williams, 1983). The influence of a mantle plume on the emplacement of CAMP dikes is debated (McHone, 2000; Beutel, 2009).

Previous Geophysical Investigations

Crustal structure of the southern Appalachians

Inboard of the ocean-continent transition, seismic studies show that the crust gradually thickens from ~35 km beneath the Atlantic Coastal Plain to ~54 km across the Blue Ridge Mountains (Holbrook et al., 1994; Cook and Vasudevan, 2006; Baker and Hawman, 2011; Hawman et al., 2012). A localized crustal root (~54-km crustal thickness) is present beneath the high elevations of the Blue Ridge Mountains in northern Georgia and western North Carolina (Hawman et al., 2012), though relatively thick crust (~50 km) extends to the southwest in northern Georgia and Alabama (French et al., 2009). The thickened crust beneath the crystalline southern Appalachians is also marked by a pronounced Bouguer gravity low (Figure 1.1C). In other parts of western North Carolina, receiver function H-k stacking suggests that the crust is 46 km thick, though a deeper mantle discontinuity at 60-km depth is interpreted to mark the base of a thick eclogitic crustal root (Wagner et al., 2012b). The continental crust is up to ~55-km thick beneath the Cumberland Plateau in Tennessee (Owens et al., 1984; Prodehl et al., 1984).

Wide-angle and receiver function studies provide constraints on average crustal P-wave velocities and Vp/Vs ratios across the region. Average crustal P-wave velocities vary between 6.2 and 6.6 km/s across the crystalline terranes of the southern Appalachians (Hawman et al., 2012). The estimated ranges of average crustal Vp/Vs ratios derived from H-k stacking results from broadband stations MYNC (Blue Ridge) and GOGA (Inner Piedmont) are 1.74-1.78 and 1.72-1.76, respectively (Hawman et al., 2012).

Mantle lithosphere structure

The mantle lithosphere beneath the southeastern United States exhibits vertical stratification and lateral variations in velocity structure. Beneath the Blue Ridge, wide-angle reflectivity is observed at depths of ~59-68 km, and Ps conversions in receiver functions from station MYNC are consistent with a discontinuity at 60-65 km (Baker and Hawman, 2011). Ps conversions from the Appalachian Seismic Transect (AST) in western North Carolina also provide evidence for a discontinuity at ~60-km depth (Wagner et al., 2012b).

Studies of the velocity structure of the uppermost mantle indicate lateral variations in P-wave velocity beneath the region. Mantle p-wave velocities derived from a refraction experiment across the Cumberland Plateau and Valley and Ridge province are 7.9-8.0 km/s (Prodehl et al., 1984). A study using Pn arrivals from regional earthquakes recorded on the SESAME array indicates that mantle Vp is lower beneath the Blue Ridge Mountains (7.6-7.8 km/s) compared with portions of the crystalline southern Appalachians to the southeast (8.3-8.5 km/s) (MacDougall et al., 2015).

The nature of lithospheric thinning across the southeastern United States is also important for evaluating rift models. Sp receiver function analyses indicate that the lithosphere is 85-106 km thick beneath USNSN seismic station GOGA in central Georgia north of the suture (Abt et al., 2010). Shear-wave splitting measurements in the southeastern United States indicate complex anisotropy within the lithospheric mantle (Wagner et al., 2012a).

Figure 1.1. Regional maps of the SESAME array. A. Topography of the study area including offshore bathymetry (Amante and Eakins, 2009). SESAME stations along lines W, E, and D are shown as black dots. Dashed line marks the trend of the Suwannee suture. B. Magnetic anomaly map (Maus et al., 2009; obtained from http://www.geomag.org/models/emag2.html). Contour interval is 100 nT. SESAME stations are shown as white dots. Arrow marks the strong magnetic low associated with the Brunswick magnetic anomaly. C. Bouguer (onshore) and free-air (offshore) gravity map of the study area (obtained from http://www.unavco.org/software/visualization/idv/IDV_datasource_grav.html). Contour interval is 10 mGal. SESAME stations are shown as white dots. Figures were made using Generic Mapping Tools (Wessel et al., 2013).

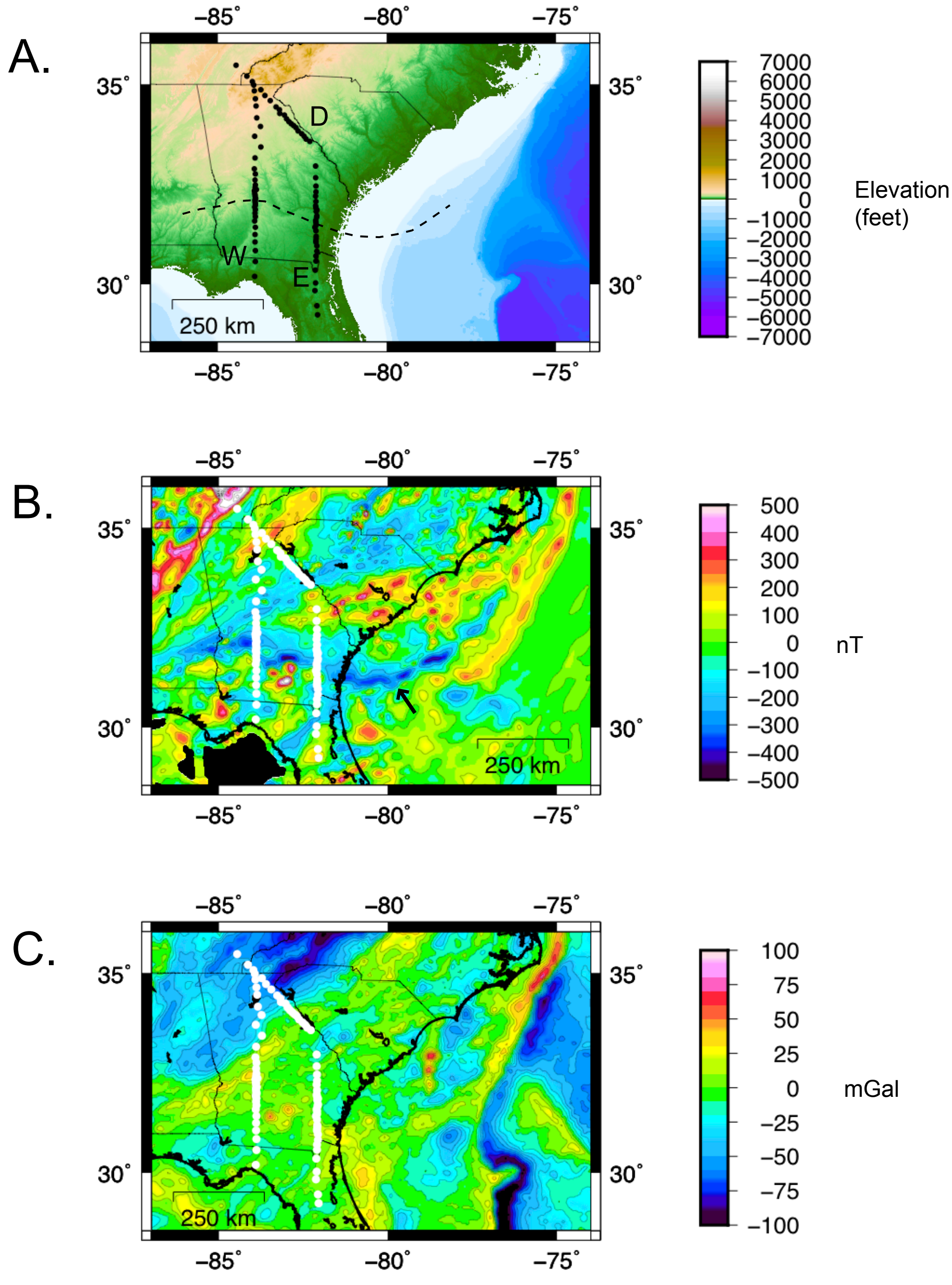
A.
-85˚
-80˚
-75˚
35˚
30˚
D
W
E
250 km
7000
6000
5000
4000
3000
2000
1000
0
−1000
−2000
−3000
−4000
−5000
−6000
−7000
Elevation
(feet)
B.
250 km
500
400
300
200
100
0
−100
−200
−300
−400
−500
nT
C.
250 km
100
75
50
25
0
−25
−50
−75
−100
mGal

CHAPTER 2

CRUSTAL EVOLUTION ACROSS THE SOUTHERN APPALACHIANS: INITIAL RESULTS FROM THE SESAME BROADBAND ARRAY[1]

[1] Parker, E.H., Jr., Hawman, R.B., Fischer, K.M., and Wagner, L.S, 2013, *Geophysical Research Letters*, v. 40, p. 3853-3857.

Reprinted here with permission of the publisher.

ABSTRACT

Receiver functions from the EarthScope SESAME broadband deployment and U.S. Transportable Array were analyzed to constrain average crustal thickness and composition across the southern Appalachians. Low Vp/Vs ratios (1.69-1.72) across the Carolina terrane and parts of the Inner Piedmont indicate the crust has a felsic average composition. The results are consistent with models of thin-skinned thrusting of Carolina arc fragments over Laurentian basement, whereas arc collision models require significant crustal modification to explain the low Vp/Vs. New crustal thickness estimates provide constraints on the extent of the Blue Ridge crustal root. The present root may be a remnant of a broader structure formed by Alleghanian thrust loading. Root preservation is attributed to Mesozoic heating and thinning of lower crust beneath outboard terranes, leaving colder Blue Ridge crust largely intact. However, thickened crust (50-55 km) across the region may also be inherited from continental collision during the Proterozoic Grenville orogeny.

INTRODUCTION

The Southeastern Suture of the Appalachian Margin Experiment (SESAME) is designed to study lithospheric evolution associated with two cycles of continental collision and break-up in the southeastern United States (Figure 2.1). During the Grenville orogeny (1.3-1.0 Ga), arc and continental collision along the eastern margin of North America (present coordinates) resulted in the formation of the supercontinent Rodinia (Hynes and Rivers, 2010). Subsequent opening of the Iapetus ocean in the Late Proterozoic was followed by renewed plate convergence, episodic terrane accretion, and strike-slip tectonics along the North American margin during the Paleozoic (Aleinikoff et al., 1995; Hibbard et al., 2012). Pangea formed during the Permo-Carboniferous Alleghanian orogeny (Hatcher, 2010), while continental break-up occurred in the Triassic-Jurassic (Hames et al., 2000). In this paper, we use Ps receiver functions to evaluate the extent to which Alleghanian thin-skinned tectonics and continental rifting modified Grenville-age lower crust along the Laurentian margin. The implications for crustal evolution, crustal root preservation, and lower crustal petrology are briefly discussed.

Consortium for Continental Reflection Profiling (COCORP) studies indicate that terranes exposed in the southern Appalachians are part of a west-vergent, thin-skinned (3-15 km thick) thrust belt emplaced over the Laurentian margin during the Alleghanian orogeny (Cook and Vasudevan, 2006). The Inner Piedmont, Carolina terrane, and Coastal Plain may be underlain by Grenville basement beneath the detachment (Figure 2.2) (Phinney and Roy-Chowdhury, 1989). Alternatively, the Carolina terrane or Inner Piedmont may have been underthrust beneath the Laurentian margin in the vicinity of the Central Piedmont suture zone prior to Alleghanian collision (e.g. Anderson and Moecher, 2009; Hibbard et al., 2012).

Previous wide-angle reflection and receiver function studies show that crustal thickness increases northwestward from ~35 km beneath the Coastal Plain to 50-56 km across the Blue Ridge Mountains (French et al., 2009; Hawman et al., 2012; Wagner et al., 2012b). The relationship between the root and present topography suggests isostatic balance, but the timing, mechanisms, and original extent of root formation remain uncertain (Hawman et al., 2012). We present two alternative models involving Permo-Triassic and pre-Alleghanian deformation.

DATA AND METHODS

The SESAME array consists of 85 broadband seismometers deployed along three transects in Georgia, Florida, North Carolina, and Tennessee (Figure 2.1). In this paper, we focus on results from SESAME stations within the Carolina terrane, Inner Piedmont, Blue Ridge, and

Valley & Ridge. We also incorporate data from the U.S. Transportable Array to help assess the regional significance of the SESAME results.

For receiver function computation, we employed a frequency domain method to isolate P-to-S conversions within the crust and mantle (Langston, 1979). For stations that exhibited strong Ps conversions and clear crustal multiples (PpPs, PpSs+PsPs), we used the Zhu and Kanamori (2000) grid search method to determine variations in crustal thickness (H) and Vp/Vs (k) across the region. To constrain the results, we used a range of average crustal Vp values (6.2-6.6 km/s) derived from previous wide-angle experiments in the southern Appalachians (Prodehl et al., 1984; Hawman et al., 2012). For stations that did not exhibit clear multiples, we estimated crustal thickness using Ps delay times and an assumed range of average crustal Vp and Vp/Vs values. Uncertainties range from ± 1.0 to ± 5.0 km for crustal thickness and ± 0.01 to ± 0.07 for Vp/Vs (Tables 2.1 and 2.2). Methodology and error analysis are discussed in greater detail in Appendix A.

CRUSTAL STRUCTURE ACROSS THE SOUTHERN APPALACHIANS

Stations D02-D09 within the Carolina terrane exhibit particularly strong Ps conversions and crustal multiples (Figures 2.1 and 2.2). The resulting H-k stacks from these stations provide estimates for crustal thickness of 36-37 km and average crustal Vp/Vs of 1.69-1.72 (Table 2.1). These results are anchored by well-constrained receiver function analyses using a Gaussian value of 5.0 for stations D02, D05, and D08 (Figure 2.3; Table 2.1). Previous wide-angle profiling across the Carolina terrane (Hawman et al., 2012) yielded crustal thickness estimates of 37-39 km and slightly higher Vp/Vs of 1.75 ± 0.01 (see Appendix A for discussion).

The results from the Inner Piedmont show a slight increase in Vp/Vs and a gradual increase in crustal thickness towards the Blue Ridge, in agreement with previous wide-angle results. Stations D15 and D17 yield H-k estimates of 41-43 km and 1.76-1.77 (Figure 2.3). Stations W29 and W31 yield similar crustal thickness estimates (40-42 km), but lower Vp/Vs ratios of 1.72-1.74. For comparison, a well-constrained H-k estimate from station GOGA (near the Inner Piedmont/Carolina terrane boundary) indicates a crustal thickness of 41-43 km and Vp/Vs of 1.72-1.76, and the average Vp/Vs across the Inner Piedmont derived from wide-angle data is 1.73 ± 0.02 (Hawman et al., 2012).

For Inner Piedmont stations with weak multiples, crustal thickness estimates using Ps delay times and an assumed Vp/Vs of 1.76 show a gradual increase in thickness from 36 to 43 km (delay time: 4.5-5.3 s) towards the Blue Ridge (Figure 2.4, Table 2.1). Allowing for a range of 6.2-6.6 km/s for average crustal Vp and 1.73-1.78 for average crustal Vp/Vs resulted in perturbations of 2-3 km in crustal thickness (Table 2.1).

Crustal thickness estimates across the Blue Ridge and Valley & Ridge provinces show considerable variability. Assuming an average crustal Vp of 6.5 km/s based on refraction results and a Vp/Vs of 1.76 based on a well-constrained value for MYNC (Hawman et al., 2012), Ps delay times of 5.5 to 7.1 s in the Blue Ridge correspond with crustal thickness estimates between 45 and 58 km (Figure 2.4; Tables 2.1 and 2.2). The location of maximum crustal thickness (~55 km) appears localized beneath stations D20, W34, W35 and W53A, in agreement with previous wide-angle results (54-56 km) and a receiver function estimate of 50-52 km at MYNC. To the northeast at V53A, crustal thickness decreases to 46 km (5.7 s), which is consistent with estimates of 46 km from the AST array (Wagner et al., 2012b). In the Tennessee Valley and Ridge, estimates of H indicate the Moho shallows to 45-48 km (5.5-6.0 s), but the crust thickens again to 54 km (6.6 s) to the northwest at station V50A along the southeast flank of the Cumberland Plateau. At stations X51A and Y51A, H-k stacks indicate thickened crust (47-50 km; 5.7-6.3 s) persists to the southwest of the Blue Ridge, despite the lower elevations. Estimated crustal thickness from FLED station FA07 (elevation: 178 m) in northern Alabama is also 50 ± 2.6 km (French et al., 2009).

DISCUSSION

The low average crustal Vp/Vs ratios (1.69-1.72) across the Carolina terrane and parts of the Inner Piedmont indicate a felsic average crustal composition (Christensen, 1996). The bulk composition is consistent with average crustal Vp of 6.2-6.6 km/s derived from wide-angle experiments across the region (Hawman et al., 2012). The upper limit for average Vp (6.6 km/s) is similar to the average Vp of 6.5 km/s determined for middle-to-lower crustal felsic rocks from the exhumed Pikwitonei granulite belt in Canada (Fountain and Salisbury, 1996). In the southern Appalachians, the low Vp/Vs ratios and low-to-moderate average Vp values (6.2-6.6 km/s) may be explained by a combination of quartzo-feldspathic gneisses, metasedimentary rocks, and felsic granulites in the lower crust (e.g. Kern and Schenk, 1988). The increase in Vp to ~7.0 km/s in the lowermost crust (Hawman et al., 2012) may be indicative of metasedimentary rocks containing garnet or sillimanite and possibly significant amounts of quartz (Fountain, 1976; van den Berg et al., 2005), rather than mafic granulites or arc rocks.

The felsic average crustal composition across the Carolina arc terrane is consistent with thin-skinned tectonic models for the southern Appalachians, but not with lateral accretion of an intact arc complex in the vicinity of the Central Piedmont suture zone (Hibbard et al., 2012) unless significant modification of the crust occurred during or after collision. The low Vp/Vs values indicate that the crust is more silica-rich than intact arc crust of andesitic-to-mafic composition (Jagoutz and Schmidt, 2012), which implies that volcanic and plutonic arc rocks exposed at the surface are not representative of lithologies at depth. Instead, arc rocks likely accreted farther outboard during the Neo-Acadian (380-355 Ma) were later transported northwestward during Alleghanian thin-skinned thrusting over either North American or Inner Piedmont basement (Anderson and Moecher, 2009). The results are consistent with models that show that the Alleghanian detachment extends southeastward beneath the Carolina terrane and possibly the Coastal Plain (Hatcher et al., 1989).

In the context of thin-skinned tectonics, the incorporation of Carolina arc fragments into the Appalachian orogen represents the process of crustal re-working accompanying continental collision (e.g. Ernst, 2010), rather than continental growth by lateral arc accretion (e.g. Taylor and McLennan, 1995). The felsic composition is consistent with models of crustal recycling involving delamination of dense mafic rocks and relamination of buoyant felsic material at convergent margins (Ernst, 2010; Hacker et al., 2011). In particular, the preservation of large volumes of felsic material may be a result of exhumation of quartzofeldspathic ultra-high pressure domains during continental collision (e.g. Western Gneiss Region of Norway; Hacker et al., 2011). The global implication is that crustal refining during convergence may be an effective means of recycling mafic rocks into the mantle and enriching the crust in felsic components (Ernst, 2010; Hacker et al., 2011). This hypothesis is consistent with the felsic crustal structure in other orogenic domains such as the Variscides (Villaseca et al., 1999) and Irish Caledonides (van den Berg et al., 2005; Hauser et al., 2008).

Receiver function Ps delay times indicate that a crustal root (total crustal thickness: ~55 km) is preserved beneath the high elevations of the Blue Ridge, consistent with local compensation of present topography. The correlation between topography and crustal thickness persists to the northwest, suggesting isostatic balance beneath subdued topography of the Tennessee Valley and Ridge and higher elevations beneath the Cumberland Plateau as well.

Models of local and regional isostatic compensation of the Blue Ridge are generally consistent with gravity profiles and seismic constraints on crustal thickness, but the planar nature of the Appalachian detachment suggests that the middle crust has not been significantly down-warped, as would be expected for both models (Hawman et al., 2012).

We suggest instead that the present root is a remnant of a much broader region of thickened crust developed across the orogen in response to Alleghanian thrust loading. During Mesozoic extension, the combination of thickened crust and heating by mafic intrusions triggered thinning of the lower crust by lateral flow (McKenzie et al., 2000), allowing rebound of the Moho without significant warping of the overlying Alleghanian detachment. Extension and crustal thinning were concentrated beneath outboard terranes, leaving the crust beneath the Blue Ridge largely intact. The lower temperatures suggested by the more rigid response of Blue Ridge crust are consistent with the lack of Triassic dikes northwest of the Inner Piedmont (King, 1961). Alternatively, given the persistence of roots for over one billion years (e.g. Fischer, 2002), the deep structure may be partly related to thickening inherited from Grenville continental collision. In either case, both the Blue Ridge root and thickened crust (~50 km) beneath the lower elevations in west Georgia and northern Alabama may have been preserved by retrograde metamorphic reactions in a cooling lower crust that caused an increase in lower crustal density, inhibiting uplift (Fischer, 2002; French et al., 2009).

CONCLUSIONS

The low average crustal Vp/Vs from SESAME stations across the Carolina terrane and parts of the Inner Piedmont indicates a felsic average crustal composition, which is consistent with Alleghanian thin-skinned tectonics. The bulk composition suggests that crustal refining during continental collision is an effective means of enriching the crust in felsic material and recycling mafic components into the mantle. The low Vp/Vs ratios are incompatible with models of continental growth by island-arc accretion along the Central Piedmont suture zone, unless removal of mafic lower crust and addition of felsic components has also occurred. The formation of the present root beneath the Blue Ridge and adjacent areas is consistent with Alleghanian collision followed by Mesozoic rifting, but the regional structure is also consistent with thickening inherited from Proterozoic Grenville tectonics.

Figure 2.1. Maps of seismic deployments. A: Regional map of the southeastern United States showing the SESAME array (W, E, and D), U.S. Transportable array (TA), and other regional broadband deployments. Dipping seismic reflectors on COCORP profiles and the Brunswick magnetic anomaly mark the Suwannee-Wiggins suture (SWS) between Laurentia and the Suwannee terrane. The Fall Line marks the onlap of Coastal Plain sediments onto exposed crystalline rock of the southern Appalachians. FLED: Florida-to-Edmonton deployment, including station FA07 (French et al., 2009); AST: Appalachian Seismic Transect (Wagner et al., 2012b). USNSN: U.S. National Seismic Network. B: Location of stations analyzed in this study with respect to major terrane boundaries. SESAME station numbers increase from S-to-N and SE-to-NW on the N-trending W-line and NW-trending D-line, respectively. CP: Cumberland Plateau; VR: Valley and Ridge; BR: Blue Ridge; IP: Inner Piedmont; CT: Carolina terrane; ACP: Atlantic Coastal Plain.

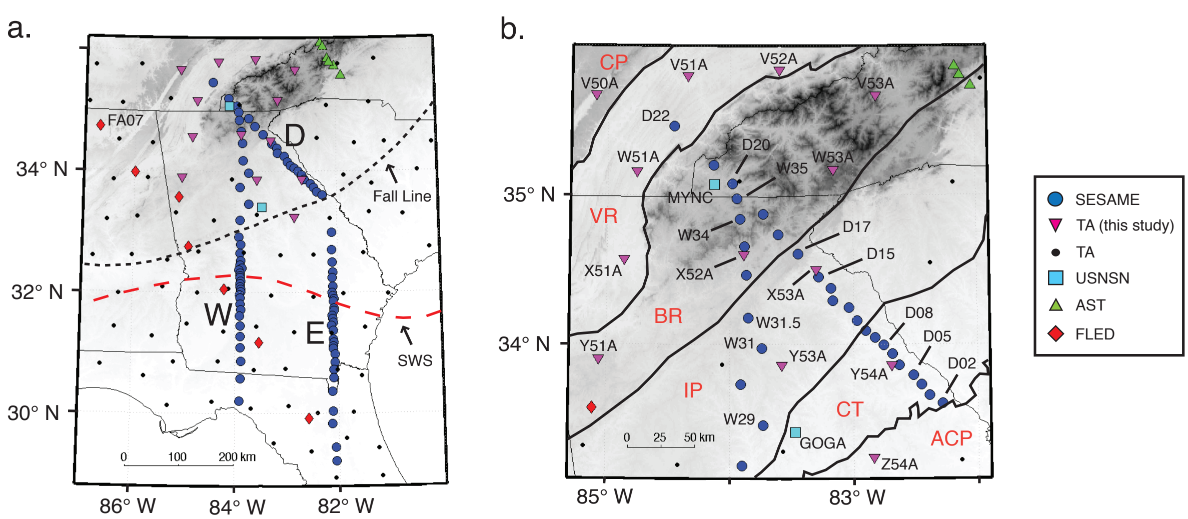

Figure 2.2. Stacked receiver function traces from stations along the D-line. Before stacking, the traces were corrected for moveout to a common ray parameter of 0.06 s/km. The Ps delay time increases from the Carolina terrane to the Blue Ridge province, and then decreases beneath the Valley and Ridge. Crustal multiples (PpPs and PsPs+PpSs) are clearly visible on stations within the Carolina terrane. The depth of the subhorizontal Alleghanian detachment and locations of major thrust faults are based on surface geology and COCORP reflectivity profiles from Cook and Vasudevan (2006). Terrane abbreviations same as Figure 2.1. CPSZ: Central Piedmont suture zone.

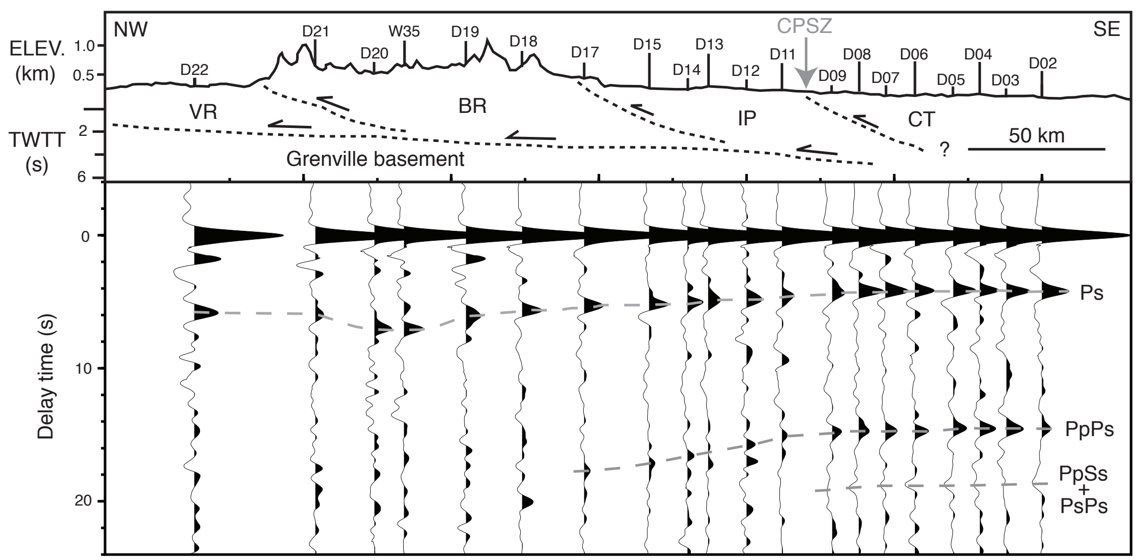

Figure 2.3. H-k stacking analysis. A: Receiver function gather for station D05 showing clear Ps and PpPs conversions (Gaussian value = 5.0). B: H-k stacking results for stations D02, D05, D15, and D17 (Table 2.1).

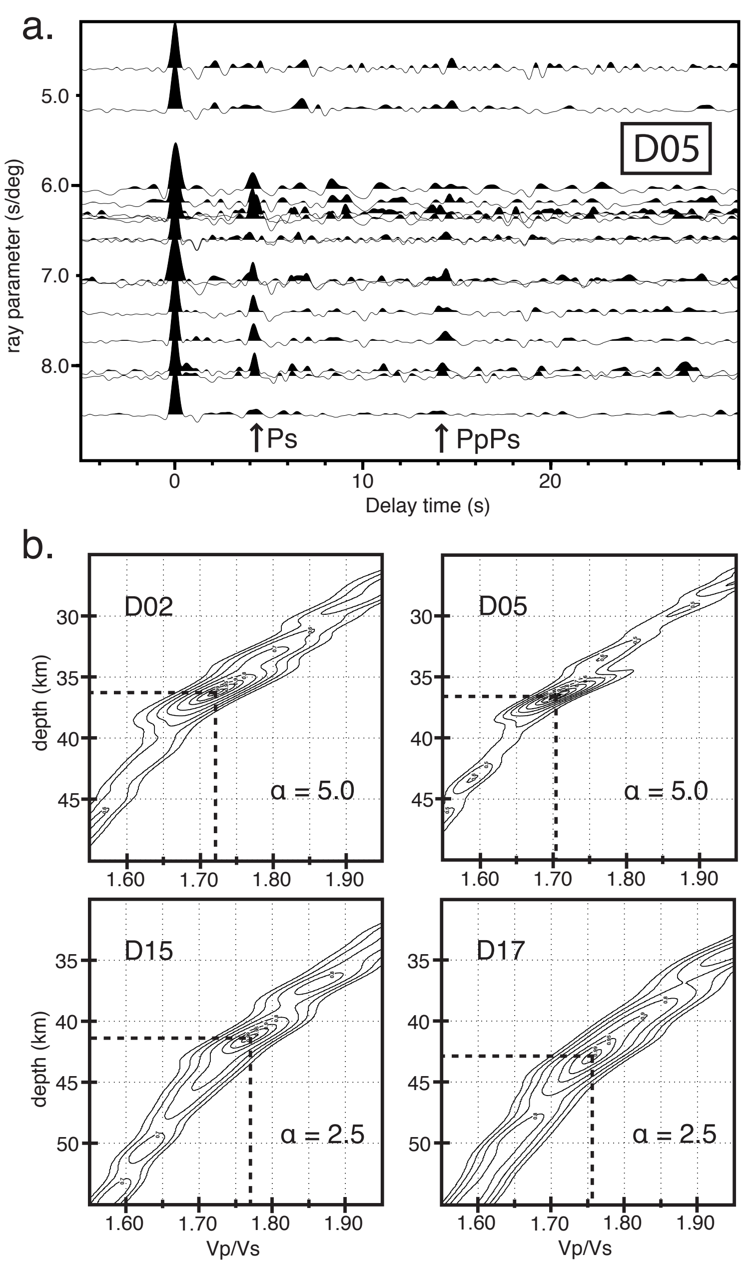

Figure 2.4. Map showing the H-k stacking results and estimated crustal thicknesses using Ps delay times for selected SESAME and TA stations (see Appendix A for details).

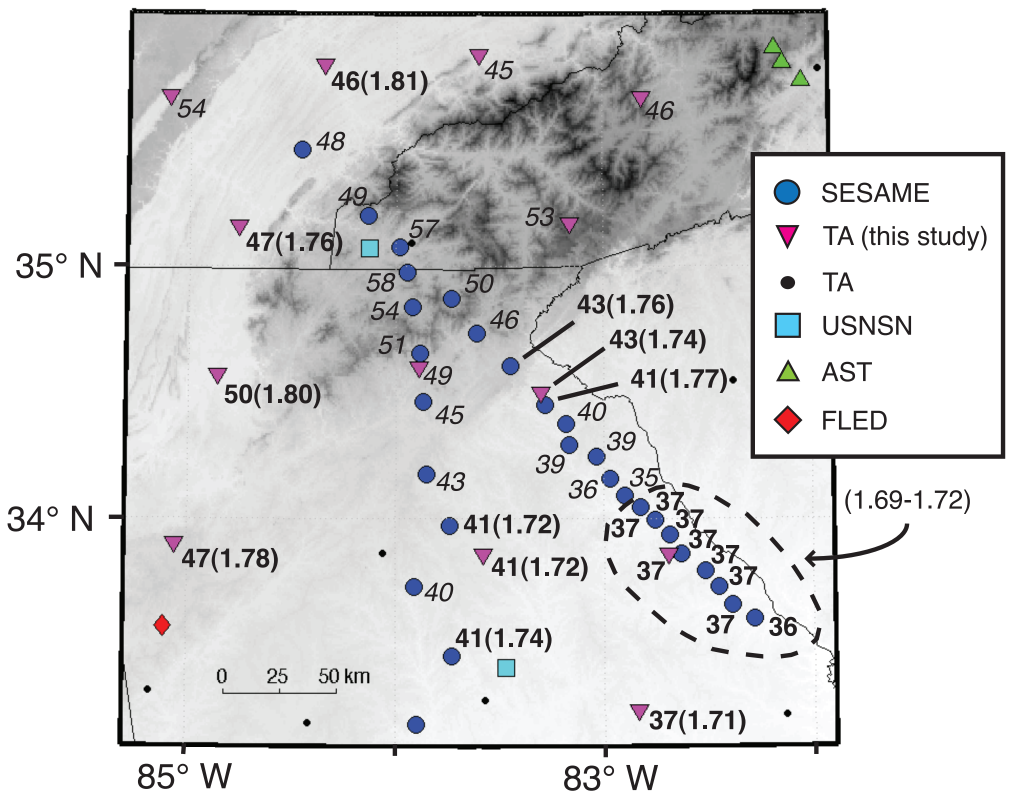

Table 2.1: Crustal thickness and Vp/Vs estimates for selected SESAME stations

Station	Province[1]	Lat/Lon	Elev. (m)	Alpha	Events	w1:w2:w3	H[2]	k[2]	Ps delay (s)
D02	CT	33.60/-82.28	124	5.0	21	0.34:0.33:0.33	36.2 (35.4-37.2)	1.72 (1.71-1.73)	4.2
D03	CT	33.66/-82.39	130	2.5	6	0.34:0.33:0.33	36.6 (34.9-37.4)	1.71 (1.70-1.74)	4.2
D04	CT	33.73/-82.45	128	2.5	6	0.34:0.33:0.33	36.8 (35.0-37.6)	1.70 (1.69-1.73)	4.2
D05	CT	33.79/-82.52	146	5.0	16	0.34:0.33:0.33	36.6 (35.8-37.4)	1.70 (1.69-1.71)	4.1
D06	CT	33.86/-82.63	152	2.5	6	0.34:0.33:0.33	37.1 (36.3-38.1)	1.69 (1.67-1.71)	4.2
D07	CT	33.94/-82.69	140	2.5	6	0.34:0.33:0.33	37.0 (36.2-38.5)	1.70 (1.68-1.71)	4.2
D08	CT	33.99/-82.76	127	5.0	18	0.34:0.33:0.33	37.1 (36.3-38.0)	1.71 (1.69-1.72)	4.3
D09	CT	34.04/-82.83	149	2.5	7	0.34:0.33:0.33	37.2 (36.0-39.1)	1.72 (1.68-1.75)	4.3
D10	CT	34.09/-82.90	186	2.5	2		35 (34-37)*		4.3
D11	IP	34.16/-82.97	216	2.5	19		36 (34-39)*		4.5
D12	IP	34.25/-83.03	247	2.5	4		39 (37-41)*		4.8
D13	IP	34.29/-83.17	200	2.5	18		39 (37-41)*		4.8
D14	IP	34.38/-83.18	211	2.5	17		40 (37-42)*		4.9
D15	IP	34.45/-83.28	254	2.5	18	0.5:0.5:0.0	41.4 (39.0-44.5)	1.77 (1.73-1.80)	5.1
D17	IP	34.60/-83.45	456	2.5	22	0.5:0.3:0.2	42.8 (40.5-44.9)	1.76 (1.74-1.78)	5.3
D18	BR	34.73/-83.61	487	2.5	7		46 (45-49)*		5.7
D19	BR	34.87/-83.73	665	2.5	5		50 (48-53)*		6.1
D20	BR	35.07/-83.98	478	2.5	6		57 (55-60)*		7.0
D21	BR	35.20/-84.14	526	2.5	6		49 (47-52)*		6.0
D22	VR	35.46/-84.46	272	2.5	9		48 (46-51)*		5.9

[1]CT: Carolina terrane; IP: Inner Piedmont; BR: Blue Ridge; VR: Valley & Ridge

[2] H-k uncertainties are based on standard deviations from bootstrapping using a Vp range of 6.2-6.6 km/s for the IP and 6.4-6.6 km/s for the CT, BR, and VR. (*) denotes estimated crustal thickness using Ps delay times. For the CT, BR, and VR, the estimates were determined using an assumed Vp=6.5 km/s and Vp/Vs=1.76, while the uncertainties in parentheses were calculated using Vp=6.4-6.6 and Vp/Vs=1.73-1.78. For the Inner Piedmont, the estimates were determined using Vp=6.4 and Vp/Vs=1.76, while the uncertainties were calculated using Vp=6.2-6.6 and Vp/Vs=1.73-1.78.

Table 2.1 (continued): Crustal thickness and Vp/Vs estimates for selected SESAME stations

Station	Province[1]	Lat/Lon	Elev. (m)	Alpha	Events	w1:w2:w3	H[2]	k[2]	Ps delay (s)
W29	IP	33.46/-83.73	193.4	2.5	16	0.34:0.33:0.33	40.8 (37.3-45.5)	1.74 (1.67-1.79)	5.0
W30	IP	33.73/-83.91	246.3	2.5	16		40 (38-43)*		5.0
W31	IP	33.97/-83.74	292	2.5	13	0.34:0.33:0.33	41.4 (39.3-43.5)	1.72 (1.70-1.74)	4.9
W31.5	IP	34.18/-83.85	334.6	2.5	5		43 (40-46)*		5.3
W32	BR	34.47/-83.87	396.1	2.5	13		45 (43-47)*		5.5
W33	BR	34.65/-83.89	533.4	2.5	19		51 (49-53)*		6.2
W34	BR	34.84/-83.92	649.6	2.5	15		54 (52-57)*		6.6
W35	BR	34.98/-83.94	539	2.5	19		58 (56-61)*		7.1

[1]CT: Carolina terrane; IP: Inner Piedmont; BR: Blue Ridge; VR: Valley & Ridge

[2] H-k uncertainties are based on standard deviations from bootstrapping using a Vp range of 6.2-6.6 km/s for the IP and 6.4-6.6 km/s for the CT, BR, and VR. (*) denotes estimated crustal thickness using Ps delay times. For the CT, BR, and VR, the estimates were determined using an assumed Vp=6.5 km/s and Vp/Vs=1.76, while the uncertainties in parentheses were calculated using Vp=6.4-6.6 and Vp/Vs=1.73-1.78. For the Inner Piedmont, the estimates were determined using Vp=6.4 and Vp/Vs=1.76, while the uncertainties were calculated using Vp=6.2-6.6 and Vp/Vs=1.73-1.78.

Table 2.2: Crustal thickness and Vp/Vs estimates for selected TA stations

Station	Province[1]	Lat/Lon	Elev. (m)	Alpha	Events	w1:w2:w3	H[2]	k[2]	Ps delay (s)
Z54A	ACP	33.24/-82.84	134	2.5	13	0.34:0.33:0.33	36.9 (33.8-40.4)	1.71 (1.66-1.77)	4.2
Y54A	CT	33.86/-82.69	176	2.5	20	0.34:0.33:0.33	36.8 (36.0-37.7)	1.71 (1.69-1.72)	4.2
X53A	IP	34.50/-83.30	240	2.5	15	0.34:0.33:0.33	43.3 (39.8-46.2)	1.74 (1.71-1.78)	5.2
Y53A	IP	33.86/-83.58	234	2.5	14	0.34:0.33:0.33	41.0 (36.4-46.8)	1.72 (1.64-1.78)	4.7
V53A	BR	35.67/-82.81	681	2.5	8		46 (45-49)*		5.7
W53A	BR	35.17/-83.16	1180	2.5	12		53 (51-56)*		6.5
X52A	BR	34.60/-83.89	481	2.5	17		49 (47-52)*		6.0
Y51A	BR	33.90/-85.06	380	2.5	12	0.34:0.33:0.33	47.1 (43.2-51.5)	1.78 (1.70-1.84)	5.7
V51A	VR	35.80/-84.35	243	2.5	17	0.34:0.33:0.33	46.4 (44.8-48.3)	1.81 (1.78-1.84)	6.0
V52A	VR	35.84/-83.60	328	2.5	15		45 (43-47)*		5.5
W51A	VR	35.16/-84.76	260	2.5	12	0.34:0.33:0.33	46.8 (45.6-48.0)	1.76 (1.74-1.78)	5.7
X51A	VR	34.57/-84.86	214	2.5	12	0.34:0.33:0.33	49.8 (46.3-55.0)	1.80 (1.73-1.85)	6.3
V50A	CP	35.67/-85.10	287	2.5	13		54 (52-57)*		6.6

[1] ACP: Atlantic Coastal Plain; CT: Carolina terrane; IP: Inner Piedmont; BR: Blue Ridge; VR: Valley and Ridge; CP: Cumberland Plateau

[2] H-k uncertainties are based on standard deviations from bootstrapping using a Vp range of 6.2-6.6 km/s for the IP and 6.4-6.6 km/s for the ACP, CT, BR, VR, and CP. (*) denotes estimated crustal thickness using Ps delay times. For the ACP, CT, BR, VR, and CP, the estimates were determined using an assumed Vp=6.5 km/s and Vp/Vs=1.76, while the uncertainties in parentheses were calculated using Vp=6.4-6.6 and Vp/Vs=1.73-1.78. For the Inner Piedmont, the estimates were determined using Vp=6.4 and Vp/Vs=1.76, while the uncertainties were calculated using Vp=6.2-6.6 and Vp/Vs=1.73-1.78.

CHAPTER 3

CONSTRAINING LITHOLOGIC VARIABILITY ALONG THE ALLEGHANIAN DETACHMENT IN THE SOUTHERN APPALACHIANS USING PASSIVE-SOURCE SEISMOLOGY[1]

---

[1] Parker, E.H., Jr., Hawman, R.B., Fischer, K.M., and Wagner, L.S, 2015, *Geology*, v. 43, p. 431-434.

Reprinted here with permission of the publisher.

ABSTRACT

Polarities and amplitudes of intracrustal P-SV conversions in receiver functions from the Southeastern Suture of the Appalachian Margin Experiment and U.S. Transportable arrays provide new constraints on the origin of seismic reflectivity delineating the Alleghanian detachment in the southern Appalachians. Forward modeling of receiver functions is consistent with a 3.5-km thick, high shear-wave velocity (Vs = 3.9 km/s) section of deformed Paleozoic platform metasedimentary rocks beneath the Blue Ridge at 3–6.5 km depth. In the Inner Piedmont, conversions from the top and base of a low-Vs zone (3.1 km/s) at depths of 5–9 km are interpreted as a package of metasedimentary rocks or a shear zone characterized by radial anisotropy. The detachment continues to the southeast beneath the Carolina terrane, where high-amplitude negative conversions at 10–13 km depth are consistent with arc rocks (Vs = 4.0 km/s) overlying sheared rocks with lower Vs (3.2 km/s). Southeast-dipping conversions at 5-10 km depth mark the boundary between the Inner Piedmont and Carolina terrane. This study demonstrates that relatively high-frequency receiver functions (up to ~3 Hz), though still lower in frequency than P-wave energy analyzed for reflection profiling (>20 Hz), can provide important links between surface geology and active-source experiments to better constrain models of crustal structure.

INTRODUCTION

During the late Paleozoic Alleghanian orogeny, shortening within the southern Appalachian fold-thrust belt was driven by indentation and translation of the Blue Ridge – Inner Piedmont (BR-IP) allochthon over the Laurentian margin (Hatcher et al., 2007). Consortium for Continental Reflection Profiling (COCORP) and Appalachian Ultradeep Core Hole (ADCOH) seismic reflection profiles show that the Appalachian detachment extends laterally at least 200-

km beneath the BR-IP to depths of 10–15 km beneath the Inner Piedmont (Figure 3.1) (Hubbard et al., 1991). Strong reflectivity in the upper crust is interpreted as a thick section of deformed platform metasediments beneath the BR-IP that correlates with Cambrian-Ordovician carbonates and siliciclastic rocks in Valley and Ridge thrust sheets to the northwest (Hatcher et al., 1987). To the southeast beneath the Carolina terrane, complex reflectivity patterns have been attributed to the continuation of passive-margin rocks (Cook and Vasudevan, 2006) or mylonitic shear zones (Iverson and Smithson, 1983). Improved resolution of velocity structure is needed to refine crustal models inferred from regional geology and reflection profiling.

In this paper, we present constraints on the origin of seismic reflectivity associated with the Alleghanian detachment beneath the southern Appalachians using high-frequency receiver functions derived from earthquakes recorded by the Southeastern Suture of the Appalachian Margin Experiment (SESAME) and U.S. Transportable arrays. We use polarities of P-SV conversions to aid in the interpretation of complex reflectivity observed in COCORP and ADCOH profiles across the BR-IP and peri-Gondwanan Carolina arc terrane. The observations provide new constraints on the composition of buried passive-margin rocks beneath the BR-IP as well as deep structure of the Carolina terrane – IP contact.

REFLECTION PROFILING ACROSS THE SOUTHERN APPALACHIANS

Seismic evidence from COCORP and ADCOH reflection profiles combined with balanced cross sections from the Appalachian fold-thrust belt suggest that the BR-IP allochthon overlies deformed Cambro-Ordovician strata deposited on Grenville basement along the Iapetan passive margin (Hubbard et al., 1991; Hatcher et al., 2007). In ADCOH lines 1 and 3 (Figure 3.1), the base of the BR-IP is marked by strong reflections at depths of 3–6 km (1.0–2.0 s TWT), and layered reflectivity at ~7.5–9 km (2.5–3.0 s TWT) is interpreted to result from metasedimentary strata of the Lower Cambrian Rome Formation overlying Grenville basement (Figure 3.1B). Antiformal structures imaged in ADCOH Line 3 within the intervening section are interpreted as duplexed platform metasedimentary rocks (Hatcher et al., 1987; Costain et al., 1989a). High reflection amplitudes have been attributed to constructive interference generated by fine-scale layering combined with large acoustic impedance contrasts between metamorphosed shales, carbonates, and sandstones (Costain et al., 1989b; Hubbard et al., 1991). Extensive transparent zones have been interpreted as thick sections of massive carbonates (Hatcher et al., 1987). In ADCOH line 1 (Figure 3.1), the Brevard fault zone dips to the southeast and merges into the Blue Ridge master décollement at 6-km depth (Hubbard et al., 1991). Metamorphosed carbonate horses within the fault zone suggest that Alleghanian thrusting along the Rosman fault (a late, brittle fault within the Brevard fault zone) incorporated slices of underlying Paleozoic strata (Edelman et al., 1987). Southeastward, beneath the Carolina terrane, the seismic reflectivity pattern in COCORP line 1 becomes increasingly complex, and the top of the basement is not as clearly imaged.

DATA AND METHODOLOGY

The SESAME broadband array consists of 85 stations across the southeastern United States. In this paper, we focus on stations northwest of the Fall Line (Figure 3.1A). We calculated receiver functions (see Appendix B for details) to identify P-SV conversions generated by large Vs contrasts across intracrustal discontinuities (e.g., Leahy et al., 2012). A major goal of the processing was to recover high frequencies to maximize resolution of structure. High values of 5-7 for α, the Gaussian parameter that controls frequency content, allowed recovery of frequencies as high as 2-3 Hz, in contrast with the 0.1-1.0 Hz range (α = 1-2.5) more commonly used for broadband studies of the crust and uppermost mantle.

Receiver functions can vary significantly with event backazimuth in regions characterized by lateral heterogeneity, dipping structure, or anisotropy. To investigate details of crustal structure, we grouped receiver functions into south (S) and northwest (NW) backazimuths to isolate systematic waveform variations. Initial estimates of interface depths were determined using receiver function P-SV delay times, an assumed Vp of 6.0 km/s, and an upper crustal Vp/Vs ratio of 1.68 derived from regional wide-angle results (Hawman et al., 2012). Forward modeling then was used to constrain the lithologic origin of seismic reflectivity. However, the derived models are nonunique, and receiver functions cannot resolve the level of detail shown by active-source seismic reflection profiles. Our strategy was to find the simplest models that are consistent with receiver function waveforms and with geologic mapping, major transitions imaged by reflection profiling, field estimates of Vp/Vs, and laboratory measurements of seismic wave velocities. Layer velocities represent bulk averages over wavelengths recoverable from the data.

RESULTS

Platform Assemblages beneath the Blue Ridge – Inner Piedmont

At station W33 in the Blue Ridge, an emergent positive arrival (0.4 s) followed by a negative pulse (0.8 s) in receiver functions (α = 5.0) calculated using events from South America is indicative of a high-Vs layer (Figure 3.2A-C). For higher-frequency receiver functions (α = 7.0), the positive arrival is more clearly visible, especially for small offsets (Figure 3.2D). The positive-negative pair is modeled as a metasedimentary sequence at 3-6.5 km depth (Figure 3.3A) with a high Vs of 3.9 km/s representative of laboratory measurements for dolostone and quartzite (Johnston and Christensen, 1992; Christensen, 1996) that likely dominate the thick, seismically transparent zones above basement in the ADCOH profiles (Hatcher et al., 1987).

Velocities for the Blue Ridge (3.3 km/s) and Grenville basement (3.4 km/s) are consistent with the wide range of velocities for quartzofeldspathic gneiss (Vs = 3.0-3.8 km/s) (Meltzer and Christensen, 2001). The Rome Formation is also modeled using a Vs of 3.4 km/s, consistent with laboratory measurements for a mixture of shale and siltstone with lesser amounts of carbonate and quartz sandstone (Johnston and Christensen, 1992). Interfaces in the model are consistent with seismic reflections at depths of 3 and 7.5 km interpreted as the top and base of the Paleozoic shelf sequence in ADCOH line 3 in the Blue Ridge (Hubbard et al., 1991).

The high-Vs layer is also evident in receiver functions from station D19 (Figures 3.4 and B2). Near the Brevard fault zone (stations W31, W31.5, D14, D17, and Y52A), positive conversions at 0.6–0.8 seconds marking an upward decrease in velocity at depths of 5–7 km are consistent with the top-of-the-platform sequence inferred from ADCOH line 1 (Figures 3.4 and B3–4), although, except for Y52A, the base of the layer is not imaged.

Seismic discontinuities beneath the Inner Piedmont and Carolina Terrane

Across the Inner Piedmont, positive conversions marking an upward decrease in Vs at depths of 10.2–13.1 km correlate with the top of Grenville basement imaged on COCORP lines GA-1 and GA-15 (Figures 3.1A, 3.4, and B4-5) (McBride et al., 2005; Cook and Vasudevan, 2006). The switch in dominant polarity of the basement conversions between the Blue Ridge and Inner Piedmont is interpreted to result from low-Vs metasedimentary platform rocks, shearing along the detachment, or a combination thereof (e.g. Johnston and Christensen, 1992; Szymanski and Christensen, 1993). For station Z52A (Figure 3.3B), the surface velocity again is consistent with values for quartzofeldspathic gneiss (Meltzer and Christensen, 2001). The Vs of 3.1 km/s for the low velocity zone (LVZ) at depths of 5-9 km (Figure 3.3B) is consistent with a shear zone formed within either gneiss or metapelitic rocks (Meltzer and Christensen, 2001; Godfrey et al., 2002). In either case, foliation in a roughly horizontal plane would produce radial anisotropy with a vertical symmetry axis, in which the slowest S-wave velocities are for near-vertical raypaths (Godfrey et al., 2002). The base of the IP and top of the Grenville basement are modeled using a higher Vs of 3.7–3.8 km/s representative of values in the high range for quartzofeldspathic gneiss (Meltzer and Christensen, 2001). A positive conversion at 9–10 km corresponding with the basement surface is evident in the stacked receiver functions from the NW backazimuth, and there is a negative conversion at 5–6 km from both backazimuths that we interpret to mark the top of the LVZ (Figures 3.3B and B4). Varying Vs by ±10% results in a change in layer thickness of < 0.5-km for the overthrust packages (Figure 3.3A-B).

Negative conversions at 12–13 km beneath stations D03 and D04 in the Carolina terrane mark a significant upward increase in Vs (Figures 3.4 and B6). In the model for D04 (Figure 3.3C), the average velocity for the Carolina terrane (upper 12 km) is consistent with low upper-crustal Vp/Vs values from wide-angle seismic data. The discontinuity at 12 km is modeled using a velocity contrast of 0.8 km/s representative of Carolina arc rocks (gabbro/amphibolite; Vs = 4.0 km/s) overlying low-Vs metasedimentary rocks (shale/limestone; Vs = 3.1-3.3 km/s) or sheared metasediments/gneisses characterized by radial anisotropy (Vs = 3.2 km/s) (Christensen, 1996; Meltzer and Christensen, 2001; Godfrey et al., 2002). The negative conversion is strong in receiver functions from the NW backazimuth, but it is not well-developed in receiver functions from the S backazimuth (Figure 3.3C). The variation could be caused by azimuthal anisotropy or lateral heterogeneity within the crust; the azimuthal coverage is not adequate to distinguish between the two possibilities. In contrast with the complex reflectivity patterns in COCORP line 1, the low-frequency receiver functions provide strong evidence that either low-Vs passive-margin rocks or a ductile shear zone extends southeastward beneath the Carolina terrane at ~12-

km depth. Shallower conversions (5-10 km) beneath the Carolina terrane (Figures 3.4 and B6-7) likely mark contrasts between imbricated thrust sheets (see Discussion). Moho conversions are discussed in Appendix B.

DISCUSSION

Active-source seismic reflection experiments typically investigate structure within the crust, whereas passive-source broadband studies usually target the Moho and uppermost mantle. The evidence presented here suggests that structure within the upper crust can be detected by extending the generation of receiver functions to higher frequencies. Waveforms from near-offset (epicentral distance: 30-45 degrees) events in South America provide sufficient high-frequency energy (2-3 Hz) to resolve layers as thin as 0.5-1.0 km. Although they clearly do not provide the same level of detail as conventional reflection profiles (in which the minimum resolvable thicknesses are roughly an order of magnitude smaller), higher-frequency receiver functions can yield useful constraints on longer-wavelength components of velocity structure within the upper crust.

Prominent intracrustal P-SV conversions at 0.4–1.5 seconds in receiver functions provide evidence for a regional SE-dipping discontinuity increasing from 3-4 km depth beneath the Appalachian foreland to 12–13 km across the rifted hinterland (Figure 3.4), in agreement with basement contour maps derived from reflection profiling (Hatcher et al., 2007). Forward modeling of P-SV conversions indicates that a 3.5-km thick zone of metamorphosed passive-margin rocks dominated by high-Vs dolostone and quartzite underlies the Blue Ridge near station W33 (Figure 3.4). Given their longer wavelengths, receiver functions are not sensitive to thinner units of interbedded shale/phyllite indicated by exposures in the Valley and Ridge and reflection profiling. Near the Brevard fault zone, shallow conversions (5-7 km) are consistent with the continuation of high-Vs metamorphosed dolostones and sandstones beneath the northwest flank of the Inner Piedmont, as interpreted in ADCOH Line 1 (Figures 3.1 and B3). Repeated sections of the 800-m thick Knox Group dolostone in the Valley and Ridge (Johnston and Christensen, 1992) and the ~640-1175-m thick Chilhowee Group quartzite and ~240-m thick Shady Dolomite exposed in the Grandfather Mountain window (Figure 3.1A; Szymanski and Christensen, 1993) are likely representative of the buried sequence of dominantly high-Vs rocks overlying the Rome Formation and Grenville basement (Costain et al., 1989a). The southeastward decrease in the modeled Vs of rocks along the detachment is consistent with a decrease in dolostone/sandstone and an increase in the volume of low-Vs metapelitic rocks.

Ductile shearing beneath the Inner Piedmont and Carolina terrane inferred from receiver function conversion amplitudes and polarities is consistent with the change in reflective character of the detachment from a well-defined discontinuity beneath the BR-IP to an increasingly complex reflective zone beneath the Carolina terrane (Iverson and Smithson, 1983). In the Inner Piedmont, a low-Vs layer at 5-9 km depth beneath station Z52A is interpreted as either a package of metasedimentary rocks dominated by metamorphosed shale or a ductile shear zone involving higher-grade rocks, both characterized by radial anisotropy. The velocity inversion at depths of 12-13 km beneath stations D03 and D04 in the Carolina terrane is interpreted as the interface between high-Vs rocks at the base of the Carolina terrane allochthon and the top of this shear zone. Well-constrained, low average crustal Vp/Vs ratios previously reported from SESAME stations in the Carolina terrane also support the interpretation that arc rocks overlie relatively felsic Laurentian basement (Parker et al., 2013).

Although sparsely sampled, the dipping zone of negative-polarity conversions observed beneath stations D05, D06, and D07 (Figure 3.4) correlates with a prominent set of reflections imaged in COCORP Line 1 by Iverson and Smithson (1983) and Cook and Vasudevan (2006). One possible model, similar to the interpretation of Cook and Vasudevan (2006), is that the conversions mark the southeast-dipping boundary between more mafic arc rocks at depth within the Carolina terrane allochthon (hanging wall) and more felsic rocks of the Inner Piedmont (footwall). The overall geometry at depth would be similar to the contact between the Inner Piedmont and Blue Ridge along the Brevard fault zone (Hatcher et al., 1987). The Brevard fault zone is not imaged by our receiver function data, perhaps in part because of insufficient contrast in average Vs between the two crustal blocks.

CONCLUSIONS

Polarities of P-SV conversions in receiver functions from the SESAME and U.S. Transportable arrays provide new constraints on the intracrustal velocity structure across the southern Appalachians. In the Blue Ridge, a high-Vs zone at 3–6.5 km depth is consistent with passive-margin metasedimentary rocks (dominantly dolostones and sandstones) underlying the BR-IP allochthon. Conversions at depths of 6–13 km across the Inner Piedmont and Carolina terrane are attributed to either low-Vs passive margin strata (dominantly metamorphosed shales) or a ductile shear zone defining the southeastward continuation of the detachment. Receiver function conversions also delineate a southeast-dipping boundary interpreted as a low-angle fault contact between the Inner Piedmont and Carolina terrane. The results are consistent with models showing that the Appalachian décollement beneath the foreland fold-thrust belt roots into a zone of sub-horizontal shear toward the hinterland of the orogen, forming a tectonic wedge comprised of accreted terranes overlying Laurentian basement.

Figure 3.1. Map of the SESAME array and reproduction of ADCOH line 1. A: Map of the southern Appalachians (eastern USA) showing Southeastern Suture of the Appalachian Margin Experiment (SESAME) array and USArray Transportable array (TA) stations, Consortium for Continental Reflection Profiling lines (GA and TN), Appalachian Ultradeep Core Hole (ADCOH) lines (AD), and terrane boundaries. CP – Cumberland Plateau. V&R – Valley and Ridge. BR – Blue Ridge. IP – Inner Piedmont. CT – Carolina terrane. PMW – Pine Mountain window. GMW – Grandfather Mountain window. B: ADCOH line 1 showing strong reflectivity at 2.5-3.0 seconds two-way travel time (arrow) marking the contact between metasedimentary strata (Rome Formation) and Grenville basement (modified from Hubbard et al., 1991). BFZ – Brevard fault zone.

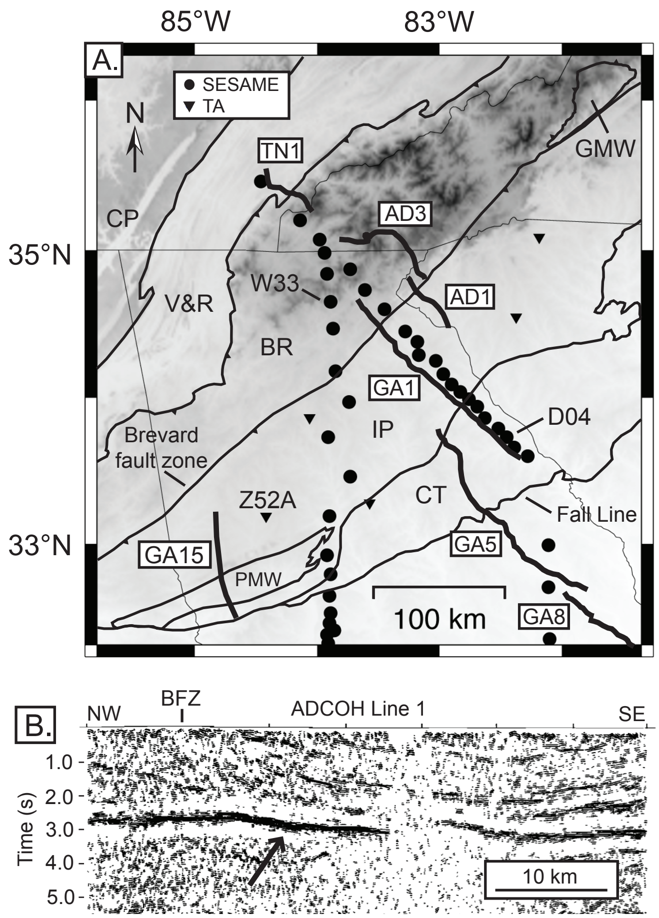

Figure 3.2. P-SV conversions at station W33. A: P-SV conversion (P waves converted to vertically polarized shear waves) polarities associated with higher-to-lower and lower-to-higher Vs contrasts are positive and negative, respectively. B: Distribution of South American earthquakes used in the analysis. C: Receiver functions ($\alpha = 5.0$) for station W33 in the Blue Ridge calculated using events from South America. The negative Ps arrival at 0.8 seconds (gray band) indicates an upward increase in velocity at 6.5 km. For large ray parameters (small event distance), there is an emergent positive phase at 0.4 seconds marking an upward decrease in velocity at 3 km (double arrow). D: Receiver functions calculated for the same events in (C) using a higher Gaussian value of 7.0. The positive-negative pair is sharpened (gray bands) and the positive arrival at 0.4 seconds (3-km) is more clearly resolved at small event offsets (double arrow).

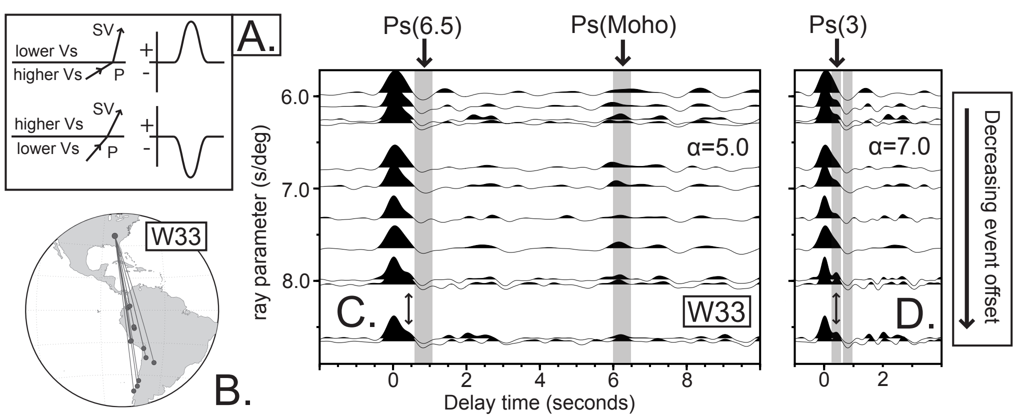

Figure 3.3. Stacked receiver function traces ($\alpha = 7.0$) compared with synthetic seismograms generated for three models of the upper crust (insets). The generalized geologic section and corresponding Vs for each layer are shown beside the velocity models (bold lines). A: Synthetic seismograms for a range of Gaussian values (2.5, 5.0, and 7.0) compared with the stacked trace for station W33 ($\alpha = 7.0$) using events from South America (Figure 3.2D). The positive and negative conversions (gray bands) marking the top and base of a 3.5-km thick, high-Vs layer agree with the positive-negative pair between 0-1 seconds. BR – Blue Ridge. GRN – Grenville basement. RF- Rome Formation. B: For station Z52A in the Inner Piedmont, positive and negative conversions from the southern (S) and northwestern (NW) backazimuths (gray bands) correlate with conversions from the top and base of a low-Vs zone at depths of 5-9 km on the synthetic trace (SYN; $\alpha = 7.0$). The absence of the Moho Ps conversion on the S backazimuth is attributed to interference with unmodeled intracrustal multiples. IP – Inner Piedmont. GRN – Grenville basement. C: For station D04 in the Carolina terrane (CT), a negative conversion on the NW backazimuth (gray band) correlates with the top of a low-Vs zone at 12-km depth on the synthetic trace (SYN; $\alpha = 7.0$).

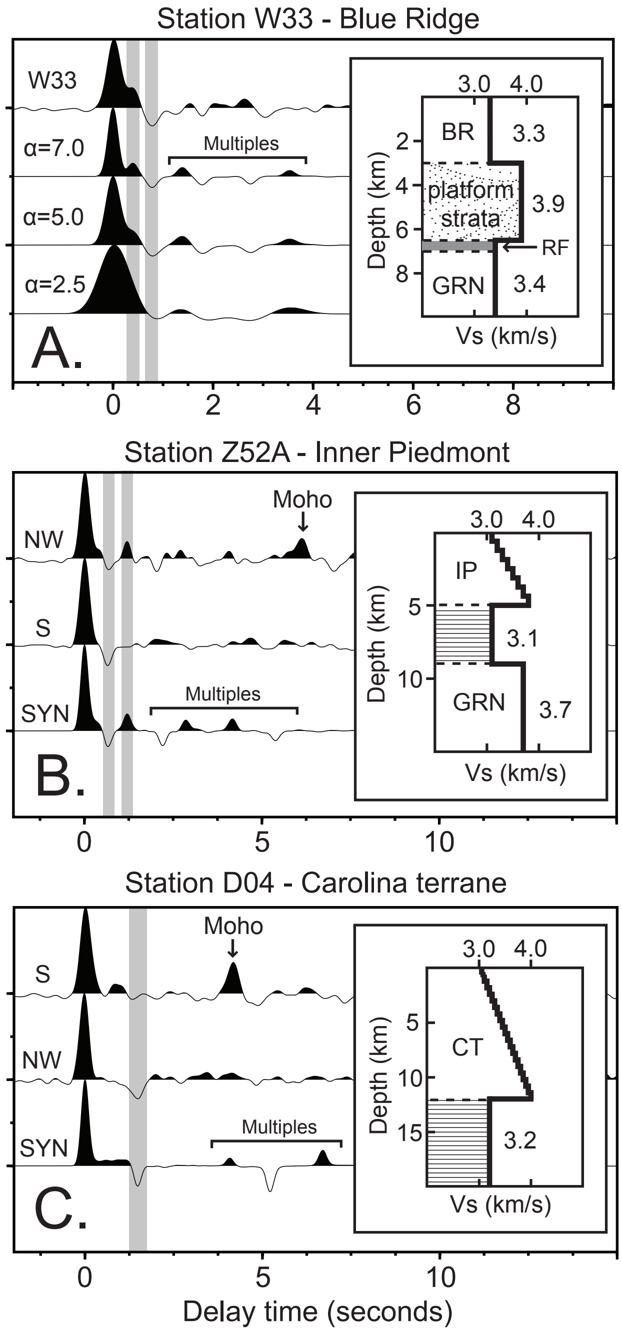
Station W33 - Blue Ridge
W33
α=7.0
α=5.0
α=2.5
Multiples
A.
3.0
4.0
BR
3.3
platform
strata
3.9
RF
GRN
3.4
Depth (km)
Vs (km/s)
Station Z52A - Inner Piedmont
Moho
NW
S
SYN
Multiples
B.
IP
3.1
GRN
3.7
Station D04 - Carolina terrane
Moho
S
NW
SYN
Multiples
C.
CT
3.2
Delay time (seconds)

Figure 3.4. P-SV conversions and interpretive cross-section. A: Station names and estimated depths of intracrustal discontinuities for positive (red) and negative (blue) polarity P-SV conversions (P waves converted to vertically polarized shear waves) from the northwest (NW; italics) and southern (S; bold) backazimuths. Positive polarities indicate an upward decrease in Vs across the discontinuity; negative polarities indicate an upward increase. B: Cross-section for the Appalachian orogen extending across strike from station D22 to D02. Depths of Ps conversions are shown for D-line (northwest-trending SESAME [Southeastern Suture of the Appalachian Margin Experiment] transect) stations as well as off-line regional stations projected onto the profile. Dashed line shows the approximate basement surface from reflection profiling (Cook and Vasudevan, 2006). Moho depths are updated from Parker et al. (2013). V&R – Valley and Ridge. BFZ – Brevard fault zone. CPSZ – Central Piedmont suture zone.

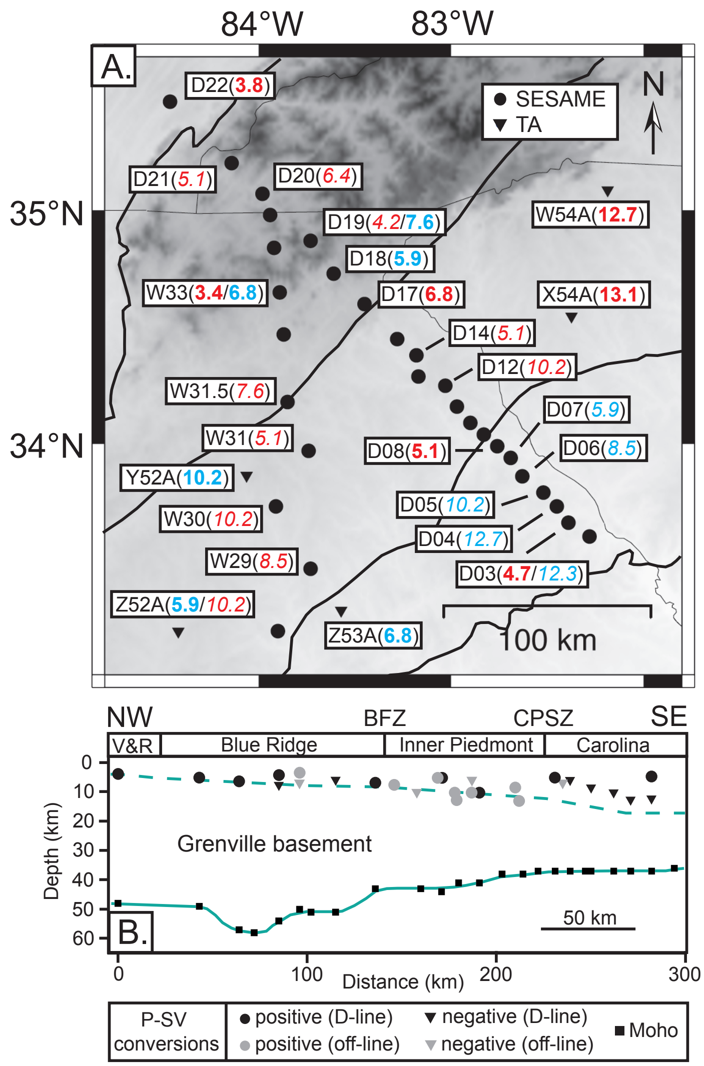
84°W
83°W
A.
D22(3.8)
SESAME
TA
N
D21(5.1)
D20(6.4)
35°N
D19(4.2/7.6)
W54A(12.7)
D18(5.9)
W33(3.4/6.8)
D17(6.8)
X54A(13.1)
D14(5.1)
D12(10.2)
W31.5(7.6)
D07(5.9)
34°N
W31(5.1)
D08(5.1)
D06(8.5)
Y52A(10.2)
D05(10.2)
W30(10.2)
D04(12.7)
W29(8.5)
D03(4.7/12.3)
Z52A(5.9/10.2)
Z53A(6.8)
100 km
NW
BFZ
CPSZ
SE
V&R
Blue Ridge
Inner Piedmont
Carolina
Depth (km)
Grenville basement
50 km
B.
Distance (km)
P-SV conversions
positive (D-line)
positive (off-line)
negative (D-line)
negative (off-line)
Moho

CHAPTER 4

CRUSTAL MAGNETISM, TECTONIC INHERITANCE, AND CONTINENTAL RIFTING IN THE SOUTHEASTERN UNITED STATES[1]

[1] Parker, E.H., Jr., 2014, *GSA Today*, v. 24, p. 4-9.

Reprinted here with permission of the publisher.

ABSTRACT

The Brunswick magnetic anomaly (BMA) in southern Georgia is coincident with seismic reflectivity marking the deep crustal suture between Laurentia and a crustal block of Gondwanan affinity. The source of the BMA remains enigmatic because of its apparent relationship with both the Permo-Carboniferous Alleghanian orogeny (~315-270 Ma) and the emplacement of the Central Atlantic Magmatic Province (~200 Ma). In this paper, the BMA is modeled using relatively weak (< 0.5 A/m) reversed-polarity remanent magnetization in lower crustal rocks (16-24 km depth) outboard of the Laurentian margin. The acquisition of this magnetic signature is consistent with transpression and strike-slip motion along the margin during the initial stage of Alleghanian convergence, which overlaps with the Kiaman Reversed Superchron (~320-263 Ma). Simple magnetic models show that the onshore segment of the BMA can be explained as an effect of continental collision rather than voluminous magmatism along the suture zone. If Central Atlantic Magmatic Province intrusions were not focused along the suture zone, then evidence for tectonic wedging at the crust-mantle boundary associated with Alleghanian convergence may be preserved along the onshore segment of the BMA, rather than over-printed by Mesozoic magmatism.

INTRODUCTION

The Brunswick magnetic anomaly (BMA) coincides with deep seismic reflectivity marking the Late Paleozoic Suwannee-Wiggins suture zone (SWS) between Laurentia and a crustal block of Gondwanan origin (McBride et al., 2005). In southern Georgia, prominent, south-dipping reflectors on Consortium for Continental Reflection Profiling (COCORP) lines crossing the BMA define the lower crustal suture (Figures 4.1 and 4.2) (McBride and Nelson, 1988). The reflectivity is interpreted as a mylonitic zone between Grenville-age North American basement and a Gondwanan crustal block accreted during the Permo-Carboniferous Alleghanian orogeny (Thomas, 2010). Drilling data across the Atlantic Coastal Plain show that the BMA is roughly coincident with the boundary between accreted peri-Gondwanan terranes and the Gondwanan Suwannee terrane (Chowns and Williams, 1983; Dallmeyer et al., 1987). However, rocks related to the Suwannee terrane are found north of the BMA (Tauvers and Muehlberger, 1987), suggesting the magnetic anomaly is more closely associated with the deep crustal suture than the upper-crustal terrane boundary.

Mesozoic rifting and emplacement of the Central Atlantic Magmatic Province (CAMP) overprint Alleghanian structure across the southeastern United States. The Triassic-Jurassic South Georgia basin cuts across the BMA (McBride, 1991), and rift basin formation was followed by extensive magmatism across the southeastern United States prior to Atlantic sea-floor spreading (McBride et al., 1989). Approximately 1-2 km of Atlantic Coastal Plain sediments now cover the basin and suture zone, and it is unknown whether the origin of the BMA is ultimately related to continental collision or rift-related mafic intrusions concentrated along the suture (Figure 4.2). Lower crustal seismic reflectors coincident with the magnetic low in southern Georgia (McBride and Nelson, 1988), offshore South Carolina (Austin et al., 1990), and offshore Virginia (Sheridan et al., 1993) suggest the source of the anomaly is related to continental collision (Figure 4.1). On the other hand, the BMA appears to merge with the East Coast magnetic anomaly (ECMA), a prominent magnetic high interpreted to result from rift-related mafic underplating and magmatism along the ocean-continent transition (Figure 4.1) (Holbrook et al., 1994). Discontinuous magnetic highs south of the BMA, extension across the South Georgia basin, and flood basalts/sills within rift basin strata suggest the BMA may represent a continuation of the ECMA (McBride and Nelson, 1988; McBride et al., 1989).

Distinguishing between these alternatives is important for understanding the role of inherited structure during continental rifting and emplacement of CAMP intrusions in the southeastern United States.

In this paper, the BMA is modeled using reversed-polarity remanent magnetization in lower crustal rocks (16-24 km depth) along the SWS and outboard of the Laurentian margin. Strong remanent magnetization (> 3.0 A/m) of exhumed granulites in other collision zones (e.g. Australia, Adirondacks, Sweden) suggests that remanence may be the source of long-wavelength magnetic anomalies in the deep crust (McEnroe et al., 2004, and references therein). The reversed-polarity remanent magnetization of Gondwanan basement blocks may have been acquired during the Kiaman Reversed Superchron (c. 320-263 Ma), the longest reversed polarity event in Earth history (Garcia et al., 2006). New magnetic models assuming relatively weak remanence (< 0.5 A/m) provide a simple explanation for the long-wavelength character of the BMA and the coincidence with seismic reflectors along its entire length.

ALLEGHANIAN OROGENY

The Permo-Carboniferous Alleghanian orogeny in the southern Appalachians involved transpression and dextral strike-slip motion along the North American margin followed by terrane transport over Grenville-age continental crust along the Blue Ridge-Piedmont megathrust (Hatcher, 2010). Sub-horizontal reflections on COCORP profiles crossing the orogenic belt suggest a major detachment underlies the Blue Ridge and Inner Piedmont and possibly extends eastward beneath the Atlantic Coastal Plain (Figure 4.2) (Cook and Vasudevan, 2006). In southern Georgia, the detachment is interpreted to merge with seismic reflectors marking the Suwannee-Wiggins suture (McBride et al., 2005; Steltenpohl et al., 2008), but it may also cross over the suture and merge with a proposed Alleghanian suture marked by the Gulf Coast-East

Coast magnetic anomalies (Hall, 1990). Alternatively, the detachment may terminate near the Central Piedmont suture zone, and the peri-Gondwanan Carolina terrane may underlie much of the Atlantic Coastal Plain in the southeastern United States (Figure 4.2) (Hibbard et al., 2010).

In southern Georgia, the deep crustal suture is interpreted to separate Grenville-age Laurentian crust from Gondwanan basement (McBride et al., 2005). The collision of the crustal block underlying the Suwannee terrane is generally considered a Permo-Carboniferous event, though accretion may have occurred during the Late Devonian (Hibbard et al., 2010).

MESOZOIC CONTINENTAL RIFTING

The Atlantic and Gulf of Mexico rifts developed outboard of the Suwannee-Wiggins suture during the Mesozoic, leaving Gondwanan lower crust and the Suwannee terrane attached to North America. Alleghanian faults and post-orogenic collapse structures were reactivated during Mesozoic extension (Steltenpohl et al., 2013), and the Suwannee terrane was possibly down-dropped from higher crustal levels (Steltenpohl et al., 2008). The Triassic-Jurassic South Georgia basin formed along the boundary between accreted peri-Gondwanan terranes and the Suwannee terrane (McBride et al., 1989; McBride, 1991). Beneath the Coastal Plain, the basin separates the Suwannee terrane from the buried Brunswick-Charleston terrane for most of the length of the BMA (Hatcher, 2010).

Drilling data show that an extensive network of mafic dikes and sills is present beneath the Atlantic Coastal Plain (Chowns and Williams, 1983). Geochronological constraints indicate that the magmatism is closely related to the emplacement of the Central Atlantic Magmatic Province at ~200 Ma (Heatherington and Mueller, 2003). The J-reflector on regional seismic reflection profiles across the basin and offshore South Carolina was initially interpreted as an extensive sub-surface basalt flow or diabase sill beneath the Coastal Plain (shaded area; Figure

4.2) (McBride et al., 1989). However, Heffner et al. (2012) recently interpreted the J-reflector as simply the base of the Coastal Plain based on re-analysis of well data and seismic reflection profiles. In general, the relationship between dike and sill complexes emplaced within the South Georgia rift strata and lower crustal intrusion and under-plating along the suture remains uncertain.

CRUSTAL STRUCTURE ACROSS THE BMA AND ECMA

In the eastern United States, the transition from largely unmodified crust beneath the Coastal Plain to highly stretched, transitional crust across the continental margin occurs over a distance of ~75-km (Lizarralde and Holbrook, 1997). On EDGE line 801 (Figure 4.1), crustal thickness decreases from 35 to 15-km across the ECMA (Sheridan et al., 1993). On lines USGS 32 and BA-6 across the Carolina trough (Figure 4.1), elevated velocities (6.5-7.5 km/s) indicative of mafic underplating are largely restricted to thinned crust along the ECMA, while 35-km thick continental crust inboard of the ECMA with Vp of 6.4-6.8 km/s appears unmodified by rift magmatism (Tréhu et al., 1989; Holbrook et al., 1994). In general, crustal thinning and underplating appear to be highly focused along the ocean-continent transition (Lizarralde and Holbrook, 1997).

As the BMA diverges from the ECMA, evidence for crustal thinning and magmatic underplating becomes limited. A velocity model for Line BA-3 (Figure 4.1), which crosses the BMA offshore, indicates that crustal thickness is ~35-40 km across the entire profile (Lizarralde et al., 1994). Middle and lower crustal velocities are 6.4-6.75 km/s, and there is a thin, poorly resolved 7.2 km/s layer at the base of the crust. On the eastern and western COCORP transects crossing the onshore segment of the BMA (Figures 4.1 and 4.2), discontinuous Moho reflectors indicate uniform crustal thickness of 33-36 km with little relief at the crust-mantle boundary

(McBride and Nelson, 1988). Truncation of dipping reflectors marking the SWS suggests the Moho formed as a result of Mesozoic extension (McBride and Nelson, 1988), though this interpretation is not unique.

PREVIOUS MAGNETIC MODELS

McBride and Nelson (1988) modeled the source of the onshore segment of the BMA as a tabular mafic intrusive complex outboard of the suture zone beneath the South Georgia basin. They make two important assumptions: 1) induced magnetization of high susceptibility mafic rocks dominates the magnetic signature; 2) the discontinuous magnetic highs that flank the south side of the BMA are paired with the continuous magnetic low (Figure 4.1). In their model, the high-low pair is generated by a south-dipping block outboard of the suture. As the trend of the BMA changes from E-W to N-S off the Georgia coast, the disappearance of the magnetic low is related to the azimuthal dependence of the anomaly. The major implication of this model is that the ECMA and BMA have a common source related to mafic magmatism.

REMANENT MAGNETIZATION OF LOWER CRUSTAL ROCKS

Remanent magnetization of lower crustal granulites is a possible source of long-wavelength magnetic anomalies originating in the deep crust (McEnroe et al., 2004), and the common assumption of induced magnetization of magnetite-bearing rocks for analysis of crustal-scale anomalies may not be completely justified (McEnroe et al., 2001). Rock magnetism and petrologic studies show that magnetite-bearing rocks can retain a strong remanent component over long periods of geologic time (Kelso et al., 1993; McEnroe and Brown, 2000). In the Arunta Block of Australia, felsic-to-mafic granulites possess a median remanent magnetization of 4.1 A/m, compared with induced magnetization of <1.0 A/m (Kelso et al., 1993).

The recognition of strong magnetism associated with the hematite-ilmenite solid solution series is also an important consideration in crustal magnetism studies (Robinson et al., 2002). Magnetization of hematite-ilmenite exsolution microstructures is thermally stable (demagnetization occurs between 530-650 ˚C) and resistant to alternating field demagnetization (McEnroe et al., 2004). These properties suggest that magnetite (Curie temperature = 580 ˚C) is not the only important magnetic phase at lower crustal depths (McEnroe et al., 2004). Exhumed granulites in Sweden containing hematite-ilmenite exsolution lamellae and minor magnetite are characterized by strong remanent magnetization of ~9.2 A/m (McEnroe et al., 2001).

NEW MAGNETIC MODELS

The magnetic models presented here are based on thin-skinned tectonic models of the southern Appalachians (Cook and Vasudevan, 2006) and the interpretation that deep crustal reflectivity marks the suture between Grenville-age Laurentian basement and Gondwanan lower crust (McBride et al., 2005). The BMA is modeled as the juxtaposition of lower crustal blocks with differing magnetic character (e.g. Daniels et al., 1983). Gondwanan crustal blocks may have acquired a localized remanent magnetic signature during Alleghanian transpression focused in deep crustal levels outboard of the Laurentian margin. Inboard of the suture, the thin-skinned nature of the orogen suggests that Grenville lower crust behaved as a stable block and escaped pervasive lower crustal metamorphism. The presence of Alleghanian granitoids north of the suture (Heatherington et al., 2010) is attributed to westward over-thrusting of rocks onto the Laurentian margin during the final stages of continental collision (e.g. Hatcher, 2010), rather than heating and metamorphism of Grenville lower crust by ductile thickening.

The primary goal of this study is to model the continuous long-wavelength magnetic low. Although the anomaly is often considered a high-low pair, there is no direct evidence indicating that the onshore flanking highs are related to the long-wavelength magnetic low. Because the overall magnetic character of the Suwannee terrane can be characterized by random magnetic highs (Figure 4.1), these discontinuous anomalies are interpreted as separate features. No attempt has been made to model the short-wavelength features because of the variability of the flanking magnetic signature along strike.

In the model for profile A (Figures 4.2 and 4.3A), Laurentian and Gondwanan lower crust possess the same magnetic susceptibility (k=0.01) typical of granulite-facies assemblages (Kelso et al., 1993), but the lower crust outboard of the Laurentian margin is modeled with relatively weak remanence of 0.47 A/m oriented towards the south (opposite the present magnetic field). The assumed horizontal inclination of the remanent vector is supported by paleomagnetic reconstructions that show the southern margin of North America at equatorial latitudes during the formation of Pangea (Van der Voo and Torsvik, 2001). The position of the SWS is based on seismic reflectivity on COCORP lines 13 and 14 (Figure 4.2). In the model, the lower crustal blocks extend from 16 to 24 km depth. Assuming a relatively low geothermal gradient of 22 ˚C/km (e.g. Arthur, 1982), the depth to the 550 ˚C isotherm is ~25 km. Above this depth, remanent magnetization of rocks containing magnetite and/or hematite-ilmenite will be stable (McEnroe et al., 2004). The slightly different magnetic signature between the two blocks produces the prominent magnetic low coincident with suture zone reflectivity on the western COCORP transect. The magnetic high is interpreted as a separate feature of unknown origin.

The contrast between profile A and B is intended to show that the flanking magnetic highs are localized, while the long-wavelength magnetic low is a continuous anomaly. In Figure 4.3-B, the Gondwanan basement is modeled with a remanence of 0.44 A/m. Again, the position of the suture zone is based on seismic reflectivity on COCORP lines 13, 14, and 19 (Figure 4.2).

The long-wavelength magnetic low (~300 nT) generated by the two blocks closely matches the observed profile.

The BMA along profile C in southeastern Georgia is relatively broad (80-km wide) and lower in amplitude (~200 nT) compared with profiles A and B (Figure 4.3-C). A slight contrast of 0.15 A/m between two blocks outboard of the margin accounts for the broad anomaly on this profile. In the model, the edge of the Laurentian margin is roughly coincident with dipping reflectivity imaged on line 16a of the eastern COCORP transect (Figure 4.2).

DISCUSSION

The long-wavelength aeromagnetic low associated with the BMA can be modeled using contrasts in remanent magnetization between Laurentian basement and Gondwanan crustal blocks underlying the Suwannee terrane. The magnetic models are consistent with tectonic models for the southern Appalachians involving transpression along the continental margin followed by foreland-directed thrusting of terranes over Grenville basement along a major detachment fault (Figure 4.4-A). The presence of African rocks north of the Brunswick magnetic anomaly is interpreted to result from thin-skinned thrusting of the Suwannee terrane across the trace of the deep crustal suture in the final stage of the Alleghanian orogeny (Figure 4.4-A) (e.g. Hall, 1990).

The models require that Mesozoic extension and magmatism did not overprint the magnetic signature inherited from convergence. The development of the South Georgia rift basin in the upper crust without extensive lower crustal modification along the suture is consistent with simple shear extension along the Atlantic margin (Figure 4.4-B) (Lister et al., 1991). In this model, focused magmatism is laterally offset towards the main Atlantic rift and basin formation in the upper crust is accommodated by extension above a mid-crustal detachment. Lower crustal stretching is interpreted to be minimal.

If the suture zone beneath the South Georgia basin was not completely overprinted by extension and magmatism, then structure related to Alleghanian transpression and collision may be preserved along the inboard section of the suture. The truncation of crustal-scale dipping reflectors by relatively flat Moho reflectors on COCORP line 13 may be indicative of under-thrusting of crustal material beneath the Laurentian margin during collision (Figures 4.2 and 4.4). Though speculative, the sub-Moho reflector on Line 14 (Figure 4.2) may be related to tectonic wedging or transpression along the suture. This feature appears similar to Moho structure imaged on high-resolution seismic reflection profiles from the ALCUDIA transect in Spain (Martínez Poyatos et al., 2012). The preservation of convergent structures would provide insight into the nature of continental collision during the accretion of Gondwanan basement.

CONCLUSIONS

The new magnetic models presented here suggest that the source of the BMA resides in lower crustal metamorphic rocks outboard of the Laurentian margin. The acquisition of reversed-polarity remanent magnetization along the suture and within Gondwanan lower crustal blocks is consistent with transpression along the North American margin during the Kiaman Superchron. The preservation of this signature at depths of 16-24 km is consistent with simple shear extension involving limited lower crustal stretching and a lack of focused magmatism beneath the South Georgia basin.

The main implications of the magnetic modeling are as follows: 1) relatively weak reversed-polarity remanence (0.21-0.47 A/m) in lower crustal rocks outboard of the Laurentian margin provides a simple explanation for the BMA; 2) CAMP intrusions in the lower crust were not highly concentrated along the Suwannee-Wiggins suture zone; 3) evidence for Alleghanian convergent structure at the crust-mantle boundary or within the mantle lithosphere may be preserved along the suture, rather than overprinted by Mesozoic extension.

The analysis provides an alternative to rift-related models assuming induced magnetization of mafic intrusions concentrated along the Suwannee-Wiggins suture zone. Additional geophysical constraints on crustal structure from the EarthScope SESAME broadband array (Fischer et al., 2012) and the SUGAR active-source seismic experiment (Shillington et al., 2013) targeting the suture and CAMP will help differentiate between tectonic models. Integration of seismic data with new perspectives on crustal magnetism will provide a better understanding of terrane accretion, rifting processes, and passive margin formation in the southeastern United States.

Figure 4.1. Aeromagnetic map (red = high; blue = low) of the eastern margin of North America showing the approximate locations of existing seismic profiles crossing the Brunswick magnetic anomaly (BMA) and East Coast magnetic anomaly (ECMA). Seismic profiles from EDGE 801, USGS 32, and BA-6 indicate relatively abrupt crustal thinning from ~35-km to ~15-km across the ECMA. Inboard of the ocean-continent transition, crustal thickness estimates range from 35-40 km on line BA-3 and 33-36 km for both COCORP transects. Strong dipping reflectivity marking the Suwannee-Wiggins suture (SWS) is evident on EDGE 801, BA-6, and both COCORP transects. The dipping reflectivity and change in crustal structure as the BMA diverges from the ECMA suggest the magnetic low is related to continental collision. BSFZ: Blake Spur fracture zone. (Map modified from Tréhu et al., 1989; Austin et al., 1990; Sheridan et al., 1993; Lizarralde et al., 1994; North American Magnetic Anomaly Group, 2002; Bartholomew and Hatcher, 2010).

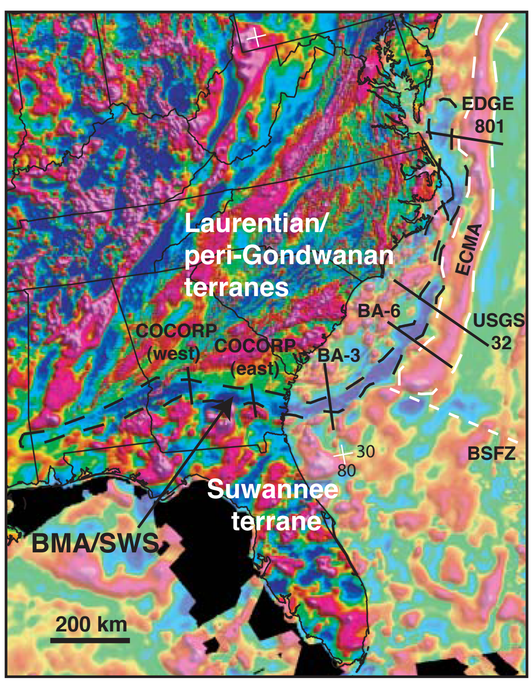

Figure 4.2. Map showing magnetic profiles and reproduction of COCORP lines 11-15. Top: Regional map showing the locations of magnetic profiles (A-C) with respect to selected COCORP profiles. The red circle on each profile marks the location of the magnetic minimum within the BMA (dashed line). Dipping seismic reflectors are evident on lines 13, 14, 16a, and 19. The Fall Line marks the onlap of Atlantic Coastal Plain (ACP) sediments onto the exposed terranes of the southern Appalachians. The shaded area defines the inferred extent of mafic magmatism across the South Georgia basin and offshore South Carolina. CT: Carolina terrane; IP: Inner Piedmont; BR: Blue Ridge; VR: Valley and Ridge. (Map modified from Dallmeyer, 1988; McBride et al., 1989; Lizarralde et al., 1994). Bottom: Seismic section for COCORP lines 11-15 showing strong dipping reflectivity coincident with the BMA (after McBride and Nelson, 1988).

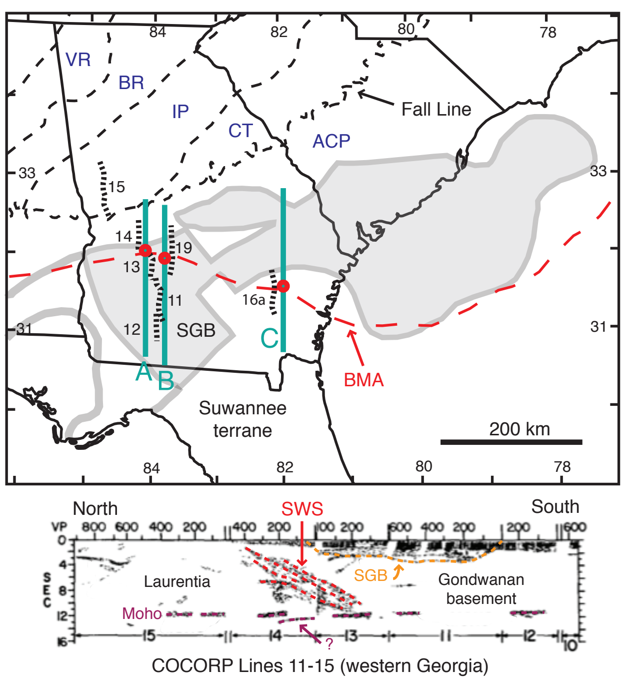

Figure 4.3. Observed total magnetic intensity (dots) and magnetic models (solid line) for profiles A-C. Magnetic profiles were obtained from Zietz et al. (1980) and then shifted to the datum of Daniels (2001). The present field is modeled using a magnetic declination of 0˚, inclination of -63˚, and total field intensity of 52,500 nT based on 1977 values when the surveys were flown. The continuous magnetic low is modeled using remanent magnetization oriented toward the south (arrow). All lower crustal blocks are modeled with a susceptibility of k=0.01 SI. The position of the Suwannee-Wiggins suture (SWS) is based on COCORP seismic reflectivity. A: Model for profile A showing general agreement with the magnetic low. The flanking magnetic high to the south is interpreted as a separate anomaly. B: Model for profile B showing close agreement with the long-wavelength signature of the magnetic low. C: Model for profile C using two crustal blocks with slightly different remanent magnetizations.

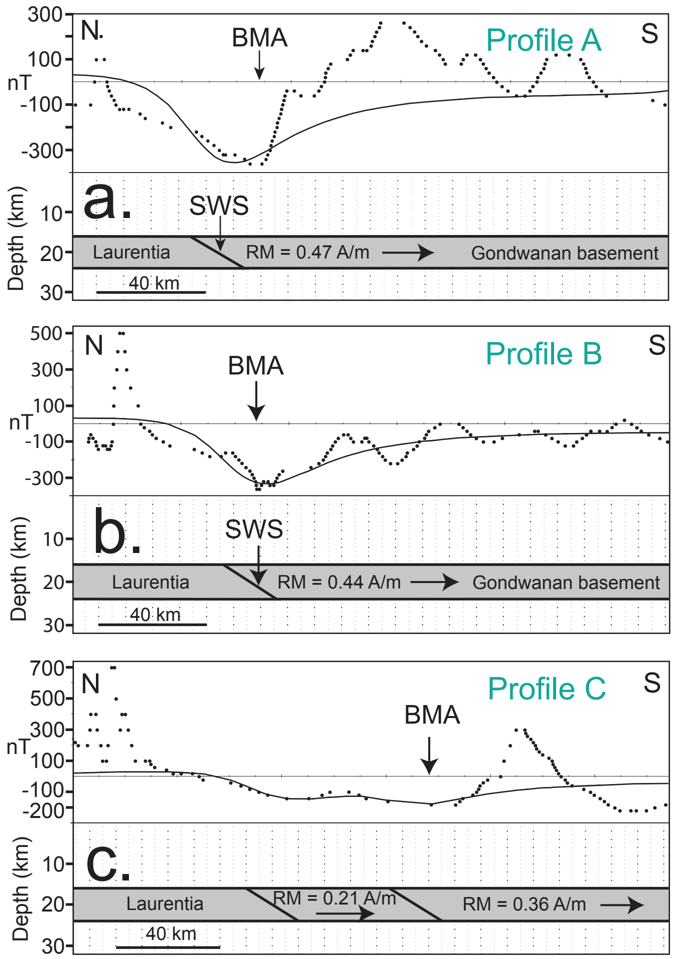

Profile A
N.
S
BMA
SWS
a.
Laurentia
RM = 0.47 A/m
Gondwanan basement
40 km
Depth (km)
nT
300
100
-100
-300
10
20
30
Profile B
N
S
BMA
SWS
b.
Laurentia
RM = 0.44 A/m
Gondwanan basement
40 km
500
300
100
-100
-300
Profile C
N
S
BMA
c.
Laurentia
RM = 0.21 A/m
RM = 0.36 A/m
40 km
700
500
300
100
-100
-200

Figure 4.4. Conceptual tectonic model for the southeastern United States. A) Strike-slip motion along the deep crustal suture followed by the initiation of Alleghanian thin-skinned thrusting on the eastern flank of accreted Gondwanan basement. B) Simple shear extension along the Atlantic margin controlled by reactivation of thin-skinned structures (after Lister et al., 1991). Localized ductile thinning along the margin suggests that complex structure (tectonic wedging) may be preserved along the Suwannee-Wiggins suture zone.

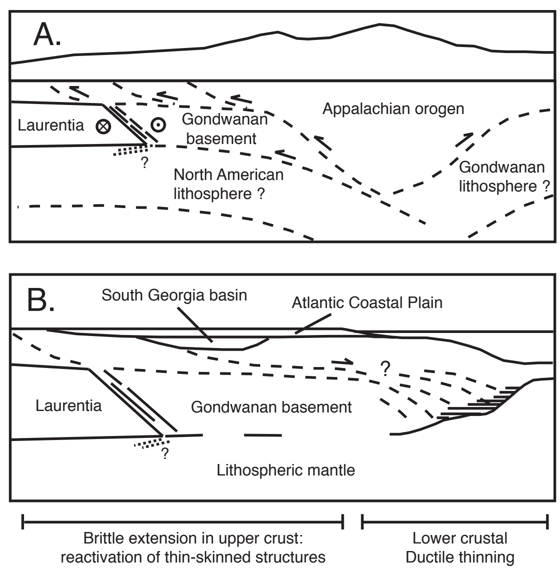

CHAPTER 5

ERRATUM FOR CRUSTAL MAGNETISM, TECTONIC INHERITANCE, AND CONTINENTAL RIFTING IN THE SOUTHEASTERN UNITED STATES[1]

---

[1] Parker, E.H., Jr., 2015, *GSA Today*, v. 25, p. 41.

Reprinted here with permission of publisher.

CORRECTION FOR MAGNETIC MODELS

An error has been found in the modeling used to generate magnetic anomalies in Figure 4.3. During construction of crustal models, the coordinates of the polygons used to represent Gondwanan crust were entered incorrectly (counterclockwise). This resulted in two errors: 1) it reversed the polarities of the computed anomalies, which then necessitated a reversal in magnetic polarity (assignment of a 180-degree declination) for remanent magnetization, in order to match the overall pattern of the observed anomalies, and 2) it generated an unintended lateral variation in the contribution to the magnetic anomaly from induced magnetization. The second error was small, because of the small value for susceptibility (k=0.01 SI) assigned to all polygons, but the first error resulted in a 180-degree error in the orientation of the contrast in remanent magnetization between Gondwanan and Laurentian crust.

Figure 5.1 shows the corrected anomalies. The changes in the overall shapes of the anomalies are relatively minor, but the remanent magnetization is now shown as localized and reversed in Laurentian rather than Gondwanan crust. This is equivalent to reversed magnetization for both crustal blocks, where (e.g., for profile A) the value of 0.47 A/m then represents the contrast due to slightly stronger magnetization for Laurentian crust. This is consistent with the original interpretation that magnetization was acquired during the Kiaman superchron (320 - 263 Ma) and Alleghanian collision, while the region was near the equator.

Figure 5.1: Corrected magnetic models for Chapter 4

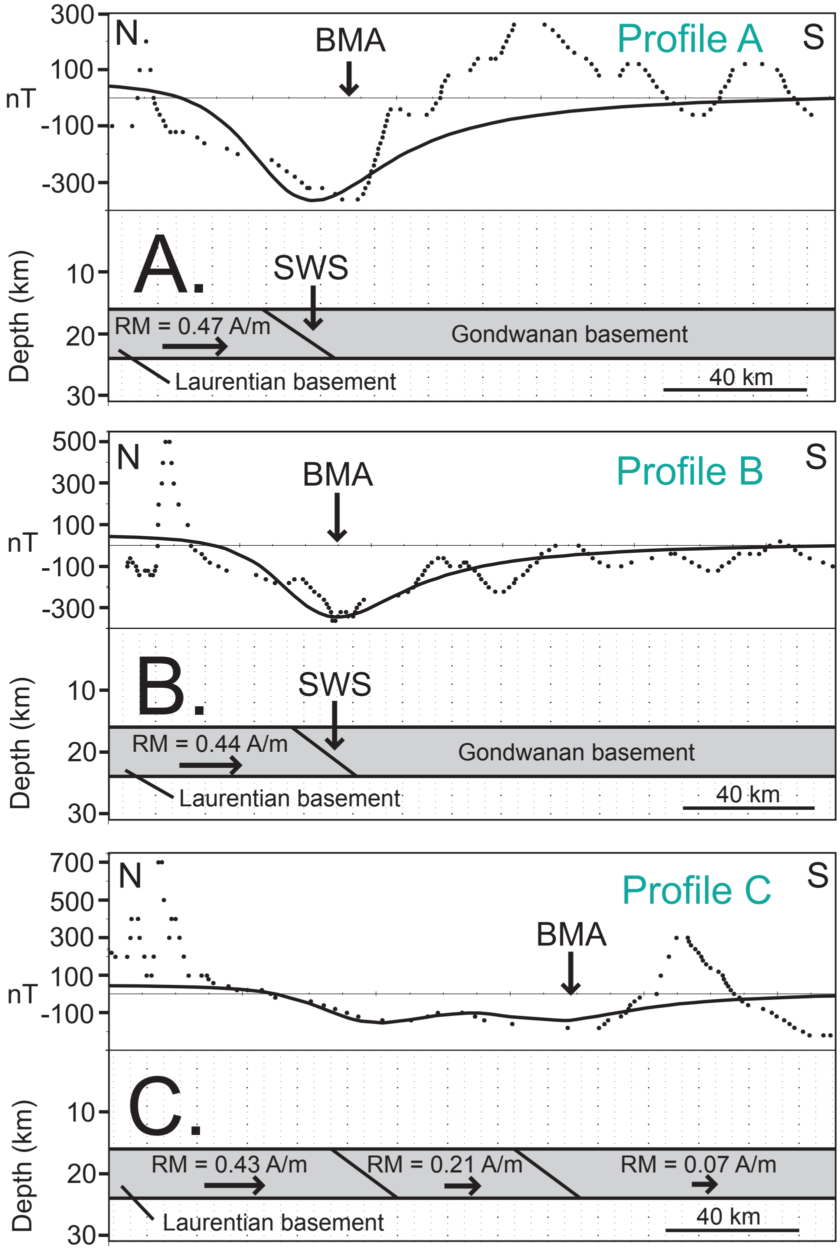

CHAPTER 6

CONCLUSIONS

SOUTHERN APPALACHIAN CRUSTAL STRUCTURE

Terrane transport during the Alleghanian orogeny

The receiver function results presented in Chapters 2 and 3 comprise important baseline constraints on the crustal structure of the southern Appalachians and help resolve questions concerning the dynamics of the Late Paleozoic Alleghanian orogeny. The forward models and H-k stacking results provide two new lines of evidence for the southeastward continuation of the Appalachian detachment beneath the peri-Gondwanan Carolina arc terrane, strengthening models of terrane overthrusting during continental collision. The seismic discontinuity at ~12 km depth beneath the Carolina terrane provides strong evidence for an interface between high-Vs arc rocks and lower-Vs passive-margin metasedimentary rocks or Grenville basement. Low Vp/Vs ratios across the Carolina terrane are consistent with a middle/lower crust largely composed of Grenville basement gneisses, rather than intermediate-to-mafic Carolina arc rocks.

Global implications of Appalachian crustal composition

Globally, the well-constrained low Vp/Vs ratios are consistent with the hypothesis that parts of the continental crust may be more felsic than generally thought (Hacker et al., 2011). In general, the lower continental crust is considered to be mafic in composition (Christensen and Mooney, 1995). The low average crustal Vp/Vs ratios, moderate average crustal Vp of 6.5 km/s, and lower crustal velocities of ~7.0 km/s instead point to the possibility that relatively felsic rocks comprise a major portion of the lower crust in this region. The presence of high-velocity minerals (garnet, sillimanite) in otherwise quartz-rich lithologies can explain the observed P-wave velocities and Vp/Vs ratios.

Possible mechanisms for 'felsification' of the crust include relamination of buoyant felsic material during subduction of sediments, arc material, or continental crust (Hacker et al., 2011). In the southern Appalachians, the evolution of the continental crust towards a felsic bulk composition may reflect the occurrence of these processes during repeated episodes of arc and continent collision along the eastern margin of Laurentia. If the crust beneath the detachment is truly Grenville in age, then the crustal evolution towards a felsic composition may have started as early as the Neoproterozoic, with subsequent modification during Paleozoic arc activity and Alleghanian continental collision.

Blue Ridge crustal root

Receiver function Ps conversions from SESAME and TA stations combined with previous wide-angle and receiver function data confirm that a localized crustal root (up to ~58-km crustal thickness) underlies the high elevations of the Blue Ridge in northern Georgia and western North Carolina (Chapter 2). Root preservation is attributed to thinning of the lower crust by ductile flow during Mesozoic rifting. Alternatively, the root may be an inherited feature from Neoproterozoic Grenville continental collision. The strong correlation between topography and crustal thickness suggests local isostatic balance, though low-velocity mantle could also provide a source of buoyancy to support the high elevations (MacDougall et al., 2015).

CRUSTAL STRUCTURE ACROSS THE ATLANTIC COASTAL PLAIN

The Suwannee suture and Brunswick Magnetic Anomaly

Magnetic modeling based on contrasts in remanent magnetization between Laurentian and Gondwanan crust suggests that continental suturing is the source of the Brunswick Magnetic

Anomaly (Chapter 4). The correlation between the BMA and dipping reflectors marking the Suwannee suture is the basis for this interpretation. The new modeling approach is motivated by observations that strong remanent magnetization associated with hematite-ilmenite microstructures may be a significant factor in understanding crustal-scale magnetic anomalies. In the context of Mesozoic rifting, the main implication is that voluminous intra-crustal CAMP magmatism is not required to explain the BMA. Although the suture itself has been hypothesized as a zone of weakness, Mesozoic rifting and magmatism have clearly not overprinted dipping reflectivity marking the collision zone, and the Florida block (Suwannee terrane and underlying basement) remains attached to North America. Surface geology and drilling show that CAMP dike swarms intruded the Atlantic margin and South Georgia basin, but the volume and extent of crustal modification by CAMP intrusive activity and the mechanics of continental rifting (brittle extension vs. ductile thinning) remain open questions and active research targets.

End-member models for dike intrusion during large igneous province emplacement include: 1) mafic underplating at the base of the crust with rapid intrusion of dikes through the crust. 2) mafic underplating with more extensive intra-crustal fractionation at higher crustal levels preceding dike intrusion in the uppermost crust and extrusive flood basalt volcanism (e.g. Bryan et al., 2010; Ridley and Richards, 2010). The hypothesis that extensive intra-crustal magmatism was preferentially concentrated outboard of the preserved suture is plausible, but this does not explain the much larger extent of CAMP magmas emplaced across four continents. In other words, there is not a unique relationship between CAMP, the South Georgia basin, and the suture zone. The timing (202-195 Ma), rapid emplacement (peak activity at ~201 Ma), and geographic extent of dike intrusion along the entire eastern margin of the United States suggests that the igneous activity is fundamentally related to lithospheric rupture prior to the initial formation of Atlantic oceanic crust (200-185 Ma) (Holbrook and Kelemen, 1993; McHone, 2000; Schettino and Turco, 2009; Callegaro et al., 2013), rather than localized extension beneath the Triassic South Georgia basin.

Speculative model for CAMP emplacement

Additional seismic constraints on the velocity structure of the continental crust are needed to differentiate between models of mafic underplating and localized intra-crustal intrusion beneath the Atlantic Coastal Plain. For the intrusion of large volumes of gabbro (Vp/Vs = 1.85), an increase in average crustal Vp/Vs ratio is expected. However, in the crystalline southern Appalachians intruded by CAMP dikes, the low Vp/Vs ratios clearly show that dike intrusion may not necessarily result in a significant increase in Vp/Vs. In addition, geochemical data from CAMP dikes along the eastern margin of North America also suggest that crustal contamination may have been limited (Callegaro et al., 2013). The major implication is that CAMP emplacement inboard of the volcanic rifted margin may be characterized by mafic underplating at the base of the crust, rapid intrusion of dikes, and more isolated, volumetrically limited plutonic activity.

FUTURE WORK

The last major tectonic event to affect the southeastern United States was the Mesozoic break-up of the supercontinent Pangea, and the present structure of the rifted Appalachian orogen and Atlantic passive margin largely reflects modification in response to extensional tectonics and erosion. Fundamental seismic constraints on crustal and lithospheric thickness and velocity structure are still needed to characterize the effects of rifting across the Atlantic Coastal Plain. Constraints on extensional deformation are, in turn, critical for evaluating the potential for tectonic overprinting of pre-Mesozoic structure. Thinning of the lithosphere may have obliterated fabrics developed during Paleozoic convergence. Alternatively, evidence for suturing may be preserved within the mantle if deformation was localized within discrete shear zones. In the latter case, the concept of tectonic inheritance (i.e. the reactivation of structures formed during convergence) is an important consideration.

In terms of rifting, the mechanical response (e.g. ductile thinning; shear zone formation; brittle faulting) of the lithosphere to extension and the nature of rift magmatism are two fundamental outstanding issues. Analyses of SsPmp phases across the Atlantic Coastal Plain will provide new constraints on crustal thickness beneath the South Georgia basin, and Sp receiver functions will provide new insight on variations in lithospheric thickness across the region. Anisotropy studies using SKS measurements and Rayleigh waves will provide additional information on strain patterns within the lithosphere resulting from convergent and extensional tectonics, or a combination of both. The possible effects of differential crustal stretching between the brittle upper crust and ductile lower crust along low-angle detachments is difficult to assess, though additional constraints on crustal reflectivity from PKIKP analyses may yield insight on post-rift crustal structure.

Extensive rift magmatism is expected to modify the velocity structure of the crust and increase average crustal P-wave velocities and Vp/Vs ratios. In the crystalline southern Appalachians affected by CAMP magmatism, detailed Ps receiver function analyses of the crust-mantle boundary will provide new insight on the effects of magmatic underplating. Across the Atlantic Coastal Plain, analyses of SsPmp phases can provide new constraints on the average P-wave velocity structure of the crust. It may also be possible to analyze crustal multiples in Ps receiver functions to determine average crustal Vp/Vs ratios across the Atlantic Coastal Plain, though constraints on the velocity structure of the 1-2 km thick unconsolidated sediments are also needed to evaluate the relative contributions of high Vp/Vs sediments and mafic magmatism on average crustal Vp/Vs estimates.

REFERENCES

Abt, D.L., Fischer, K.M., French, S.W., Ford, H.A., Yuan, H., and Romanowicz, B., 2010, North American lithospheric discontinuity structure imaged by Ps and Sp receiver functions: Journal of Geophysical Research, v. 115, B09301, doi:10.1029/2009JB006914.

Aleinikoff, J.N., Zartman, R.E, Walter, M., Rankin, D.W., Lyttle, P.T, and Burton, W.C., 1995, U-Pb ages of metarhyolites of the Catoctin and Mount Rogers formations, central and southern Appalachians: Evidence for two pulses of Iapetan rifting: American Journal of Science, v. 295, p. 428-454.

Amante, C. and Eakins, B.W., 2009, ETOPO1 1 arc-minute global relief model: Procedures, data sources and analysis: NOAA Technical Memorandum NESDIS NGDC-24, National Geophysical Data Center, NOAA, doi:10.7289/V5C8276M [accessed 08-11-14].

Anderson, E.D., and Moecher, D.P., 2009, Formation of high-pressure metabasites in the southern Appalachian Blue Ridge via Taconic continental subduction beneath the Laurentian margin: Tectonics, v. 28, TC5012, doi:10.1029/2008TC002319.

Arthur, M.A., 1982. Thermal history of the Georges Bank basin, *in* Scholle, P.A., Wenkham, C.R., eds., Geological studies of the COST Nos. G-1 and G-2 wells, United States North Atlantic outer continental shelf: Geological Survey Circular 861, p. 143-152.

Austin, J.A., Jr., Stoffa, P.L., Phillips, J.D., Oh, J., Sawyer, D.S., Purdy, G.M., Reiter, E., and Makris, J., 1990, Crustal structure of the Southeast Georgia embayment-Carolina trough: Preliminary results of a composite seismic image of a continental suture(?) and a volcanic passive margin: Geology, v. 18, p. 1023-1027.

Baker, M.S., and Hawman, R.B., 2011, Crustal structure in the southern Appalachians: A comparison of results obtained from broadband data and three-component, wide-angle P and S reflection data: Bulletin of the Seismological Society of America, v. 101, p. 2796-2809, doi:10.1785/0120100341.

Bartholomew, M.J., and Hatcher, R.D., Jr., 2010, The Grenville orogenic cycle of southern Laurentia: Unraveling sutures, rifts, and shear zones as potential piercing points for Amazonia: Journal of South American Earth Sciences, v. 29, p. 4-20.

Beck, S.L., and Zandt, G., 2002, The nature of orogenic crust in the central Andes: Journal of Geophysical Research, v. 107, doi:10.1029/2000JB000124.

Becker, T.P., Thomas, W.A., and Gehrels, G.E., 2006, Linking Late Paleozoic sedimentary provenance in the Appalachian basin to the history of Alleghanian deformation: American Journal of Science, v. 306, p. 777-798, doi: 10.2475/10.2006.01.

Beutel, E.K., 2009, Magmatic rifting of Pangaea linked to onset of South American plate motion: Tectonophysics, v. 468, p. 149-157.

Bryan, S.E., Peate, I.U., Peate, D.W., Self, S., Jerram, D.A., Mawby, M.R., Marsh, J.S., and Miller, J.A., 2010, The largest volcanic eruptions on Earth: Earth-Science Reviews, v. 102, p. 207-229.

Bryant, B., and Reed, J.C., Jr., 1970, Geology of the Grandfather Mountain window and vicinity, North Carolina and Tennessee: United States Geological Survey Professional Paper 615, p. 1-190.

Callegaro, S., Marzoli, A., Bertrand, H., Chiaradia, M., Reisberg, L., Meyzen, C., Bellieni, G., Weems, R.E., and Merle, R., 2013, Upper and lower crust recycling in the source of CAMP basaltic dykes from southeastern North America: Earth and Planetary Science Letters, v. 376, p. 186-199.

Carrigan, C.W., Miller, C.F., Fullagar, P.D., Bream, B.R., Hatcher, R.D., Jr., and Coath, C.D., 2003, Ion microprobe age and geochemistry of southern Appalachian basement, with implications for Proterozoic and Paleozoic reconstructions: Precambrian Research, v. 120, p. 1-36.

Cassidy, J.F., 1992, Numerical experiments in broadband receiver function analysis: Bulletin of the Seismological Society of America, v. 82, p. 1453-1474.

Chakraborty, S., Moecher, D.P., and Samson, S.D., 2012, Provenance of the Lower Ocoee Supergroup, eastern Great Smoky Mountains: Geological Society of America Bulletin, v. 124, p. 1278-1292, doi: 10.1130/B30578.1.

Chowns, T.M., and Williams, C.T., 1983, Pre-Cretaceous rocks beneath the Georgia Coastal Plain – Regional implications, *in* Gohn, G.S., ed., Studies related to the Charleston, South Carolina, earthquake of 1886 – Tectonics and seismicity: USGS Professional Paper 1313-L, L1-L42.

Christensen, N.I., and Mooney, W.D., 1995, Seismic velocity structure and composition of the continental crust: A global view: Journal of Geophysical Research, v. 100, p. 9761-9788.

Christensen, N.I., 1996, Poisson's ratio and crustal seismology: Journal of Geophysical Research, v. 101, p. 3139-3156.

Clendenin, C.W., Jr., 2013, Insights into the mode of the South Georgia rift extension in eastern Georgia, USA: Tectonophysics, v. 608, p. 613-621.

Cook, F.A., Albaugh, D.S., Brown, L.D., Kaufman, S., Oliver, J.E., and Hatcher, R.D., Jr., 1979, Thin-skinned tectonics in the crystalline southern Appalachians; COCORP seismic-reflection profiling of the Blue Ridge and Piedmont: Geology, v. 7, p. 563-567.

Cook, F.A. and J.E. Oliver, 1981, The Late Precambrian-Early Paleozoic continental edge in the Appalachian orogen: American Journal of Science, v. 281, p. 993-1008.

Cook, F.A., and Vasudevan, K., 2006, Reprocessing and enhanced interpretation of the initial COCORP Southern Appalachians traverse: Tectonophysics, v. 420, p. 161-174.

Coruh, C., Costain, J.K., Hatcher, R.D., Jr., Pratt, T.L., Williams, R.T., and Phinney, R.A., 1987, Results from regional vibroseis profiling: Appalachian ultra-deep core hole site study: Geophysical Journal of the Royal Astronomical Society, v. 89, p. 147-156, doi:10.1111/j.1365-246X.1987.tb04401.x.

Costain, J.K., Hatcher, R.D., Jr., and Çoruh, C., 1989a, Appalachian ultradeep core hole (ADCOH) project site investigation, regional seismic lines, and geologic interpretation, *in* Hatcher, R.D., Jr., Viele, G.W., and Thomas, W.A., eds., The Appalachian-Ouachita orogen in the United States: Boulder, Colorado, Geological Society of America, The Geology of North America, v. F-2, Plate 12.

Costain, J.K., Hatcher, R.D., Jr., Çoruh, C., Pratt, T.L., Taylor, S.R., Litehiser, J.J., and Zietz, I., 1989b, Geophysical characteristics of the Appalachian crust, *in* Hatcher, R.D., Jr., Viele, G.W., and Thomas, W.A., eds., The Appalachian-Ouachita orogen in the United States: Boulder, Colorado, Geological Society of America, The Geology of North America, v. F-2, p. 385-416.

Crotwell, H.P., and Owens, T.J., 2005, Automated receiver function processing: Seismological Research Letters. v. 76, p. 702-709.

Dallmeyer, R.D., Caen-Vachette, M., and Villeneuve, M., 1987, Emplacement age of post-tectonic granites in southern Guinea (West Africa) and the peninsular Florida subsurface:

Implications for origins of southern Appalachian exotic terranes: Geological Society of America Bulletin, v. 99, p. 87-93.

Dallmeyer, R.D., 1988, Late Paleozoic tectonothermal evolution of the western Piedmont and eastern Blue Ridge, Georgia: Controls on the chronology of terrane accretion and transport in the southern Appalachian orogen: Geological Society of America Bulletin, v. 100, p. 702-713.

Daniels, D.L., Zietz, I., and Popenoe, P., 1983, Distribution of subsurface lower Mesozoic rocks in the Southeastern United States as interpreted from regional aeromagnetic and gravity maps, *in* Gohn, G.S., ed., Studies related to the Charleston, South Carolina, earthquake of 1886 – Tectonics and seismicity: U.S. Geological Survey Professional Paper 1313, K1-K24.

Daniels, D.L., 2001, Georgia aeromagnetic and gravity maps and data: a website for distribution of data. U.S. Geological Survey Open-File Report 01-0106, http://pubs.usgs.gov/of/2001/of01-106/ (accessed December 2012).

Dennis, A.J., and Wright, J.E., 1997, The Carolina terrane in northwestern South Carolina, U.S.A.: Late Precambrian-Cambrian deformation and metamorphism in a peri-Gondwanan oceanic arc: Tectonics, v. 16, p. 460-473.

Dennis, A.J., Shervais, J.W., Mauldin, J., Maher, H.D., Jr., and Wright, J.E., 2004, Petrology and geochemistry of Neoproterozoic volcanic arc terranes beneath the Atlantic Coastal Plain, Savannah River Site, South Carolina: Geological Society of America Bulletin, v. 116, p. 572-593.

Edelman, S.H., Liu, A., and Hatcher, R.D., Jr., 1987, The Brevard zone in South Carolina and adjacent areas: An Alleghanian orogen-scale dextral shear zone reactivated as a thrust fault: The Journal of Geology, v. 95, p. 793–806, doi:10.1086/629178.

Efron, B., and Tibshirani, R., 1991, Statistical data analysis in the computer age: Science, v. 253, p. 390-395, doi:10.1126/science.253.5018.390.

Ernst, W.G., 2010, Subduction-zone metamorphism, calc-alkaline magmatism, and convergent-margin crustal evolution: Gondwana Research, v. 18, p. 8-16.

Fischer, K.M., 2002, Waning buoyancy in the crustal roots of old mountains: Nature, v. 417, p. 933-936.

Fischer, K.M., MacDougall, J.G., Hawman, R.B., Parker, E.H., and Wagner, L.S., 2012, The lithosphere of the Appalachian orogen and Atlantic passive margin, Abstract T43G-03 presented at 2012 Fall Meeting, AGU, San Francisco, Calif., 3-7 Dec.

Fountain, D.M., 1976, The Ivrea-Verbano and Strona-Ceneri zones, northern Italy: A cross-section of the continental crust – new evidence from seismic velocities of rock samples: Tectonophysics, v. 33, p. 145-165.

Fountain, D.M., and Salisbury, M.H, 1996, Seismic properties of rock samples from the Pikwitonei granulite belt – God's Lake domain crustal cross section, Manitoba: Canadian Journal of Earth Sciences, v. 33, p. 757-768.

French, S.W., Fischer, K.M., Syracuse, E.M., and Wysession, M.E., 2009, Crustal structure beneath the Florida-to-Edmonton broadband seismometer array: Geophysical Research Letters, v. 36, L08309, doi: 10.1029/2008GL036331.

Garcia, A.S., Thomas, D.N., Liss, D., and Shaw, J., 2006, Low geomagnetic field intensity during the Kiaman superchron: Thellier and microwave results from the Great Whin Sill intrusive complex, northern United Kingdom: Geophysical Research Letters, v. 33, L16308, doi:10.1029/2006GL026729.

Godfrey, N.J., Christensen, N.I., and Okaya, D.A., 2002, The effect of crustal anisotropy on reflector depth and velocity determination from wide-angle seismic data: A synthetic example based on South Island, New Zealand: Tectonophysics, v. 355, p. 145–161, doi:10.1016/S0040-1951(02)00138-5.

Hacker, B.R., Kelemen, P.B., and Behn, M.D., 2011, Differentiation of the continental crust by relamination: Earth and Planetary Science Letters, v. 307, p. 501-516.

Hall, D.J., 1990, Gulf Coast-East Coast magnetic anomaly 1: Root of the main crustal decollement for the Appalachian-Ouachita orogen: Geology, v. 18, p. 862-865.

Hames, W.E., Renne, P.R., and Ruppel, C., 2000, New evidence for geologically instantaneous emplacement of earliest Jurassic Central Atlantic magmatic province basalts on the North American margin: Geology, v. 28, p. 859-862.

Hatcher, R.D., Jr., 1971, Stratigraphic, petrologic, and structural evidence favoring a thrust solution to the Brevard problem: American Journal of Science, v. 270, p. 177-202, doi:10.2475/ajs.270.3.177.

Hatcher, R.D., Jr., 1987, Tectonics of the southern and central Appalachian internides: Annual Review of Earth and Planetary Sciences, v. 15, p. 337-362, doi:10.1146/annurev.ea.15.050187.002005.

Hatcher, R.D., Jr., Costain, J.K., Coruh, C., Phinney, R.A., and Williams, R.T., 1987, Tectonic implications of new Appalachian Ultradeep Core Hole (ADCOH) seismic reflection data from the crystalline southern Appalachians: Geophysical Journal of the Royal Astronomical Society, v. 89, p. 157–162, doi:10.1111/j.1365-246X.1987.tb04402.x.

Hatcher, R.D., Jr., Thomas, W.A., Geiser, P.A., Snoke, A.W., Mosher, S., and Wiltschko, D.V., 1989, Alleghanian orogen, *in* R.D. Hatcher, Jr., et al., eds., The Appalachian-Ouachita Orogen in the United States: Boulder, Colorado, Geological Society of America, The Geology of North America, v. F-2, p. 233-318.

Hatcher, R.D., Jr., 1991, Interactive property of large thrust sheets with footwall rocks – the subthrust interactive duplex hypothesis: A mechanism of dome formation in thrust sheets: Tectonophysics, v. 191, p. 237-242, doi:10.1016/0040-1951(91)90059-2.

Hatcher, R.D., Jr., 2001, Rheological partitioning during multiple reactivation of the Palaeozoic Brevard fault zone, southern Appalachians, USA, *in* Holdsworth, R.E., Strachan, R.A., Magloughlin, J.F., and Knipe, R.J., eds., The nature and tectonic significance of fault zone weakening: Geological Society of London Special Publication 186, p. 257-271, doi:10.1144/GSL.SP.2001.186.01.15.

Hatcher, R.D., Jr., Lemiszki, P.J., and Whisner, J.B., 2007, Character of rigid boundaries and internal deformation of the southern Appalachian foreland fold-thrust belt, *in* Sears, J.W., Harms, T.A., and Evenchick, C.A., eds., Whence the Mountains? Inquiries into the Evolution of Orogenic Systems: A Volume in Honor of Raymond A. Price: Geological Society of America Special Paper 433, p. 243–276, doi: 10.1130/2007.2433(12).

Hatcher, R.D., Jr., 2010, The Appalachian orogen: A brief summary, *in* Tollo, R.P, et al., eds., From Rodinia to Pangea: The Lithotectonic Record of the Appalachian Region: Boulder, Colorado, Geological Society of America Memoir 206, p. 1-19.

Hauser, F., O'Reilly, B.M., Readman, P.W., Daly, J.S., and van den Berg, R., 2008, Constraints on crustal structure and composition within a continental suture zone in the Irish

Caledonides from shear wave wide-angle reflection data and lower crustal xenoliths: Geophysical Journal International, v. 175, p. 1254-1272.

Hawman, R.B., Khalifa, M.O., and Baker, M.S., 2012, Isostatic compensation for a portion of the southern Appalachians: Evidence from a reconnaissance study using wide-angle, three-component seismic soundings: Geological Society of America Bulletin, v. 124, p. 291-317, doi: 10.1130/B30464.1.

Heatherington, A.L., and Mueller, P.A., 2003, Mesozoic igneous activity in the Suwannee terrane, southeastern USA: Petrogenesis and Gondwanan affinities: Gondwana Research, v. 6, p. 296-311.

Heatherington, A.L., Mueller, P.A., and Wooden, J.L., 2010, Alleghanian plutonism in the Suwannee terrane, USA: Implications for late Paleozoic tectonic models, *in* Tollo, R.P., Bartholomew, M.J., Hibbard, J.P., and Karabinos, P.M., eds., From Rodinia to Pangea: The Lithotectonic Record of the Appalachian Region: Geological Society of America Memoir 206, p. 607-620, doi:10.1130/2010.1206(24).

Heffner, D.M., Knapp, J.H., Akintunde, O.M., and Knapp, C.C., 2012, Preserved extent of Jurassic flood basalt in the South Georgia Rift: A new interpretation of the J horizon: Geology, v. 40, p. 167-170, doi:10.1130/G32638.1.

Hibbard, J.P., Stoddard, E.F., Secor, D.T., and Dennis, A.J., 2002, The Carolina Zone: overview of Neoproterozoic to Early Paleozoic peri-Gondwanan terranes along the eastern flank of the southern Appalachians: Earth-Science Reviews, v. 57, p. 299-339.

Hibbard, J., and Waldron, J.W.F., 2009, Truncation and translation of Appalachian promontories: Mid-Paleozoic strike-slip tectonics and basin initiation: Geology, v. 37, p. 487-490.

Hibbard, J.P., van Staal, C.R., and Rankin, D.W., 2010, Comparative analysis of the geological evolution of the northern and southern Appalachian orogen: Late Ordovician-Permian, *in* Tollo, R.P., Bartholomew, M.J., Hibbard, J.P., and Karabinos, P.M., eds., From Rodinia to Pangea: The Lithotectonic Record of the Appalachian Region: Geological Society of America Memoir 206, p. 51-69, doi:10.1130/2010.1206(03).

Hibbard, J.P., Miller, B.V., Hames, W.E., Standard, I.D., Allen, J.S., Lavallee, S.B., and Boland, I.B., 2012, Kinematics, U-Pb geochronology, and $^{40}Ar/^{39}Ar$ thermochronology of the Gold Hill shear zone, North Carolina: The Cherokee orogeny in Carolinia, Southern Appalachians: Geological Society of America Bulletin, v. 124, p. 643-656, doi: 10.1130/B30579.

Holbrook, W.S., and Kelemen, P.B., 1993, Large igneous province on the US Atlantic margin and implications for magmatism during continental breakup: Nature, v. 364, p. 433-436.

Holbrook, W.S., Reiter, E.C., Purdy, G.M., Sawyer, D., Stoffa, P.L, Austin, J.A. Jr., Oh, J., and Makris, J., 1994, Deep structure of the U.S. Atlantic continental margin, offshore South Carolina, from coincident ocean bottom and multichannel seismic data: Journal of Geophysical Research, v. 99, p. 9155-9178.

Holm-Denoma, C.S., and Das, R., 2010, Bimodal volcanism as evidence for Paleozoic extensional accretionary tectonism in the southern Appalachians: Geological Society of America Bulletin, v. 122, p. 1220-1234.

Hubbard, S.S., Çoruh, C., and Costain, J.K., 1991, Paleozoic and Grenvillian structures in the southern Appalachians: Extended interpretation of seismic reflection data: Tectonics, v. 10, p. 141–170, doi:10.1029/90TC01854.

Hynes, A., and Rivers, T., 2010, Protracted continental collision – evidence from the Grenville Orogen: Canadian Journal of Earth Sciences, v. 47, p. 591-620, doi:10.1139/E10-003.

Iverson, W.P., and Smithson, S.B., 1983, Reprocessing and reinterpretation of COCORP southern Appalachian profiles: Earth and Planetary Science Letters, v. 62, p. 75–90, doi:10.1016/0012-821X(83)90072-9.

Jagoutz, O., and Schmidt, M.W., 2012, The formation and bulk composition of modern juvenile continental crust: The Kohistan arc: Chemical Geology, v. 298-299, p. 79-96.

Johnston, J.E., and Christensen, N.I., 1992, Shear wave reflectivity, anisotropies, Poisson's ratios, and densities of a southern Appalachian Paleozoic sedimentary sequence: Tectonophysics, v. 210, p. 1–20, doi:10.1016/0040-1951(92)90124-O.

Kelso, P.R., Banerjee, S.K., and Teyssier, C., 1993, Rock magnetic properties of the Arunta block, central Australia, and their implication for the interpretation of long-wavelength magnetic anomalies: Journal of Geophysical Research, v. 98, p. 15987-15999.

Kennett, B.L.N., and Engdahl, E.R., 1991, Traveltimes for global earthquake location and phase identification: Geophysical Journal International, v. 105, p. 429-465.

Kern, H., and Schenk, V., 1988, A model of velocity structure beneath Calabria, southern Italy, based on laboratory data: Earth and Planetary Science Letters, v. 87, p. 325-337.

King, P.B., 1961, Systematic pattern of Triassic dikes in the Appalachian region: U.S. Geological Survey Professional Paper 424-B, p. B93-B95.

Langston, C.A., 1979, Structure under Mount Rainier, Washington, inferred from teleseismic body waves: Journal of Geophysical Research, v. 84, p. 4749-4762, doi:10.1029/JB084iB09p04749.

Leahy, G.M., Saltzer, R.L., and Schmedes, J., 2012, Imaging the shallow crust with teleseismic receiver functions: Geophysical Journal International, v. 191, p. 627–636, doi:10.1111/j.1365-246X.2012.05615.x.

Levin, V., and Park, J., 1997, Crustal anisotropy in the Ural Mountains foredeep from teleseismic receiver functions: Geophysical Research Letters, v. 24, p. 1283-1286, doi:10.1029/97GL51321.

Lister, G.S., Etheridge, M.A., and Symonds, P.A., 1991, Detachment models for the formation of passive continental margins: Tectonics, v. 10, p. 1038-1064.

Lizarralde, D., Holbrook, W.S., and Oh, J., 1994, Crustal structure across the Brunswick magnetic anomaly, offshore Georgia, from coincident ocean bottom and multi-channel seismic data: Journal of Geophysical Research, v. 99, p. 21741-21757.

Lizarralde, D., and Holbrook, W.S., 1997, U.S. mid-Atlantic margin structure and early thermal evolution: Journal of Geophysical Research, v. 102, p. 22855-22875.

Lombardi, D., Braunmiller, J., Kissling, E., and Giardini, D., 2008, Moho depth and Poisson's ratio in the Western-Central Alps from receiver functions: Geophysical Journal International, v. 173, p. 249-264.

MacDougall, J.G., Fischer, K.M., Forsyth, D.W., Hawman, R.B., and Wagner, L.S., 2015, Shallow mantle velocities beneath the southern Appalachians from Pn phases: Geophysical Research Letters, v. 42, p. 339-345, doi:10.1002/2014GL062714.

Maher, H.D., Jr., Dallmeyer, R.D., Secor, D.T., Jr., and Sacks, P.E., 1994, $^{40}Ar/^{39}Ar$ constraints on chronology of Augusta fault zone movement and late Alleghanian extension, southern Appalachian Piedmont, South Carolina and Georgia: American Journal of Science, v. 294, p. 428-448.

Martínez Poyatos, D., Carbonell, R., Palomeras, I., Simancas, J.F., Ayarza, P., Martí, D., Azor, A., Jabaloy, A., González Cuadra, P., Tejero, R., Martín Parra, L.M., Matas, J., González Lodeiro, F., Pérez-Estaún, A., García Lobón, J.L., and Mansilla, L., 2012, Imaging the crustal structure of the Central Iberian Zone (Variscan Belt): The ALCUDIA deep seismic reflection transect: Tectonics, v. 31, TC3017, doi:10.1029/2011TC002995.

Maus, S., et al., 2009, EMAG2: A 2-min resolution Earth Magnetic Anomaly Grid compiled from satellite, airborne, and marine magnetic measurements: Geochemistry Geophysics Geosystems, v. 10, Q08005, doi:10.1029/2009GC002471.

McBride, J.H., and Nelson, K.D., 1988, Integration of COCORP deep reflection and magnetic anomaly analysis in the southeastern United States: Implications for origin of the Brunswick and East Coast magnetic anomalies: Geological Society of America Bulletin, v. 100, p. 436-445.

McBride, J.H., Nelson, K.D., and Brown, L.D., 1989, Evidence and implications of an extensive early Mesozoic rift basin and basalt/diabase sequence beneath the southeast Coastal Plain: Geological Society of America Bulletin, v. 101, p. 512-520.

McBride, J.H., 1991, Constraints on the structure and tectonic development of the early Mesozoic south Georgia rift, southeastern United States; seismic reflection data processing and interpretation: Tectonics, v. 10, p. 1065-1083.

McBride, J.H., Hatcher, R.D., Jr., Stephenson, W.J., and Hooper, R.J., 2005, Integrating seismic reflection and geological data and interpretations across an internal basement massif: The southern Appalachian Pine Mountain window, USA: Geological Society of America Bulletin, v. 117, p. 669–686, doi:10.1130/B25313.1.

McEnroe, S.A., and Brown, L.L., 2000, A closer look at remanence-dominated aeromagnetic anomalies: Rock magnetic properties and magnetic mineralogy of the Russell Belt microcline-sillimanite gneiss, northwest Adirondack Mountains, New York: Journal of Geophysical Research, v. 105, p. 16437-16456.

McEnroe, S.A., Harrison, R.J., Robinson, P., Golla, U., and Jercinovic, M.J., 2001, Effect of fine-scale microstructures in titanohematite on the acquisition and stability of natural remanent magnetization in granulite facies metamorphic rocks, southwest Sweden: Implications for crustal magnetism: Journal of Geophysical Research, v. 106, p. 30523-30546.

McEnroe, S.A., Langenhorst, F., Robinson, P., Bromiley, G.D., and Shaw, C.S.J., 2004, What is magnetic in the lower crust?: Earth and Planetary Science Letters, v. 226, p. 175-192.

McHone, J.G., 2000, Non-plume magmatism and rifting during the opening of the central Atlantic Ocean: Tectonophysics, v. 316, p. 287-296.

McKenzie, D., Nimmo, F., Jackson, J.A., Gans, P.B., and Miller, E.L., 2000, Characteristics and consequences of flow in the lower crust: Journal of Geophysical Research, v. 105, p. 11029-11046.

McLelland, J.M., Selleck, B.W., and Bickford, M.E., 2010, Review of the Proterozoic evolution of the Grenville Province, its Adirondack outlier, and the Mesoproterozoic inliers of the Appalachians, *in* Tollo, R.P, et al., eds., From Rodinia to Pangea: The Lithotectonic Record of the Appalachian Region: Boulder, Colorado, Geological Society of America Memoir 206, p. 21-49.

Meltzer, A., and Christensen, N., 2001, Nanga Parbat crustal anisotropy: Implications for interpretation of crustal velocity structure and shear-wave splitting: Geophysical Research Letters, v. 28, p. 2129–2132, doi:10.1029/2000GL012262.

Merschat, A.J., Hatcher, R.D. Jr., and Davis, T.L., 2005, The northern Inner Piedmont, southern Appalachians, USA: kinematics of transpression and SW-directed mid-crustal flow: Journal of Structural Geology, v. 27, p. 1252-1281.

Miller, B.V., Fetter, A.H., and Stewart, K.G., 2006, Plutonism in three orogenic pulses, Eastern Blue Ridge Province, southern Appalachians: Geological Society of America Bulletin, v. 118, p. 171-184, doi: 10.1130/B25580.1.

Mueller, P.A., Heatherington, A.L., Foster, D.A., Thomas, W.A., and Wooden, J.L., 2014, The Suwannee suture: Significance for Gondwana-Laurentia terrane transfer and formation of Pangea: Gondwana Research, v. 26, p. 365-373.

North American Magnetic Anomaly Group (NAMAG), 2002, Magnetic anomaly map of North America. United States Geological Survey, scale 1:10 000 000, 1 sheet.

Owens, T.J., Zandt, G., and Taylor, S.R., 1984, Seismic evidence for an ancient rift beneath the Cumberland Plateau, Tennessee: A detailed analysis of broadband teleseismic P waveforms: Journal of Geophysical Research, v. 89, p. 7783-7795, doi:10.1029/JB089iB09p07783.

Parker, E. H., Hawman, R.B., Fischer, K.M., Wagner, L.S., and Lekic, V., 2011, Preliminary results from the Southeastern Suture of the Appalachian Margin Experiment (SESAME): Initial observations and a comparison between vault and direct-burial stations: Abstract T21A-2285 presented at 2011 Fall Meeting, AGU, San Francisco, Calif., 5-9 Dec.

Parker, E.H., Jr., Hawman, R.B., Fischer, K.M., and Wagner, L.S., 2013, Crustal evolution across the southern Appalachians: Initial results from the SESAME broadband array: Geophysical Research Letters, v. 40, p. 3853–3857, doi:10.1002/grl.50761.

Parker, E.H., Jr., 2014, Crustal magnetism, tectonic inheritance, and continental rifting in the southeastern United States: GSA Today, v. 24, p. 4-9, doi: 10.1130/GSAT-G192A.1.

Parker, E.H., Jr., Hawman, R.B., Fischer, K.M., and Wagner, L.S., 2015, Constraining lithologic variability along the Alleghanian detachment in the southern Appalachians using passive-source seismology: Geology, accepted February 20, 2015.

Phinney, R.A., and Roy-Chowdhury, K., 1989, Reflection seismic studies of crustal structure in the eastern United States, *in*, Pakiser, L.C., and Mooney, W.D., eds., Geophysical framework of the continental United States: Boulder, Colorado, Geological Society of America Memoir 172, p. 613-653.

Prodehl, C., Schlittenhardt, J., and Stewart, S.W., 1984, Crustal structure of the Appalachian Highlands in Tennessee: Tectonophysics, v. 109, p. 61-76.

Ridley, V.A., and Richards, M.A., 2010, Deep crustal structure beneath large igneous provinces and the petrologic evolution of flood basalts: Geochemistry, Geophysics, Geosystems, v. 11, doi:10.1029/2009GC002935.

Robinson, P., Harrison, R.J., McEnroe, S.A., and Hargraves, R.B., 2002, Lamellar magnetism in the haematite-ilmenite series as an explanation for strong remanent magnetization: Nature, v. 418, p. 517-520.

Schettino, A., and Turco, E., 2009, Breakup of Pangea and plate kinematics of the central Atlantic and Atlas regions: Geophysical Journal International, v. 178, p. 1078-1097, doi:10.1111/j.1365-246X.2009.04186.x.

Schlische, R.W., 1993, Anatomy and evolution of the Triassic-Jurassic continental rift system, eastern North America: Tectonics, v. 12, p. 1026-1042.

Secor, D.T., Jr., Snoke, A.W., and Dallmeyer, R.D., 1986, Character of the Alleghanian orogeny in the southern Appalachians: Part III. Regional tectonic relations: Geological Society of America Bulletin, v. 97, 1345-1353.

Sheridan, R.E., Musser, D.L., Glover, L. III, Talwani, M., Ewing, J.I., Holbrook, W.S., Purdy, G.M., Hawman, R., and Smithson, S., 1993, Deep seismic reflection data of EDGE U.S. mid-Atlantic continental-margin experiment: Implications for Appalachian sutures and Mesozoic rifting and magmatic underplating: Geology, v. 21, p. 563-567.

Shillington, D.J., Lizarralde, D., and Harder, S., 2013, The SUGAR experiment: an upcoming active-source seismic experiment of the South Georgia Basin to examine the relationship between extension, magmatism, and pre-existing structures, Abstract presented at EarthScope National Meeting, Raleigh, NC, May 13-15.

Sinha, A.K., Thomas, W.A., Hatcher, R.D., Jr., and Harrison, T.M., 2012, Geodynamic evolution of the central Appalachian orogen: geochronology and compositional diversity of magmatism from Ordovician through Devonian: American Journal of Science, v. 312, p. 907-966, doi: 10.2475/08.2012.03.

Snoke, A.W., and Frost, R.B., 1990, Exhumation of high pressure pelitic schist, Lake Murray spillway, South Carolina: Evidence for crustal extension during Alleghanian strike-slip faulting: American Journal of Science, v. 290, p. 853-881.

Steltenpohl, M.G., Mueller, P.M., Heatherington, A.L., Hanley, T.B., and Wooden, J.L., 2008, Gondwanan/peri-Gondwanan origin for the Uchee terrane, Alabama and Georgia: Carolina zone or Suwannee terrane(?) and its suture with Grenvillian basement of the Pine Mountain window: Geosphere, v. 4, p. 131-144.

Steltenpohl, M.G., Schwartz, J.J., and Miller, B.V., 2013, Late to post-Appalachian strain partitioning and extension in the Blue Ridge of Alabama and Georgia: Geosphere, v. 9, p. 647-666.

Szymanski, D.L., and Christensen, N.I., 1993, The origin of reflections beneath the Blue Ridge-Piedmont allochthon: A view through the Grandfather Mountain window: Tectonics, v. 12, p. 265–278, doi:10.1029/92TC01831.

Tauvers, P.R., and Muehlberger, W.R., 1987, Is the Brunswick magnetic anomaly really the Alleghanian suture?: Tectonics, v. 6, p. 331-342.

Taylor, S.R., and McLennan, S.M., 1995, The geochemical evolution of the continental crust: Reviews of Geophysics, v. 33, p. 241-265.

Thomas, W.A., 1991, The Appalachian-Ouachita rifted margin of southeastern North America: Geological Society of America Bulletin, v. 103, p. 415-431.

Thomas, W.A., 2010, Interactions between the southern Appalachian-Ouachita orogenic belt and basement faults in the orogenic footwall and foreland, *in* Tollo, R.P., Bartholomew, M.J., Hibbard, J.P., and Karabinos, P.M., eds., From Rodinia to Pangea: The Lithotectonic Record of the Appalachian Region: Geological Society of America Memoir 206, p. 897-916, doi:10.1130/2010.1206(34).

Tréhu, A.M., Ballard, A., Dorman, L.M., Gettrust, J.F., Klitgord, K.D., and Schreiner, A., 1989, Structure of the lower crust beneath the Carolina trough, U.S. Atlantic continental margin: Journal of Geophysical Research, v. 94, p. 10585-10600.

Tull, J., Holm-Denoma, C.S., and Barineau, C.I., 2014, Early to Middle Ordovician back-arc basin in the southern Appalachian Blue Ridge: Characteristics, extent, and tectonic significance: Geological Society of America Bulletin, v. 126, p. 990-1015, doi: 10.1130/B30967.1.

van den Berg, R., Daly, J.S., and Salisbury, M.H., 2005, Seismic velocities of granulite-facies xenoliths from Central Ireland: Implications for lower crustal composition and anisotropy: Tectonophysics, v. 407, p. 81-99.

van der Voo, R., and Torsvik, T.H., 2001, Evidence for Late Paleozoic and Mesozoic non-dipole fields provides an explanation for the Pangea reconstruction problems: Earth and Planetary Science Letters, v. 187, p. 71-81.

Villaseca, C., Downes, H., Pin, C., and Barbero, L., 1999, Nature and composition of the lower continental crust in central Spain and the granulite-granite linkage: Inferences from granulitic xenoliths: Journal of Petrology, v. 40, p. 1465-1496.

Wagner, L.S., Long, M.D., Johnston, M.D., and Benoit, M.H., 2012a, Lithospheric and asthenospheric contributions to shear-wave splitting observations in the southeastern United States: Earth and Planetary Science Letters, v. 341, p. 128-138, doi:10.1016/j.epsl.2012.06.020.

Wagner, L.S., Stewart, K., and Metcalf, K., 2012b, Crustal-scale shortening structures beneath the Blue Ridge Mountains, North Carolina, USA: Lithosphere, v. 4, p. 242-256.

Wessel, P., Smith W.H.F., Scharroo, R., Luis, J., and Wobbe, F., 2013, Generic Mapping Tools: Improved version released: Eos, v. 94, p. 409-410.

Zhu, L., and Kanamori, H., 2000, Moho depth variation in southern California from teleseismic receiver functions: Journal of Geophysical Research, v. 105, p. 2969-2980, doi:10.1029/1999JB900322.

Zietz, I., Riggle, F.E., and Gilbert, F.P., 1980, Aeromagnetic map of Georgia. U.S. Geological Survey Geophysical Investigations map GP-940, scale 1:500 000, 1 sheet.

APPENDIX A

SUPPLEMENTARY MATERIAL FOR CHAPTER 2

PROCESSING DETAILS

Receiver function computation

The SESAME deployment was staggered over three summer field seasons beginning in 2010. Most of the stations used in this study were deployed in May 2011, so approximately 1.5 years of data were available for this preliminary analysis. TA stations used in this study were deployed in the summer of 2012, so less than one year of data were available. We used earthquakes with magnitude (m_b) greater than or equal to 5.7 and an epicentral range of 30-95 degrees; appropriate events typically came from the Peru-Chile, Aleutian, Japan, and Kuril trenches as well as the Mediterranean region.

For receiver function processing, seismograms were initially de-trended, tapered, and band-passed filtered from 0.05 to 2.0 Hz. The seismograms were then windowed to 120 seconds, starting 30 seconds prior to the direct P-wave, and the horizontal components were rotated to the radial and tangential directions based on the back-azimuth of the teleseismic event for a given station. We used a frequency-domain (water-level) method to deconvolve the vertical component from the radial component (Langston, 1979). Water level values, typically 0.01, and Gaussian values (alpha) of 2.5 and 5.0 were chosen to maximize resolution while maintaining stable noise levels. Traces for a given station were stacked to enhance signal levels; before stacking, the traces were corrected for moveout to a common ray parameter of 0.06 s/km. The stacked traces for stations along the W-line are shown in Figure A1. Examples of receiver function gathers and corresponding stacks for selected stations along the W and D lines are shown in Figures A2 and A3.

H-k method

We used the method of Zhu and Kanamori (2000) to estimate crustal thickness (H) and average crustal Vp/Vs (k) from travel time delays for the direct Ps conversion and crustal multiples (PpPs and PpSs+PsPs) and assumed values of average crustal P-wave velocity. The ray parameter for each event was calculated using the *iasp91* velocity model of Kennett and Engdahl (1991). Using a grid search method, receiver function amplitudes at the predicted arrival times of the Ps conversion and crustal multiples (for a given pair of H and k) were then stacked for all receiver functions at a given station (Zhu and Kanamori*,* 2000; Lombardi et al.*,* 2008).

For stations that did not exhibit clear crustal multiples, we used the Ps delay time and assumed ranges of average crustal Vp and Vp/Vs to estimate crustal thickness. The results are summarized in Tables 2.1 and 2.2, and the H-k stacks are shown in Figure A4. Stacked receiver function traces from TA stations are shown in Figure A5, and Ps delay times for SESAME and TA stations are shown in Figure A6.

Error Analysis

Error estimates for the H-k analysis were obtained using the bootstrapping method of Efron and Tibshirani (1991), as implemented by Crotwell and Owens (2005). Bootstrapping was carried out using 100 iterations and repeated for a range of assumed average crustal Vp. For H-k analysis of stations in the Carolina terrane, Blue Ridge, Valley and Ridge, and Cumberland Plateau, we used an average crustal Vp range of 6.4-6.6 km/s derived from previous wide-angle studies (Prodehl et al., 1984; Hawman et al., 2012). For stations in the Inner Piedmont, we used an average crustal Vp range of 6.2-6.6 km/s (Hawman et al., 2012). The estimates for thickness and Vp/Vs are the mean values obtained using an average crustal Vp of 6.4 km/s for the Inner Piedmont and 6.5 km/s for all other stations (Tables 2.1 and 2.2). The upper and lower bounds on thickness and Vp/Vs (shown in parentheses) represent the range in mean values derived for the ranges in average Vp, including the uncertainties (+- one standard deviation) derived from bootstrapping. Small uncertainties in thickness (+- 1.0 km) and Vp/Vs (+- 0.01-0.02) for stations D02, D05, and D08 correspond with well-constrained H-k estimates across the Carolina terrane.

For crustal thickness estimates based on Ps delay times, we used an average crustal Vp/Vs of 1.76 (all stations) and an average crustal Vp of 6.4 km/s (for the Inner Piedmont) and 6.5 km/s (for all other stations). Uncertainties correspond to the minimum and maximum values found using a Vp/Vs range of 1.73-1.78 (all stations) and ranges for average crustal Vp of 6.2-6.6 km/s (Inner Piedmont) and 6.4-6.6 km/s (all other stations).

COMPARISON WITH WIDE-ANGLE RESULTS

For the Carolina terrane, the well-constrained H-k stacking estimates of Vp/Vs are generally lower than the wide-angle estimates of 1.74-1.76, though there is slight overlap in the uncertainty ranges at some stations (D03 and D09). At least part of the difference may be due to refraction effects. The wide-angle travel-time data yield estimates of Vp/Vs averaged along the ray path, where it is assumed that ray paths for PmP and SmS are identical. Because velocities generally increase with depth, refraction results in longer paths for ray segments deep in the crust, resulting in a slight bias of Vp/Vs estimates towards deeper crustal values. Estimates of average crustal Vp/Vs obtained from receiver functions rely on steeper raypaths, and so are less susceptible to this effect.

For the Inner Piedmont, the estimates for average crustal Vp/Vs show considerably more scatter. The Vp/Vs of 1.73 ± 0.02 determined for the Inner Piedmont using wide-angle methods falls within the uncertainty range determined using receiver functions. However, some of the variation may also be attributed to along-strike differences in lower crustal composition beneath the Alleghanian detachment, which may not correlate with upper crustal terrane boundaries. The estimates for Vp/Vs for stations along the W-line (W29, W31, and Y53A) are generally lower than estimates from stations along the D-line (D15, D17, and X53A). Better constraints on Vp/Vs from stations within the Inner Piedmont are required to evaluate possible along-strike variations in bulk composition across this province.

Figure A1. Stacked receiver functions from stations along the N-S trending W-line, including station D20 from the NW-trending D-line. Before stacking, the traces were corrected for moveout using a common ray parameter of 0.06 s/km. The Ps delay time increases from ~5.0 s at station W29 to ~7.0 s beneath stations W35 and D20, corresponding with an estimated increase in crustal thickness from 38-43 km to 55-61 km. Crustal reverberations are generally unclear or weak, except for station W31.

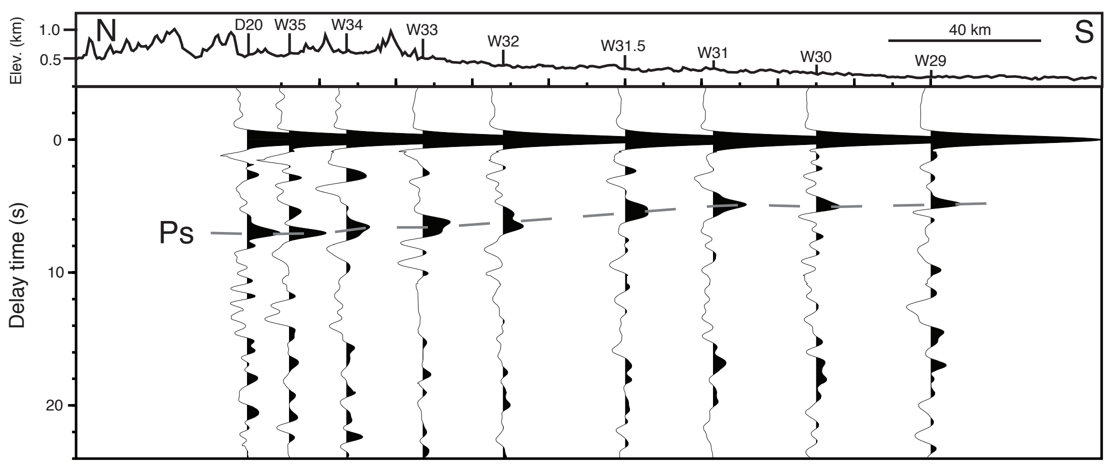

Figure A2. Receiver function gathers and stacked traces for stations D02 and D05 in the Carolina terrane using Gaussian values of 2.5 and 5.0. Before stacking, the traces were corrected for moveout using a common ray parameter of 0.06 s/km. The Ps conversion and crustal multiples (PpPs and PsPs+PpSs) are clearly visible in the stacked traces.

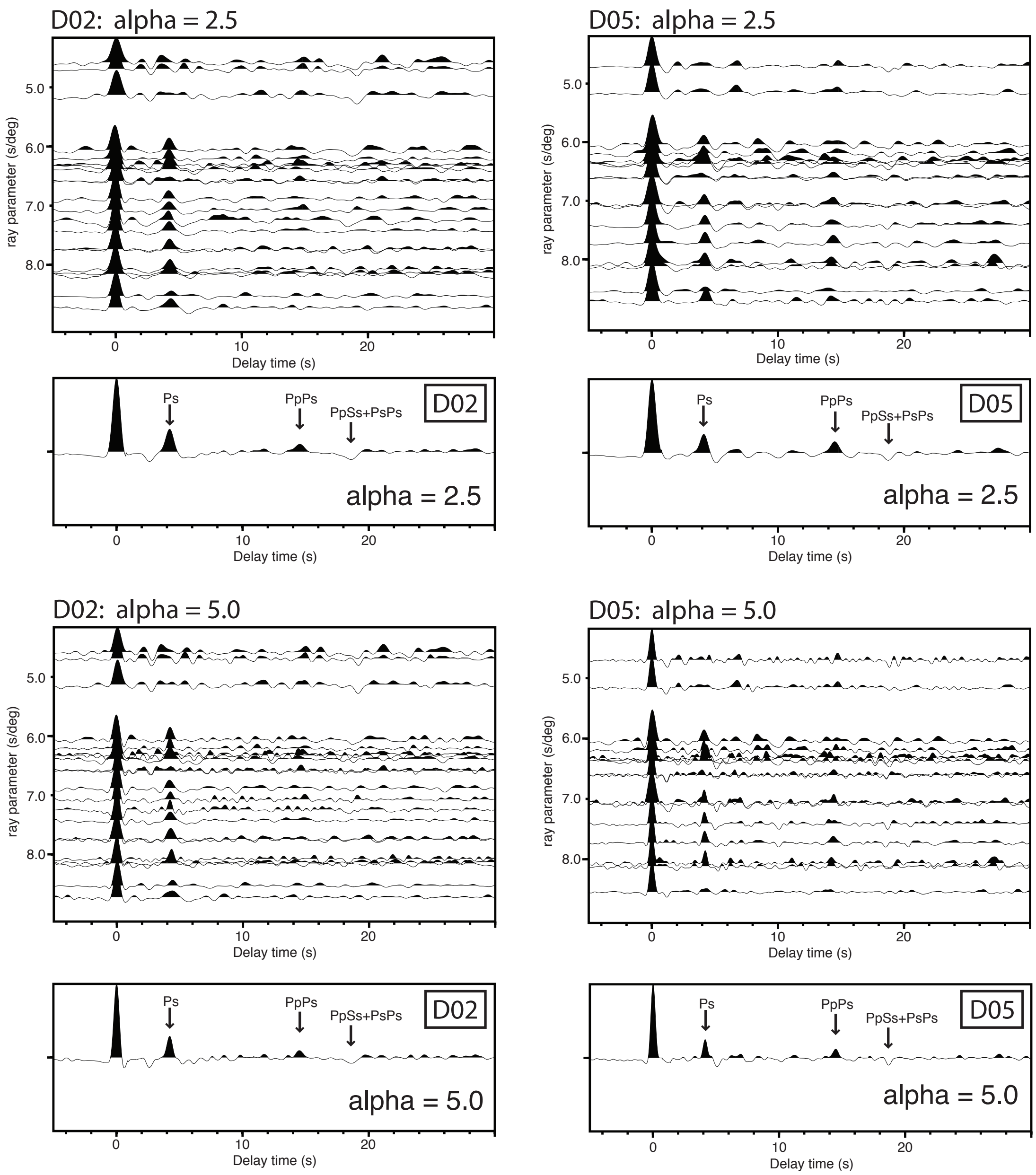

Figure A3. Receiver function gathers and stacked traces for stations D15, D17, and W35 using a Gaussian value of 2.5. For stations D15 and D17 in the Inner Piedmont, the PpPs conversion is lower in amplitude compared with stations D02 and D05 (see Figure 2.1). For station W35 in the Blue Ridge, the Ps conversion at ~7.0 seconds is clearly visible, but the crustal reverberations are unclear.

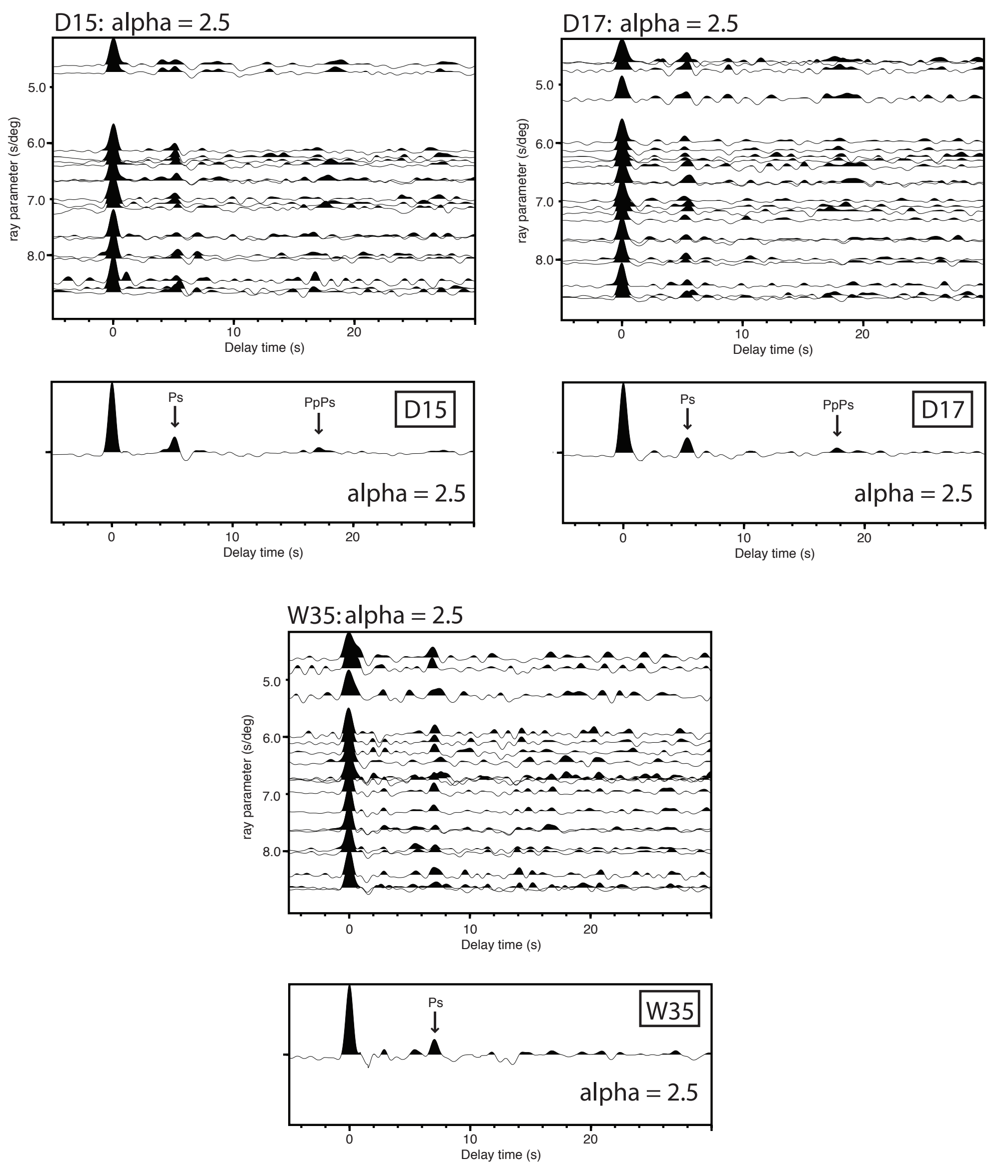

Figure A4. H-k stacks for selected SESAME and TA stations.

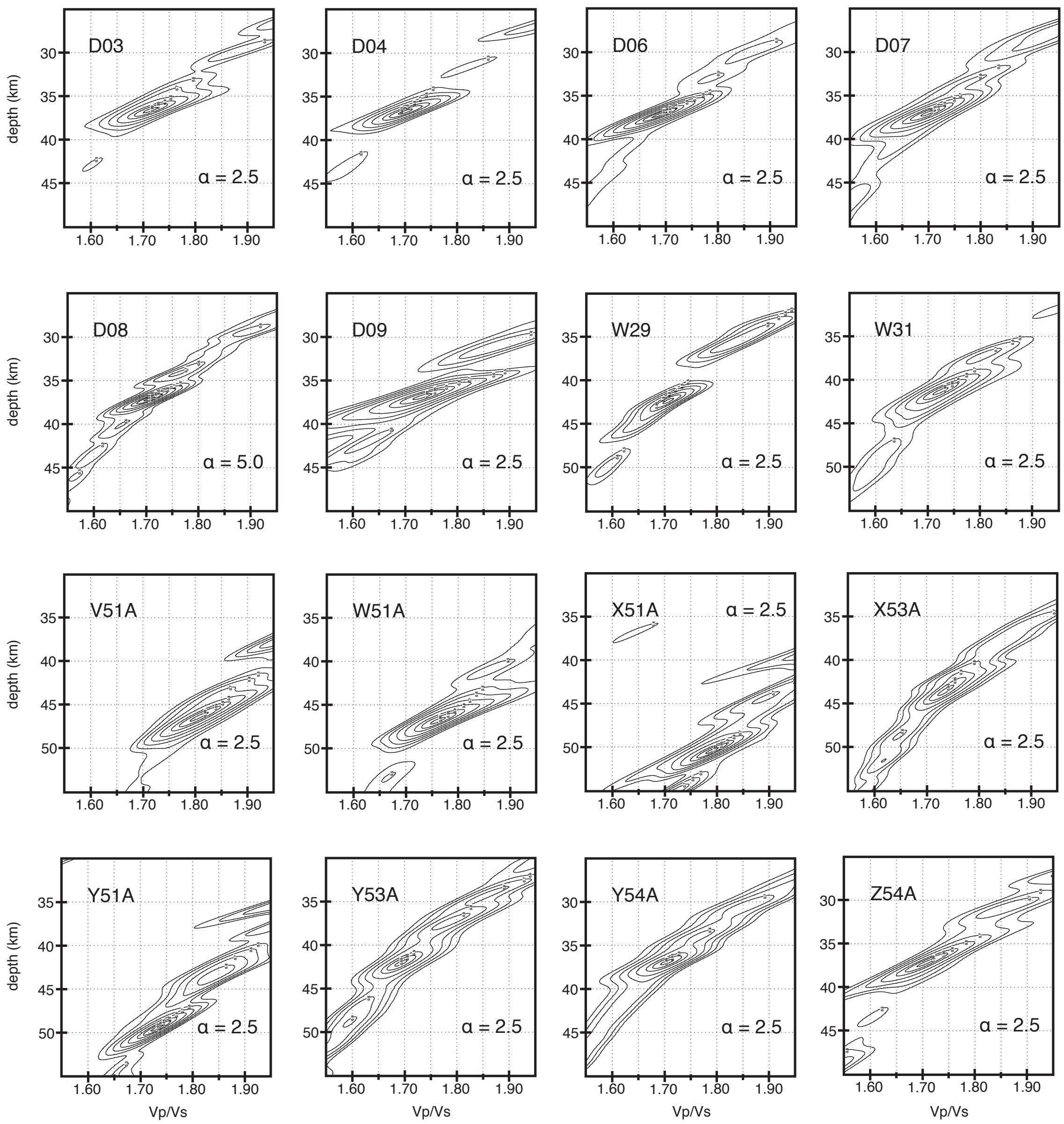

Figure A5. Stacked receiver function traces for selected TA stations projected onto a NW-trending line passing through stations V50A and Z54A. The overall pattern is consistent with the delay times observed for profiles along the W and D lines (Figures 2.2 and A1).

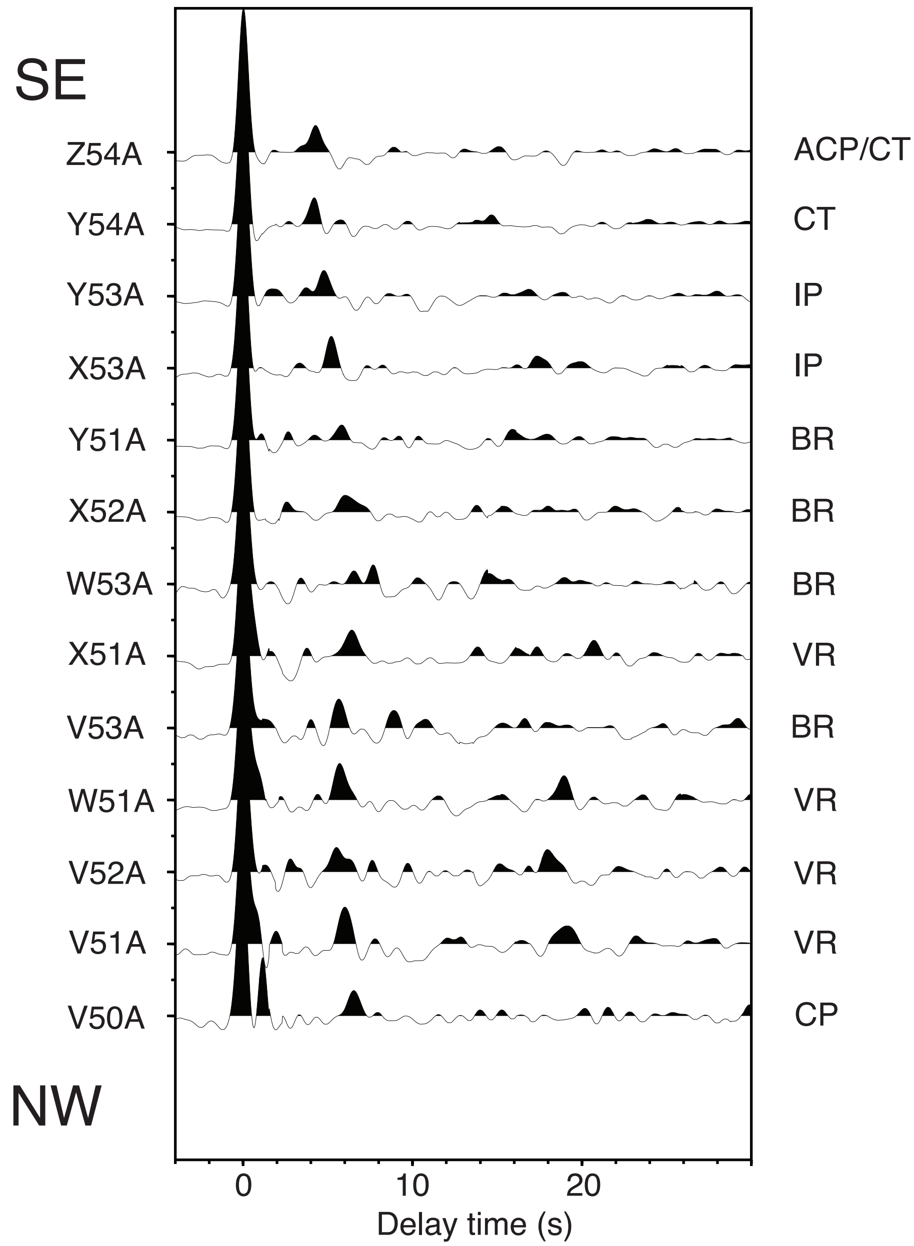

Figure A6. Contour map showing variation in Ps delay times across the southern Appalachians. Corresponding depths (see also Fig. 4) for time contours assuming Vp=6.5 km/s and Vp/Vs=1.76 are as follows: 4.5 s – 37 km; 5.0 s – 41 km; 5.5 s – 45 km; 6.0 s – 49 km; 6.5 s – 53 km; 7.0 s – 57 km.

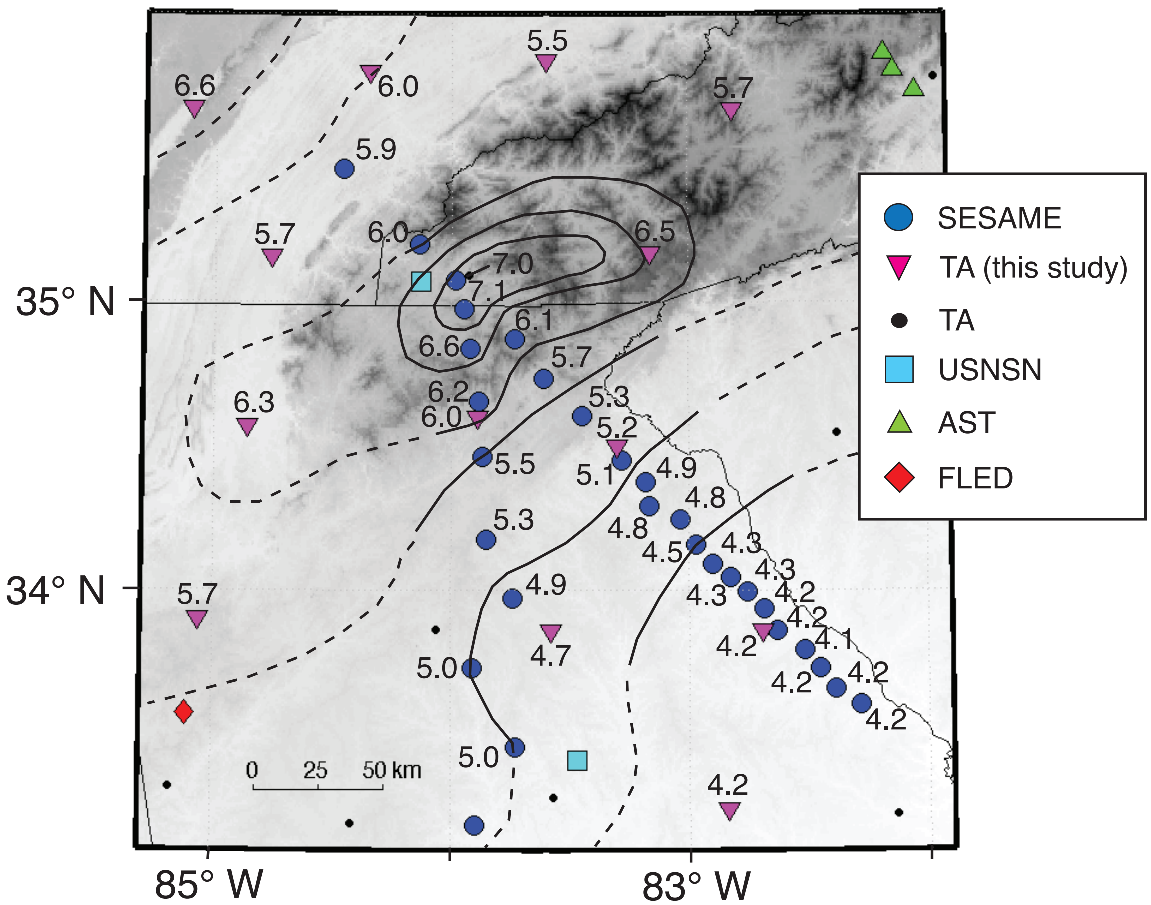

APPENDIX B

SUPPLEMENTARY MATERIAL FOR CHAPTER 3

PROCESSING DETAILS

The analysis of P-SV converted phases presented in this paper was optimized to identify shallow intracrustal discontinuities by including high-frequency energy in the receiver function calculations and then separating the waveforms by backazimuth (e.g. Owens et al., 1984). Receiver functions were generated by deconvolving the vertical-component from the radial-component seismogram using the frequency-domain method (Langston, 1979). High signal-to-noise events were chosen for the analysis, and the low pre-event noise in the receiver functions indicates that the waveforms are not contaminated by processing artifacts. Different low-pass Gaussian filters (α=5.0 and 7.0, corresponding to maximum frequencies of ~2 Hz and ~3 Hz, respectively) were applied to evaluate waveform variation with frequency content. Gaussian values of 1.0-2.5 (yielding maximum frequencies of 0.1-1.0 Hz) are typically used in broadband studies of the lower crust and uppermost mantle. Higher-frequency receiver functions (α=7.0; up to 3 Hz) provide improved resolution at the expense of increased noise levels (Cassidy, 1992). In our forward models, interface depths were determined using P-SV delay times (Zhu and Kanamori, 2000), and the velocity models were based on P-SV polarities, constraints from surface geology, seismic reflection profiling, and laboratory measurements of shear-wave velocities (Vs). In the modeling, both Vp and Vs were allowed to vary. For additional information on the geologic interpretation of reflection profiles from the southern Appalachians, the reader is referred to Hatcher (1971), Coruh et al. (1987), Hatcher (1987), Phinney and Roy-Chowdhury (1989), Hatcher (1991), and Hatcher (2001).

The receiver-function gathers and corresponding bootstrapped stacks are shown in Figures B1-B7 and B8, respectively. Bootstrap analysis was performed to evaluate the robustness of the vertically stacked conversions (Figure B8; Efron and Tibshirani, 1991). Stacked traces were corrected for moveout using a ray parameter of 0.06 s/km. In this study, the majority of earthquakes in the 30-95° epicentral range used for the analysis occurred in South America and the northern Pacific region (Figure B9; Table B1). The approximate backazimuthal ranges used for the analysis were 150-180° and 275- 345° for South America and the northern Pacific, respectively. Suitable events from other regions (e.g. Atlantic mid-ocean ridge) were less numerous and generally yielded lower-quality receiver functions.

The analysis of high-frequency receiver functions separated by backazimuth is not always ideal for imaging deeper discontinuities because waveforms can vary significantly in regions characterized by lateral heterogeneity, dipping structure, or anisotropy (e.g. Levin and Park, 1997). In this study, the weak Moho P-SV conversions for some backazimuths (e.g. D04-NW; Figure 3.3C) are attributed primarily to interference effects with unmodeled intracrustal multiples (e.g. Beck and Zandt, 2002). Lateral heterogeneity within the crust could cause these effects to vary with azimuth. Dipping structure or azimuthal anisotropy at the crust-mantle boundary remain a possibility, but these effects are difficult to assess because of the limited azimuthal event coverage for this region. Poor signal quality or a gradational Moho are also alternative explanations, but the strong PpPs multiples from the Moho observed on both backazimuths at some stations indicate that these causes are less likely.

In general, there is clear evidence for strong Moho conversions across the array when all backazimuths are considered, and the reader is referred to Parker et al. (2013) for lower-frequency ($\alpha = 2.5$) receiver-function stacks including events from both the S and NW backazimuths. These data show the strong amplitude and continuity of Moho P-SV conversions across the crystalline southern Appalachians. Receiver functions showing strong Moho P-SV conversions ($\alpha = 1.0$ and 2.0) from the Blue Ridge and Inner Piedmont are also presented in Baker and Hawman (2011).

Figures B1-B7. Receiver-function gathers showing P-SV conversion picks (gray bands) used to estimate depths shown in Figure 3.4. For each station, the Gaussian value (5.0 or 7.0) and backazimuth (s: south, nw: northwest) are shown in parentheses. The water level parameter used in the frequency-domain receiver function calculations (Langston, 1979) was 0.01.

Figure B1. P-SV conversions at stations D20, D21, and D22. Positive conversions from station D22 in the Valley & Ridge and stations D20 and D21 in the Blue Ridge show a southeastward increase in Grenville basement depth from 3.8 to 6.4 km, in agreement with estimates determined from seismic reflection profiling in this region (Hatcher et al., 2007). The upward decrease in shear-wave velocity beneath parts of the Valley and Ridge and Blue Ridge is interpreted to result from the dominance of low-velocity shale of the Rome Formation or Conasauga Group, rather than high-velocity quartzite or dolomite, overlying Grenville basement (Hatcher et al., 2007). This observation implies that receiver function conversion polarities may vary laterally depending on the lithology and thickness of platform assemblages above the basement surface.

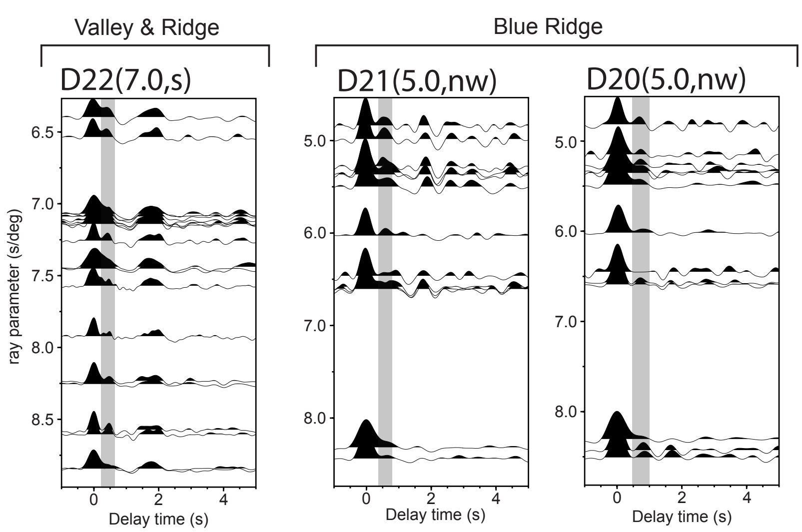

Figure B2. P-SV conversions at stations D18 and D19. For station D19, positive and negative conversions in receiver functions from the northwest and south backazimuths, respectively, are consistent with the presence of a high-velocity layer at 4.2-7.6 km depth beneath the Blue Ridge. Negative conversions are generated at the base of the high-velocity layer, and positive conversions are generated at the top. For station D18, the negative conversion at 5.9 km corresponding with the base of the high-velocity layer is evident, though the top of the layer is not imaged.

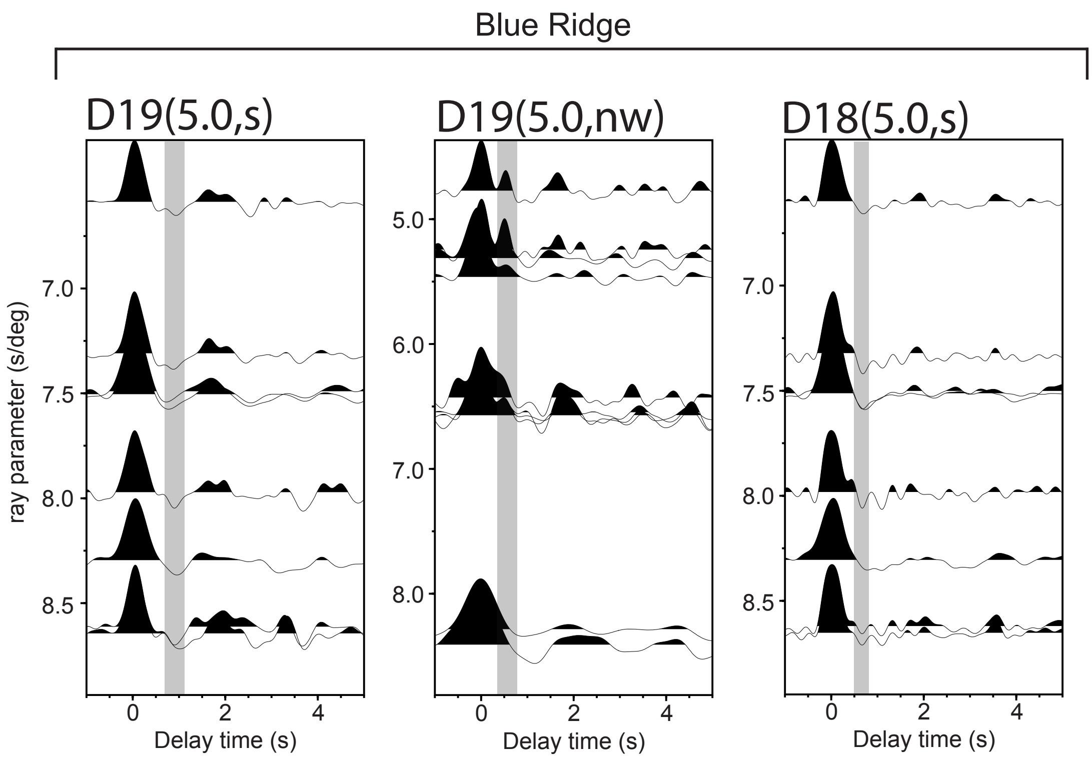

Figure B3. P-SV conversions at stations D14, W31, D17, and W31.5. Positive conversions in receiver functions from stations along the Brevard zone (D17 and W31.5) and northwestern flank of the Inner Piedmont (D14 and W31) are indicative of an upward decrease in velocity marking the top of the high-Vs meta-sedimentary layer at 5-7 km depth, consistent with the interpretation that passive margin rocks dominated by dolostone and quartzite extend slightly southeast of the Brevard zone.

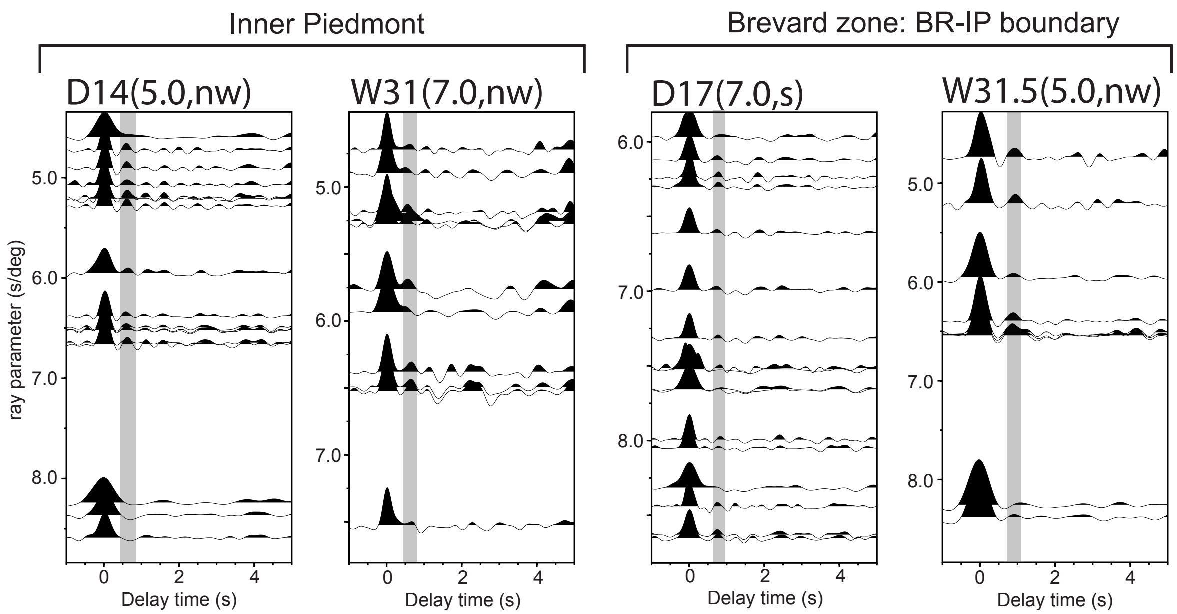

Figure B4. P-SV conversions at stations Y52A and Z52A. For station Z52A in the Inner Piedmont, positive and negative conversions in receiver functions from the northwestern and southern backazimuths, respectively, are indicative of a low-velocity zone at 6-10 km depth. Positive conversions are generated at the base of the low-velocity zone, and negative conversions are generated at the top. At station Y52A on the northwestern flank of the Inner Piedmont, the negative conversion at 10.2-km depth is interpreted to mark the base of the high-Vs platform sequence.

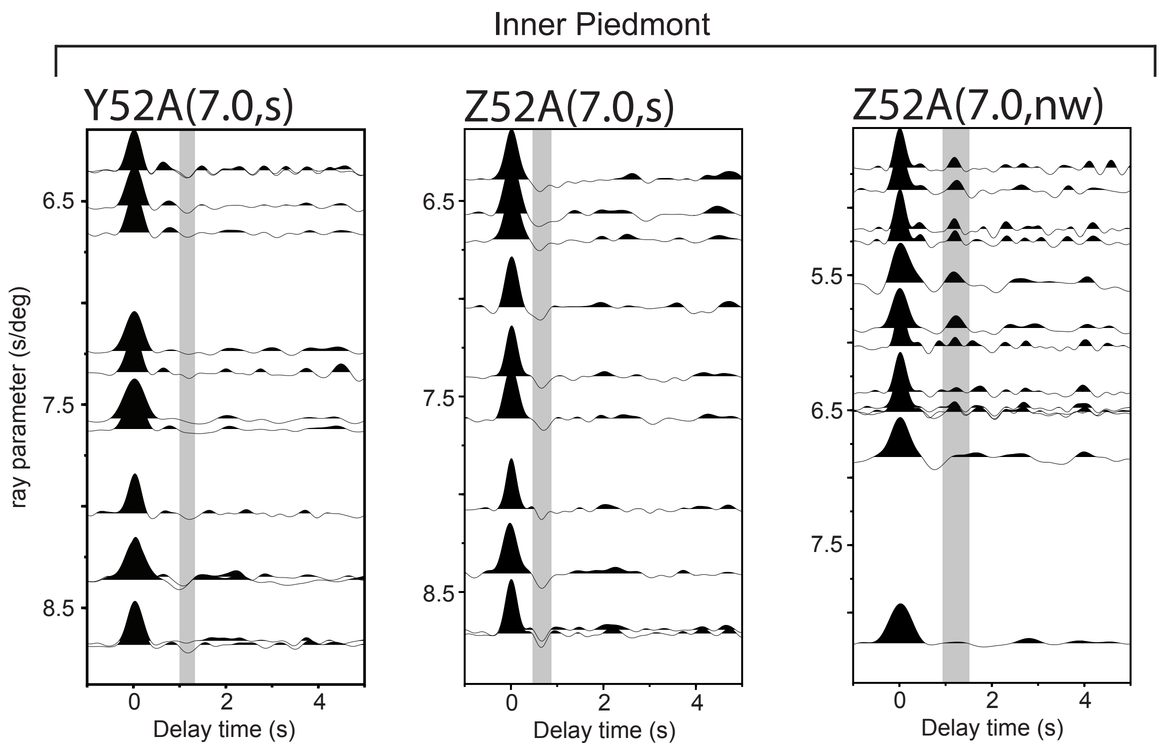

Figure B5. P-SV conversions at stations W29, W30, D12, W54A, and X54A. Positive conversions from stations across the Inner Piedmont corresponding with depths of 8.5-13.1 km are consistent with depths to Grenville basement determined from seismic reflection profiling (Hatcher et al., 2007).

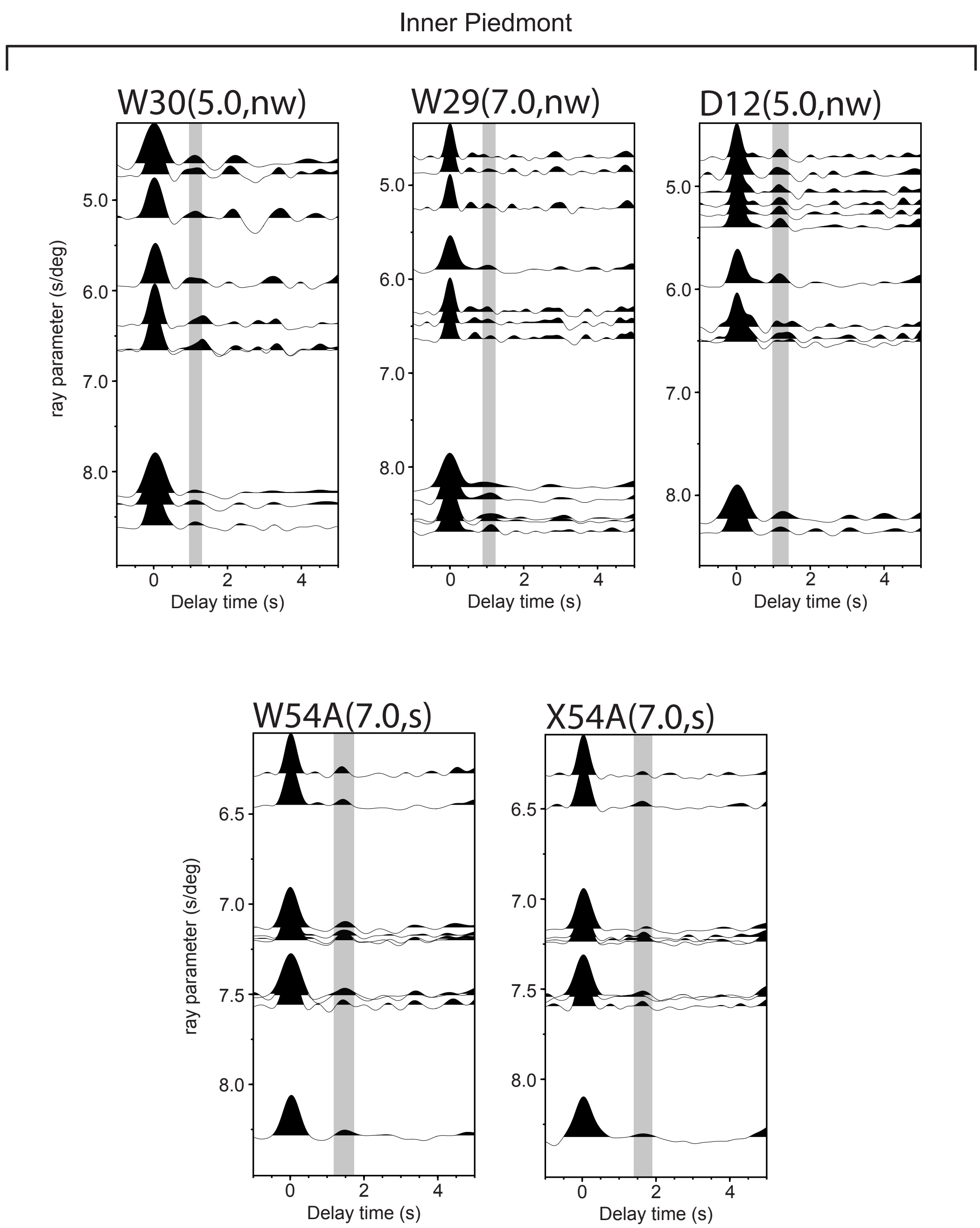

Figure B6. P-SV conversions at stations D03-D07 and Z53A. Negative conversions in receiver functions across the Carolina terrane indicate an upward increase in velocity at depths of 5.9-12.7 km. For stations D03-D05, the conversions are interpreted to mark the base of high-Vs Carolina terrane arc rocks. Earlier negative conversions from stations D05-D07 and Z53A are interpreted to mark velocity discontinuities associated with Alleghanian thrust sheet imbrication.

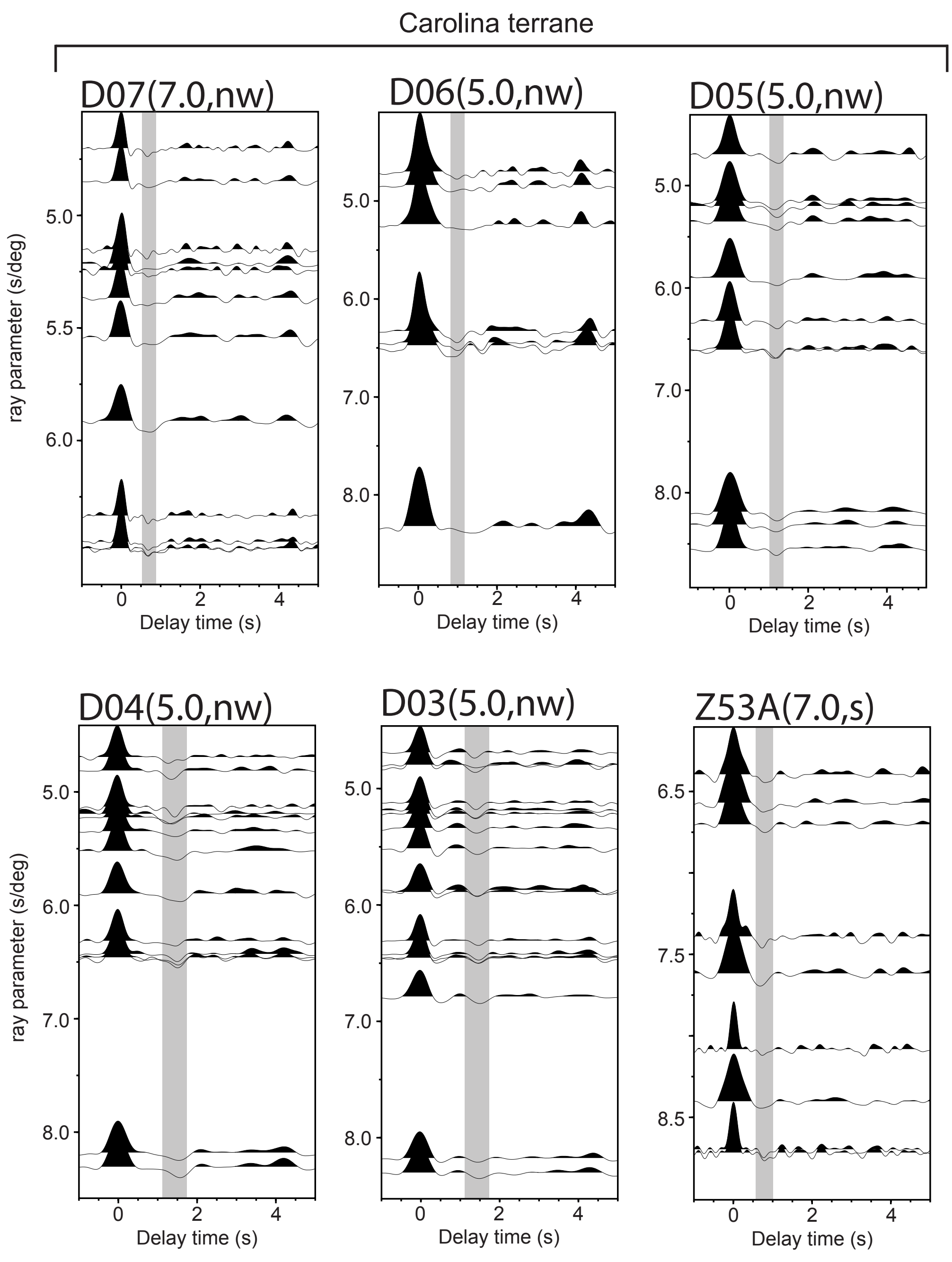

Figure B7. P-SV conversions at stations D03 and D08. Positive conversions in receiver functions from stations D03 and D08 in the Carolina terrane are indicative of an upward decrease in velocity at depths of 4.7-5.1 km, reflecting the complex internal structure of the Alleghanian thrust sheet.

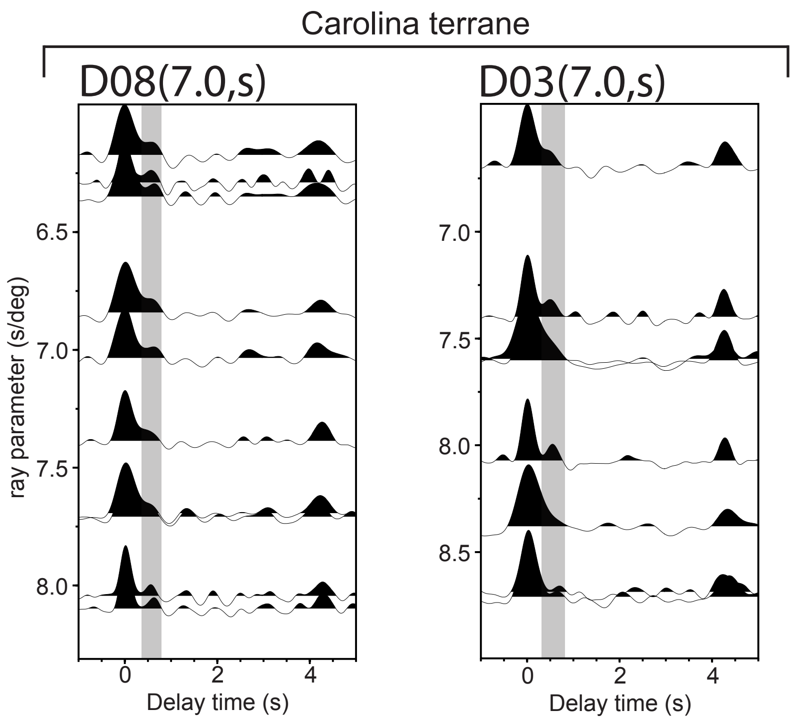

Figure B8. Bootstrapped receiver-function stacks. In each figure, the mean stacked trace is shown with 2-sigma error bounds to demonstrate the robustness of the intracrustal P-SV conversions (arrows) used to estimate conversion depths in Figure 3.4 (Figures B8, A-G) and Figure 3.3 (Figures B8, H-I). For each set of stacked traces, the corresponding event backazimuth, Gaussian value, and number of the receiver functions included in the stack (N) are shown. The bootstrapping analysis is based on the method of Efron and Tibshirani (1991). A-G: Bootstrapped receiver-function stacks for gathers shown in Figures B1-B7. H-I: Bootstrapped receiver-function stacks for stations D04 and W33 shown in Figure 3.3.

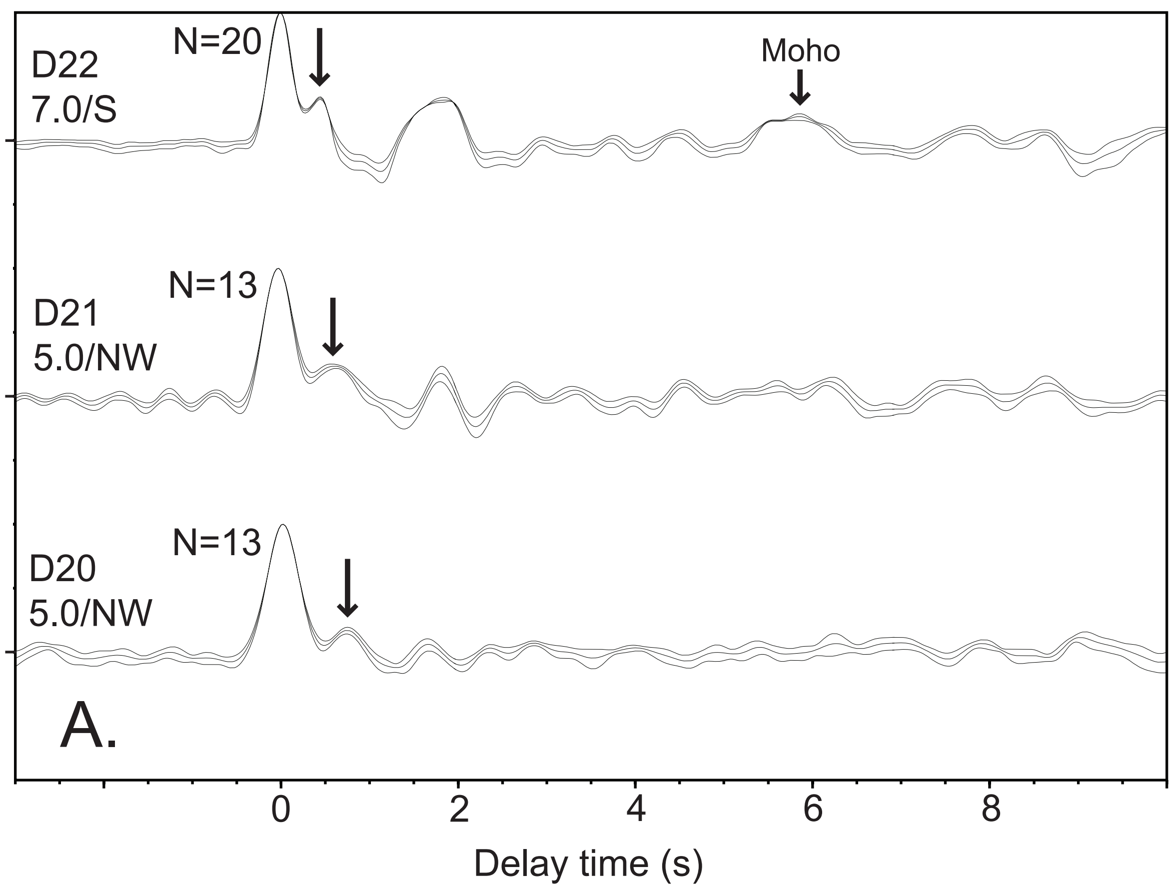

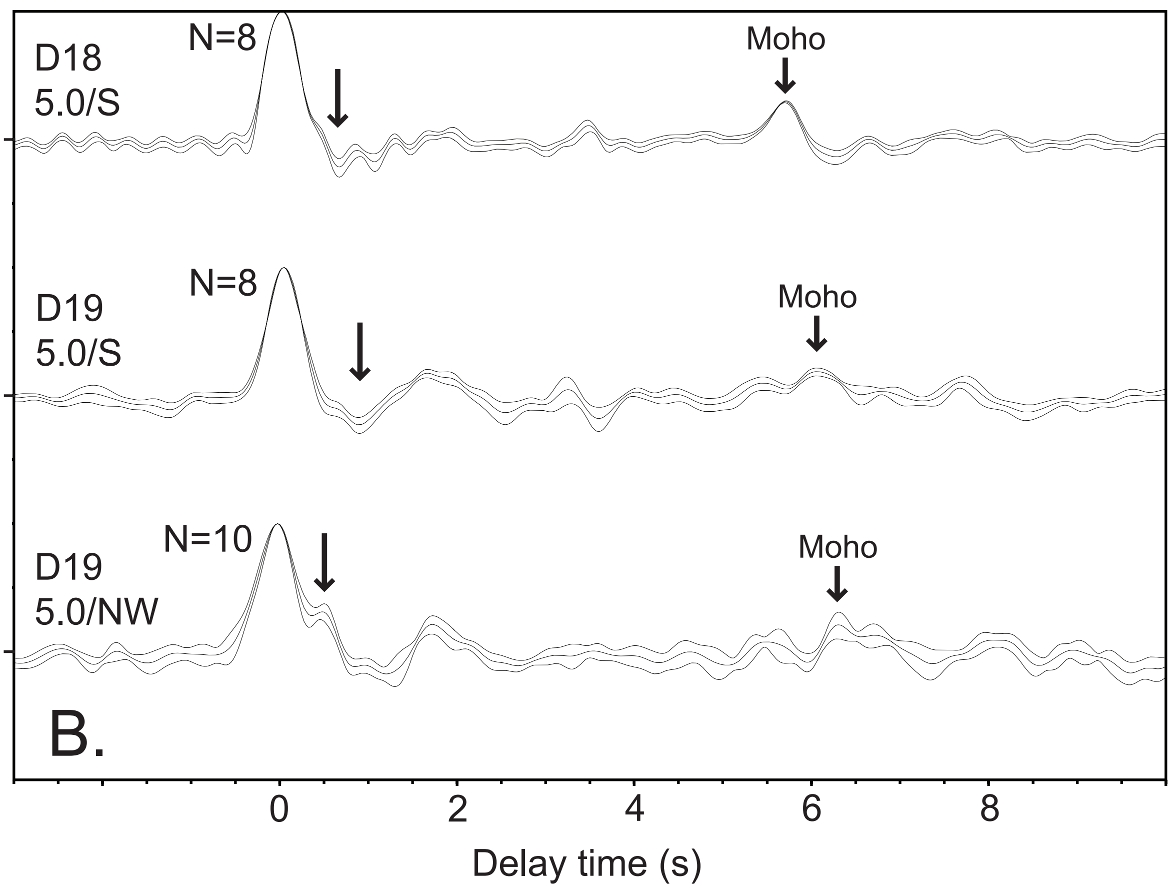

D18
5.0/S
N=8
Moho
D19
5.0/S
N=8
Moho
D19
5.0/NW
N=10
Moho
B.
0
2
4
6
8
Delay time (s)

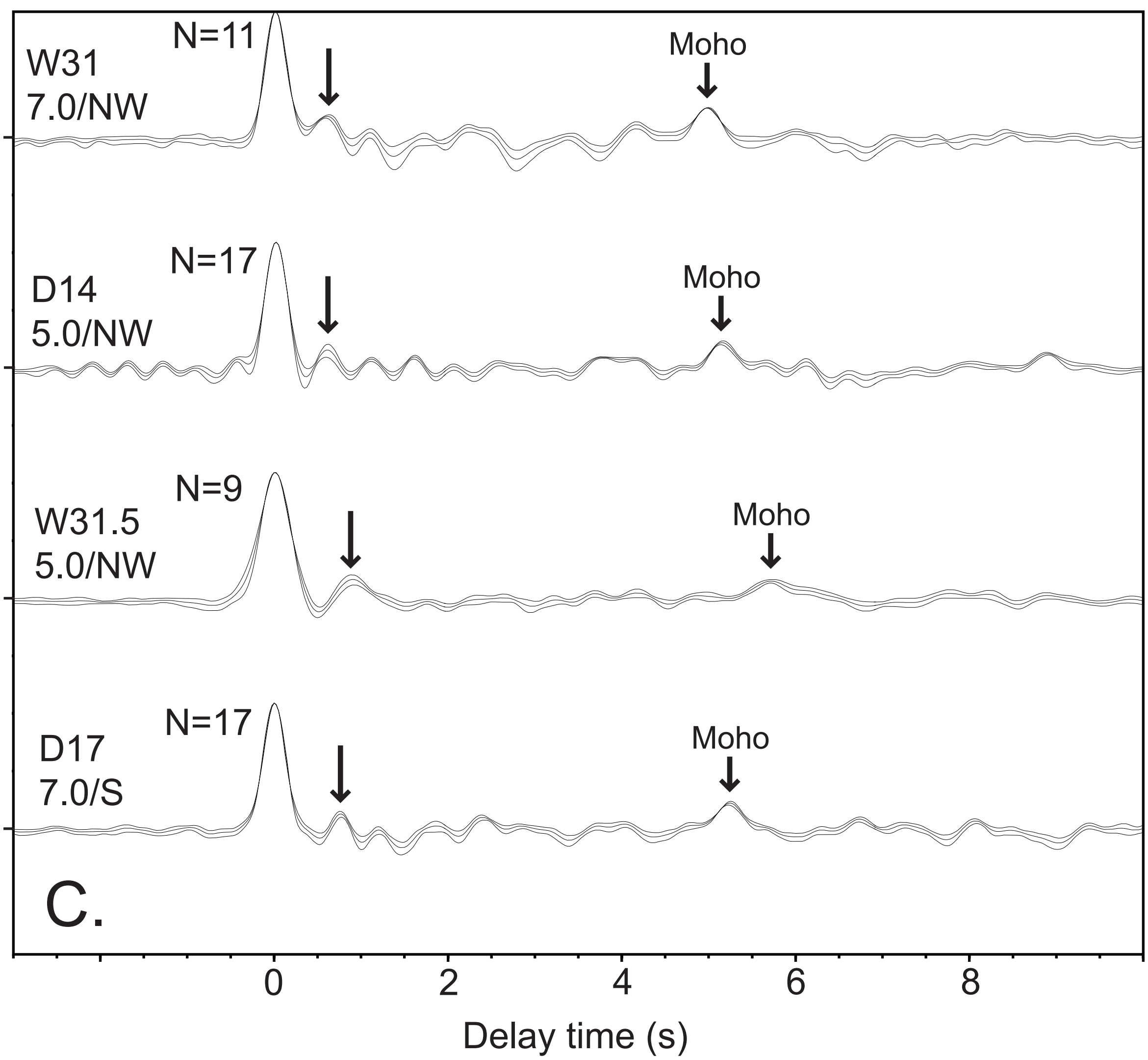
W31
7.0/NW
N=11
Moho
D14
5.0/NW
N=17
Moho
W31.5
5.0/NW
N=9
Moho
D17
7.0/S
N=17
Moho
C.
0
2
4
6
8
Delay time (s)

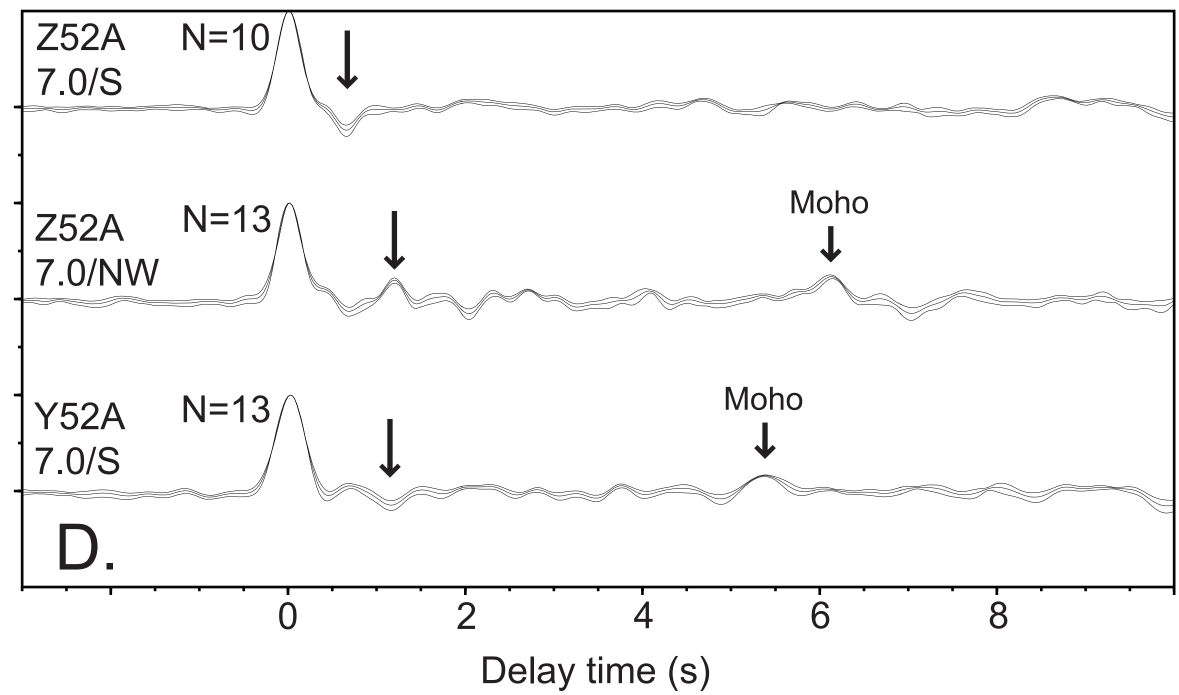

Z52A
7.0/S
N=10
Z52A
7.0/NW
N=13
Moho
Y52A
7.0/S
N=13
Moho
D.
0
2
4
6
8
Delay time (s)

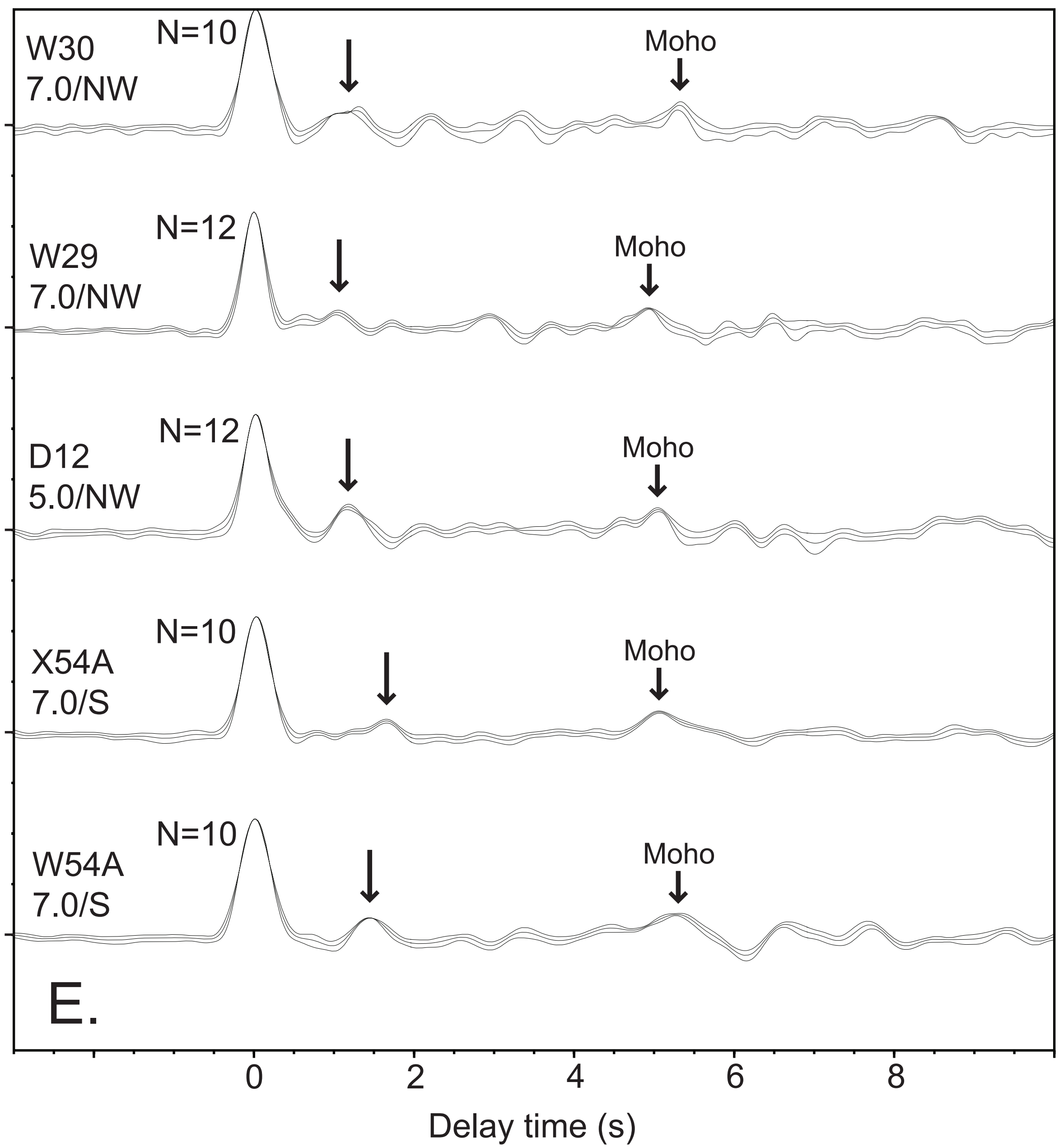
W30
7.0/NW
N=10
Moho
W29
7.0/NW
N=12
Moho
D12
5.0/NW
N=12
Moho
X54A
7.0/S
N=10
Moho
W54A
7.0/S
N=10
Moho
E.
0
2
4
6
8
Delay time (s)

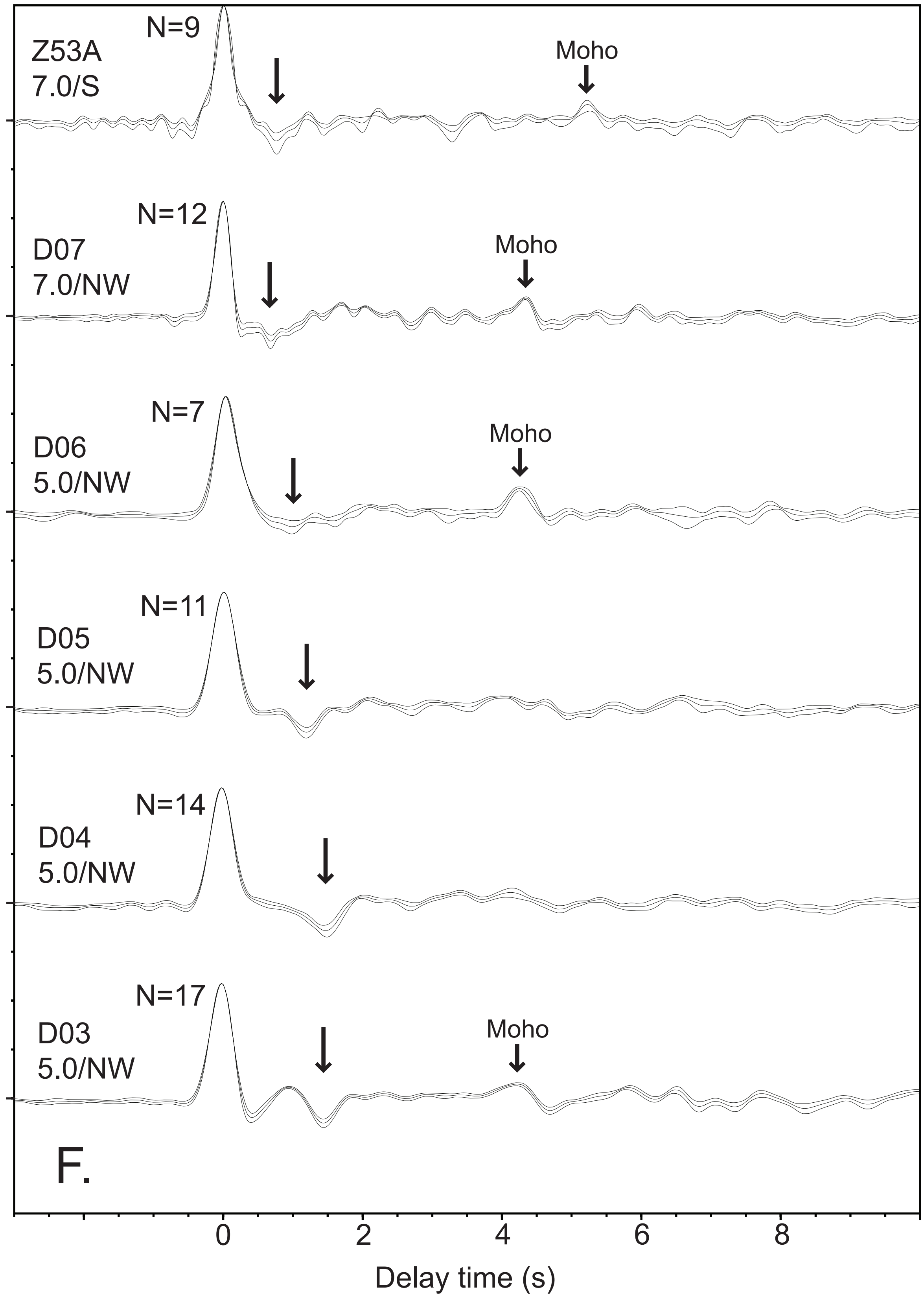

N=9
Z53A
7.0/S
Moho
N=12
D07
7.0/NW
Moho
N=7
D06
5.0/NW
Moho
N=11
D05
5.0/NW
N=14
D04
5.0/NW
N=17
D03
5.0/NW
Moho
F.
0
2
4
6
8
Delay time (s)

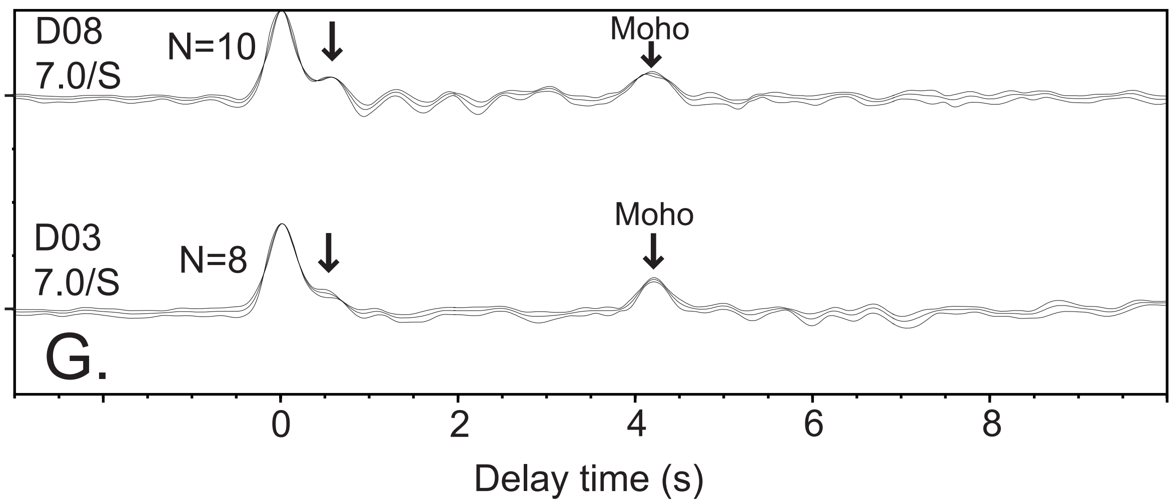
D08
7.0/S
N=10
Moho
D03
7.0/S
N=8
Moho
G.
0
2
4
6
8
Delay time (s)

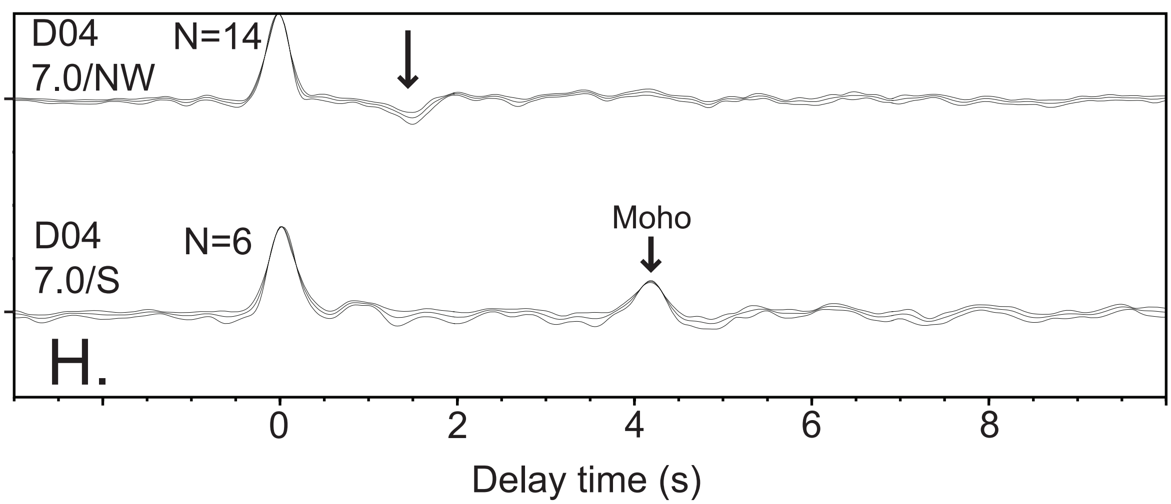
D04
7.0/NW
N=14
D04
7.0/S
N=6
Moho
H.
0
2
4
6
8
Delay time (s)

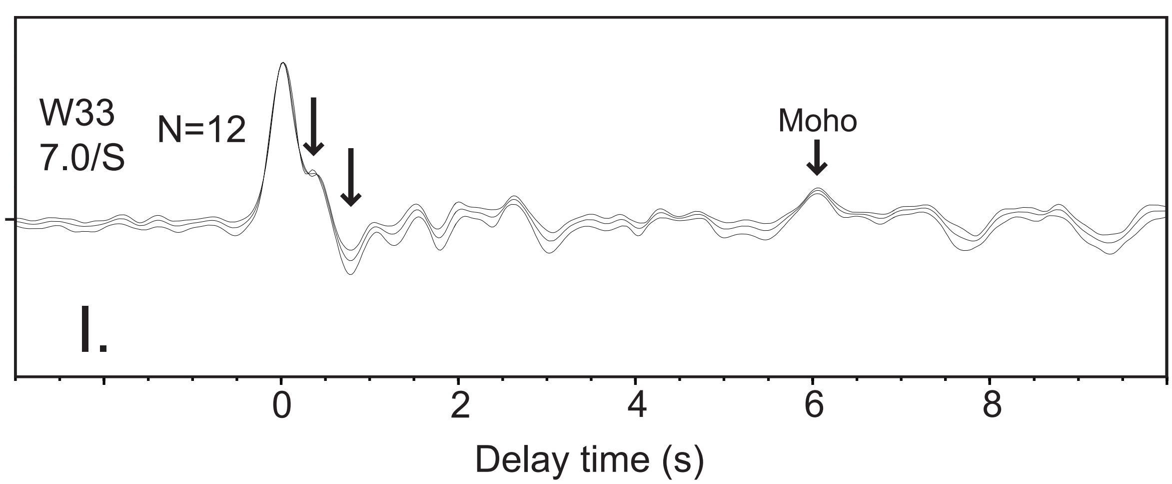
W33
7.0/S
N=12
Moho
I.
0
2
4
6
8
Delay time (s)

Figure B9. Distribution of events used in the calculation of receiver functions.

Table B1: Events used in the calculation of receiver functions for each station

Event (yr/julian day/hr/min)	Latitude	Longitude	Station
2011.152.12.55	-37.57	-73.69	d17
2011.171.16.36	-21.68	-68.19	d08, d17
2011.175.03.09	51.98	-171.82	d05, d14, w30
2011.216.13.51	48.77	154.84	d05, d14, w30
2011.227.02.53	-1.81	-76.90	d17
2011.236.17.46	-7.65	-74.51	d08, d17
2011.245.10.55	52.10	-171.72	d05, d14, w29, w30
2011.245.13.47	-28.39	-63.06	d08, d17
2011.252.19.41	49.39	-127.06	d05, d14, w29, w30
2011.279.11.12	-24.13	-64.30	d08
2011.301.18.54	-14.44	-75.99	d08, d17
2012.030.05.11	-14.16	-75.62	d08, d17
2012.074.09.08	40.89	144.94	d14, w30
2012.085.22.37	-35.18	-71.79	d08, d17
2012.108.03.50	-32.63	-71.37	d08, d17, y52a, z52a, z53a
2012.135.10.00	-17.70	-69.57	d03, d08, d17, d18, d19, d22, y52a, z52a, z53a
2012.156.00.45	5.30	-82.58	d22
2012.171.15.56	53.36	171.59	z52a
2012.176.03.15	57.61	163.20	d03
2012.184.23.31	-14.41	-75.59	d22
2012.190.11.33	45.48	151.32	d03
2012.215.09.38	-8.41	-74.26	d03, d08, d17, d18, d19, d22, y52a, z52a, z53a
2012.223.18.37	52.63	-167.42	d03, z52a
2012.227.02.59	49.80	145.06	d03, d04, d05, d06, d07, d12, d14, d19, d20, d21
			w29, w30, w31, w31.5, z52a
2012.270.23.39	51.61	-178.31	d03, d04, d05, d06, d07, d12, d14, d19, d20, d21
			w29, w30, w31, w31.5, z52a
2012.274.16.31	1.92	-76.36	d03, d17, d18, d19, d22, y52a, z52a, z53a
2012.302.03.04	52.79	-132.10	d03, d04, d05, d06, d12, d14, d19, d20, d21
			w29, w30, w31.5
2012.321.18.12	49.28	155.43	d03, d04, d05, d07, d19, d20, d21, w31

Table B1 (continued): Events used in the calculation of receiver functions for each station

Event (yr/julian day/hr/min)	Latitude	Longitude	Station
2013.005.08.58	55.39	-134.65	d03, d04, d05, d12, d14, d19, d20, d21
			w29, w30, w31.5, z52a
2013.030.20.15	-28.09	-70.65	d03, d17, d18, d19, d22, y52a, z52a, z53a
2013.040.14.16	1.14	-77.39	d03, d17, d18, d19, d22, y52a, z52a, z53a
2013.045.13.13	67.63	142.51	d03, d04, d05, d07, d12, d14, d20, d21
			w29, w30, w31, w31.5, z52a
2013.059.14.05	50.95	157.28	d03, d04, d05, d07, d12, d19, d20, d21
2013.109.03.05	46.22	150.79	d03, d04, d06, d07, d12, d14, d21, w29, w31, z52a
2013.139.18.44	52.34	160.07	d03, d04, d07, z52a
2013.144.05.44	54.89	153.22	d03, d04, d06, d07, d12, d14, d20, d21, w29, w31, z52a
2013.144.14.56	52.24	151.44	d12, d14, d20
2013.198.02.37	-15.66	-71.74	d03, d17, d18, d19, d22, w54a, x54a
2013.224.09.49	-5.40	-81.93	d03, d17, d18, d19, d22, w54a, x54a, y52a, z52a, z53a
2013.225.15.43	5.77	-78.20	d22
2013.235.08.34	-22.27	-68.59	z52a
2013.242.16.25	51.61	-175.36	d03, d04, d06, d07, d12, d14, d19, d20, d21
			w29, w31, w31.5, z52a
2013.246.20.19	51.24	-130.40	d20
2013.247.02.32	51.59	-174.73	d03, d04, d07, d14, d19, d20, d21, w31.5, z52a
2013.258.16.21	51.58	-174.72	d03, d04, d06, d07, d12, d14, d19, d21, w31, w31.5, z52a
2013.268.16.42	-15.85	-74.56	d03, d17, d18, d19, d22, z52a, w54a, x54a, y52a, z53a
2013.274.03.38	53.20	152.79	d03, d04, d07, d12, d14, d19, d20, d21, w31, w31.5, z52a
2013.304.23.03	-30.29	-71.52	d22, z52a, w54a, x54a, y52a, z53a
2013.316.07.03	54.69	162.30	w31
2014.069.05.18	40.83	-125.13	w29
2013.074.23.51	-5.57	-80.97	d22, y52a
2013.075.21.16	-19.98	-70.70	d22, w54a, y52a, x54a
2014.081.12.59	-19.76	-70.87	d22, w54a, x54a
2014.082.18.20	-19.69	-70.85	d22
2014.091.23.46	-19.61	-70.77	d22, w54a, x54a

Table B1 (continued): Events used in the calculation of receiver functions for each station

Event (yr/julian day/hr/min)	Latitude	Longitude	Station
2014.093.01.58	-20.31	-70.58	d22
2014.093.02.43	-20.57	-70.49	d22, w54a, x54a
2014.094.01.37	-20.64	-70.65	d22
2014.114.03.10	49.64	-127.73	w29
2014.130.14.16	60.00	-152.13	w31
2014.235.22.32	-32.70	-71.44	w54a, y52a, x54a
2014.236.23.21	-14.60	-73.57	w54a, y52a, x54a